Ricardo da Costa Barbedo Vieira

Alteration of GABA$_A$R Trafficking in Epilepsy

Junho 2015

· U C ·

UNIVERSIDADE DE COIMBRA

Alteration of GABA$_A$R Trafficking in Epilepsy

Ricardo da Costa Barbedo Vieira

2015

Agradecimentos / Acknowledgments

Gostava de começar por agradecer todo o carinho que me foi dado pelo CNC, desde que cheguei até ao presente momento. Não foi fácil mas teria sido muito mais difícil caso o ambiente que aqui se vive não fosse tão bom.

Um agradecimento muito especial ao Professor Carlos Duarte pelo acolhimento, apoio, toda a ajuda e conhecimento não só científico mas também musical que partilhamos. Obrigado por ter sempre uma posição sensata e calma onde muitos outros não o conseguiriam.

Miranda, não tenho palavras para descrever o quão importante foste. Todo o tempo que tiveste de lidar comigo foste sempre positiva e ajudaste-me a atravessar os percursos difíceis com apoio incondicional. Só há uma coisa a dizer. És fantástica e um devo-te um banquete pelo que tu passaste por minha causa. Nunca me vou esquecer das coisas que me ensinaste. Foi um prazer ter crescido contigo durante este ano.

Um sincero agradecimento a todos os que habitam o "Golden Aquarium" que me proporcionaram tantas horas de riso e diversão. Era algo com que eu não esperava e agora é algo que não quero deixar. Em particular, tenho de agradecer ao grandíssimo Carlos, a majestosa Tatiana, ao grande mestre Rui, e a Dona "Maria Alice" pelo grande apoio que me deram e pelas conversas fantásticas que partilhamos. É desta maneira que crescemos.

Aos meus meninos do grandioso grupo CBD, "Gracie", "Ivancipação" e "Pedrinho Alphose" um enorme agradecimento por toda a brincadeira e todo o apoio que me deram no laboratório, sem esquecer a dose recomendada de "bullying". Sinceramente, são pessoas que nunca vou esquecer e que espero que permaneçam por perto durante muito tempo.

Para aos meus amigos e família a olhar por mim do grande Porto, um enorme agradecimento pelo tempo e força que me deram para continuar a enfrentar este obstáculo. Não interessa o quão longe, levo-vos sempre no meu coração.

E finalmente, um enorme agradecimento a si, meu caro leitor, por estar a ler esta humilde dissertação que desenvolvemos ao longo de um breve mas doce ano.

Obrigado,

Ricardo

Index

Abbreviations

AED	Antiepileptic Drug
AM	Acetoxymethyl Group
AMPA	α-amino-3-hydroxy-5-methyl-4-isoxazolepropionic acid
AP2	Clathrin Adaptor Protein 2
APS	Ammonium persulfate
APV	*(2R)*-amino-5-phosphonovaleric acid
BCA	Bicinchoninic acid
BIG2	Brefeldin-A-inhibited GDP/GTP Exchange Factor 2
BSA	Bovine Serum Albumin
Ca^{2+}	Calcium Ion
$[Ca^{2+}]_i$	Intracellular Calcium Concentration
CaCl2	Calcium chloride
CAPS	N-cyclohexyl-3-aminopropanesulfonic acid
CDC42	Cell Division Control Protein 42 Homolog
CNS	Central Nervous System
DMSO	Dimethyl sulfoxide
DNA	Deoxyribonucleic acid
DOC	Sodium deoxycholate
DTT	Dithiothreitol
ECF	Enhanced Chemifluorescence
EDTA	Ethylenediaminetetraacetic acid
EGTA	Ethylene glycol-bis(2-aminoethylether)-N,N,N′,N′-tetraacetic acid
ER	Endoplasmatic Reticulum
FBS	Fetal Bovine Serum
FDU	2'-deoxy-5-fluorouridine
GABA	Gamma-Aminobutyric acid

GABA$_A$R	Gamma-Aminobutyric acid Receptor Type A
GABA$_B$R	Gamma-Aminobutyric acid Receptor Type B
GABARAP	GABA$_A$ receptor-associated protein
GAD	Glutamic acid Decarboxylase
GAT	GABA Transporter Protein
GDP	Guanosine diphosphate
GEF	Guanine Nucleotide Exchange Factor
GODZ	Golgi-specific DHHC zinc-finger-domain Protein
GRIF	GABA$_A$R-interacting Factor Protein
GTP	Guanosine triphosphate
HAP1	Huntingtin-associated Protein 1
HBSS	Hank's Balanced Salt Solution
HCl	Hydrochloric acid
HEPES	4-(2-hydroxyethyl)-1-piperazineethanesulfonic acid
ILAE	International League Against Epilepsy
K$^+$	Potassium Ion
KCC2	Potassium-chloride Transporter Member 5
KCl	Potassium chloride
KH$_2$PO$_4$	Monopotassium phosphate
Mena/VASP	Mammalian Enabled Vasodilator Stimulated Phosphoprotein
Mg^{2+}	Magnesium Ion
[Mg^{2+}]$_o$	Magnesium Free
MgCl$_2$	Magnesium chloride
mIPSC	Miniature Inhibitory Postsynaptic Currents
Na$^+$	Sodium Ion
Na$_2$HPO$_4$	Disodium phosphate
NaCl	Sodium chloride
NaF	Sodium fluoride

NaHCO$_3$	Sodium bicarbonate
NKCC1	Sodium-Potassium-Chloride Co-transporter
NLGN	Neuroligin
NMDA	N-methyl-D-aspartate
NSF	N-ethylmaleimide-sensitive Factor
PKA	Protein kinase A
PKC	Protein kinase C
PLIC1	Protein Linking IAP with Cytoskeleton 1 (Ubiquilin-1)
PLIC2	Protein Linking IAP with Cytoskeleton 2 (Ubiquilin-2)
PMSF	Phenylmethylsulfonyl fluoride
PP1α	Protein Phosphatase 1α
PRIP	Phospholipase-C-related Catalytically Inactive Protein
PVDF	Polyvinylidene fluoride
SDS	Sodium dodecyl sulfate
SE	*Status epilepticus*
SV2A	Synaptic Vesicle Protein 2A
TE	Tris-EDTA
TLE	Temporal Lobe Epilepsy
TM	Transmembrane Sequence
Tris	2-amino-2-(hydroxymethyl)-1,3-propanediol
TTX	Tetrodotoxin
UPS	Ubiquitin-Proteasome System
vGAT	Vesicular GABA Transporter
Zn^{2+}	Zinc Ion

Keywords

Epilepsy

Status epilepticus

GABA$_A$ Receptor

Gephyrin

Intracellular Calcium

GABA$_A$ Receptor Trafficking

Palavras Chave

Epilepsia

Status epilepticus

Recetor de GABA Tipo A

Gefirina

Cálcio Intracelular

Trafego de Recetores GABA$_A$

Resumo

A epilepsia é uma patologia crónica caracterizada por ataques epiléticos espontâneos. Esta patologia afeta cerca de 65 milhões de pessoas no mundo inteiro, de todas as idades e ambos os géneros. Pensa-se que a génese e/ou propagação dos ataques epiléticos tem origem na hiperexcitabilidade neuronal. No sistema nervoso central, o balanço entre a atividade excitatória e inibitória é maioritariamente mediada pelo glutamato, um neurotransmissor excitatório, e pelo ácido gama-aminobutírico (GABA), um neurotransmissor inibitório. O GABA atua, em parte, através da ativação de recetores de GABA do tipo A (GABA$_A$R), os quais são, na sua grande parte, constituídos por duas subunidades α, duas β e uma subunidade γ2. Os GABA$_A$Rs apresentam uma grande mobilidade na membrana, podendo deslocar-se entre as regiões sinápticas e extra-sinápticas. A acumulação dos GABA$_A$Rs nas sinapses inibitórias é regulada pela proteína *scaffold* gefirina, a qual desempenha um papel importante no controlo da neurotransmissão GABAérgica rápida. A expressão superficial dos recetores GABA$_A$ é também influenciada pela taxa de internalização, a qual ocorre em regiões extra-sinápticas, assim como por mecanismos de regulação intracelular que determinam a taxa de reciclagem.

Ataques epiléticos simples ou recorrentes provocam uma desregulação das sinapses GABAérgicas a diferentes níveis. Porém, os mecanismos moleculares responsáveis por esta desregulação ainda não estão completamente estudados. Resultados obtidos por imunohistoquímica sugerem que o aumento do número de axónios e de terminais GABAérgicos observados na epilepsia do lobo temporal, tanto em humanos como em modelos animais, pode estar relacionado com o *sprouting* de neurónios GABAérgicos. No entanto, a possibilidade deste efeito ser devido a um aumento da produção de GABA ou de marcadores relacionados não foi descartada. Foi também sugerido que alterações na população de GABA$_A$Rs pós-sinápticos podem contribuir para a redução da atividade inibitória do GABA em neurónios principais durante o *status epilepticus* (SE). Efectivamente, no *status epilepticus* foi demonstrada uma perda rápida de GABA$_A$Rs sinápticos que contém subunidades β e γ, enquanto que GABA$_A$Rs extra-sinápticos que contém subunidades α e δ não sofrem alterações. Estas alterações na expressão superficial dos GABA$_A$R estão correlacionadas com o decréscimo nas mIPSCs observadas após a indução de SE. Porém, os mecanismos responsáveis pela alteração na expressão superficial dos GABA$_A$Rs no SE não estão ainda bem esclarecidos. O objetivo principal deste trabalho foi o estudo das alterações pós-sinápticas induzidas pelo SE ao nível das sinapses GABAérgicas. Para este propósito, implementámos um sistema *in vitro* simples que consiste em culturas de neurónios de hipocampo que foram expostos transitoriamente a uma solução desprovida de Mg^{2+} (SE). Observámos que o SE aumenta os níveis de $[Ca^{2+}]_i$ através de um mecanismo dependente da ativação de recetores N-metil-D-aspartato (NMDA). Imagiologia de cálcio em células individuais, usando Fluo-4, permitiu observar diferentes padrões de variação de $[Ca^{2+}]_i$ em função do período de exposição ao SE. Usando o mesmo modelo, verificámos um aumento da internalização de GABA$_A$Rs, acompanhada por um decréscimo da fosforilação da subunidade β3 e uma clivagem da gefirina. Estes resultados indicam que a estabilidade sináptica dos GABA$_A$Rs é comprometida pelo SE, durante e depois da crise. Mostrámos também que o

SE provoca uma redução na taxa de reciclagem dos recetores GABA$_A$R. No conjunto, os nossos resultados demonstram que o SE provoca diversas alterações na sinapse GABAérgica, nomeadamente no tráfego dos recetores e na modulação do seu destino pós-endocitose, acompanhado por uma destabilização da homeostasia do cálcio. Esta dissertação oferece as bases para uma nova linha de investigação tendo por objetivo o estudo dos danos provocados pelo SE em neurónios de hipocampo. Uma melhor compreensão destes mecanismos moleculares pode permitir identificar novos alvos terapêuticos para o tratamento do SE e novas estratégias para prevenir o desenvolvimento de epilepsia crónica.

Abstract

Epilepsy is a chronic condition characterized by recurrent unprovoked seizures. The disease affects approximately 65 million people worldwide, from all ages and both genders. It is thought that neuronal hyper-excitability is one of the main permissive factors for the genesis and/or propagation of epileptic seizures. In the Central Nervous System (CNS) the balance between excitation and inhibition is mostly regulated by the excitatory neurotransmitter glutamate and the inhibitory γ-aminobutyric acid (GABA), respectively. The neurotransmitter GABA acts, in part, through activation of $GABA_A$ receptors ($GABA_AR$), which are mostly composed of 2α-, 2β-, and 1γ2-subunits, and the accumulation of these receptors at inhibitory synapses is regulated by the scaffold protein gephyrin. $GABA_AR$ present a dynamic mobility between synaptic and extrasynaptic localization, and modulation of the interaction between $GABA_AR$ and gephyrin plays an important role in the control of fast GABAergic signalling strength. Total surface expression of $GABA_AR$ is controlled by their internalization at extrasynaptic sites, in addition to post-internalization sorting mechanisms which determine the rate of recycling.

Single and recurrent seizures lead to a dysregulation of GABAergic synapses at different levels, but the mechanisms involved are still not fully understood. Sprouting of GABAergic neurons may account for the observed persistence or increase in labelling of GABAergic axons and terminals in human temporal lobe epilepsy and related animal models. However, the possible contribution from an increased expression of GABA or related markers in other neurons was not ruled out. Alterations in the population of postsynaptic $GABA_AR$ were also suggested to partly contribute to the reduction of GABA-mediated inhibition of principal neurons in *status epilepticus* (SE). SE was shown to trigger a rapid loss of synaptic $GABA_AR$ containing β and γ subunits, while extrasynaptic receptors containing α and δ subunits remain unaffected. These alterations in the surface expression of the receptors directly link the decrease in the miniature inhibitory post-synaptic currents observed after induction of SE with the selective internalization of synaptic $GABA_AR$ containing β and γ subunits. However, the mechanisms underlying the effects of SE on the surface expression of $GABA_AR$ is not fully elucidated. The main objective of this work was to further investigate the SE-induced post-synaptic alterations in GABAergic synapses. For this purpose we implemented a simple in vitro system consisting in cultured hippocampal neurons, which were exposed transiently to a solution lacking Mg^{2+} (*status epilepticus*; SE). We observed that SE increases the $[Ca^{2+}]_i$ by a mechanism dependent on the activation of N-methyl-D-aspartate receptors. However, single cell calcium imaging with Fluo-4 showed different patterns of $[Ca^{2+}]_i$, which were also determined by the duration of the SE period. Using the same experimental approach we found an enhanced internalization of $GABA_ARs$ which was accompanied by a decrease in the phosphorylation of the β3 subunit and a cleavage of gephyrin. Together, these results indicate that $GABA_AR$ synaptic stability is compromised during and after SE, and additional experiments showed a reduction in the rate of receptor recycling in hippocampal neurons subjected to SE. Our results demonstrate that SE evokes short- and long-term alterations in GABAergic synapses, namely in receptor trafficking and in their post-endocytotic sorting, accompanied by a disruption of calcium homeostasis. This work sets the basis

for further studies on the mechanisms underlying the SE-evoked alterations in hippocampal neurons. A better understanding of these mechanisms may provide new targets for the therapy of SE and strategies for preventing the development of chronic epilepsy.

Introduction

1. Introduction

1.1. Epilepsy: definition, classification and features

Epilepsy is a chronic condition characterized by recurrent unprovoked seizures. The disease affects approximately 65 million people worldwide, from all ages and both genders (Banerjee et al., 2009; Jacobs et al., 2009; Reddy and Kuruba, 2013). The first references to epilepsy can be traced to the Assyrian texts and several mentions to the disease are also found in the ancient Greek medical texts of the Hippocratic collection (Magiorkinis et al., 2014). It was only in the beginning of the 18th century when epilepsy started to be considered an idiopathic disease deriving from the brain, since before seizures were associated with demonic possession. The study of epilepsy for the past decades has shed light into its pathophysiology and contributed to the development of therapeutic strategies which improved the patients' quality of life. However, at the present time there is only a partial understanding of this pathology.

Currently, epilepsy is considered a multifactor and symptomatologically highly diversified neurological disorder characterized by recurrent unprovoked seizures. Epilepsy is usually diagnosed after the occurrence of two singular epileptic seizures, unprovoked by any immediate cause (Banerjee et al., 2009; Fisher et al., 2014). The disease can be classified into two types: primary epilepsy, which accounts for 50% of the cases, is idiopathic, and therefore sprouts with no known cause; secondary epilepsy, also referred as acquired epilepsy, which accounts for the other 50%, may result from a variety of conditions including trauma, anoxia, metabolic imbalances, tumours, encephalitis, drug withdrawal seizures, or neurotoxicity (Banerjee et al., 2009; Jacobs et al., 2009; Reddy and Kuruba, 2013; Fisher et al., 2014). There is a plethora of different risk factors that can increase the probability of developing epilepsy, such as cerebrovascular disease, brain tumours, alcohol, traumatic head injuries, malformation during development, genetic inheritance, and infections (Banerjee et al., 2009; Jacobs et al., 2009; Reddy and Kuruba, 2013).

The mechanisms underlying the development of epilepsy or epileptogenesis are poorly understood, but typically involve three stages: the initial insult, a latent period (seizure-free) and the chronic period with spontaneous seizures (chronic stage). The initial insult triggers events, such as inflammation, oxidation, apoptosis, neurogenesis and synaptic plasticity, which eventually lead to rearrangement of synaptic circuitry, neurogenesis and a hyper-excitability state in neurons (Dudek and Staley, 2011; Pitkänen and Lukasiuk, 2011; Reddy and Kuruba, 2013). Furthermore, the initial insult evokes mossy fiber axonal sprouting. This was observed in the dentate gyrus, subiculum and entorhinal cortex of epileptic rats, and in the hippocampal dentate gyrus and CA3 subregions of TLE patients (Curia et al., 2014). Sprouted mossy fibers grow and can establish novel synaptic connections with glutamate receptor 1, calbindin, calretinin and parvalbumin immunopositive neurons (Curia et al., 2014). Taking in account the time-dependent evolution of epilepsy, epileptogenesis can correspond to the period required for the growth

of functionally active sprouted axons. Together, the changes evoked by the initial insult are later manifested as spontaneous recurrent seizures.

Seizures are abnormal electrical discharges in the brain that cause alteration in consciousness, sensation, and behaviour (Reddy and Kuruba, 2013). These discharges are synchronous and sustained within a group of neurons, which contrasts with the normal functioning of the brain where discharges are usually non-synchronous. Seizures initiate differently in the brain and, as such, are classified in a distinct manner. Generalized seizures are characterized by abnormal electrical activity in the whole brain or at least a large portion of it, while in partial seizures there is a localized abnormal electrical activity that can propagate to other areas of the brain, eventually causing a generalized seizures (Duncan et al., 2006; Banerjee et al., 2009; Josephson and Pohlmann-Eden, 2012). Partial seizures account for approximately 60% percent of all adult cases (Engel, 2001).

The most common form of epilepsy is the temporal lobe epilepsy (TLE), that is manifested with partial seizures and accounts for approximately 20% of all patients with epilepsy (Duncan et al., 2006; Reddy and Kuruba, 2013). As the name indicates, TLE is defined as a condition characterized by recurrent, unprovoked epileptic seizures that originate in the temporal lobe of the brain. The classification of the International League Against Epilepsy (ILAE) identifies two main types of temporal lobe epilepsy, the mesial temporal lobe epilepsy, in which the seizures originate either in the hippocampus, the parahippocampal gyrus or the amygdala, and the lateral temporal lobe epilepsy, a rarer type of TLE in which seizures originate in the neocortex at the outer surface of the temporal lobe (Josephson and Pohlmann-Eden, 2012). Depending on the regions affected, seizures can have different physical manifestations (Fig.1.1). In fact, epileptic patients can show, for example, involuntary movements for simple partial seizures, or loss of consciousness for complex partial seizures (Duncan et al., 2006).
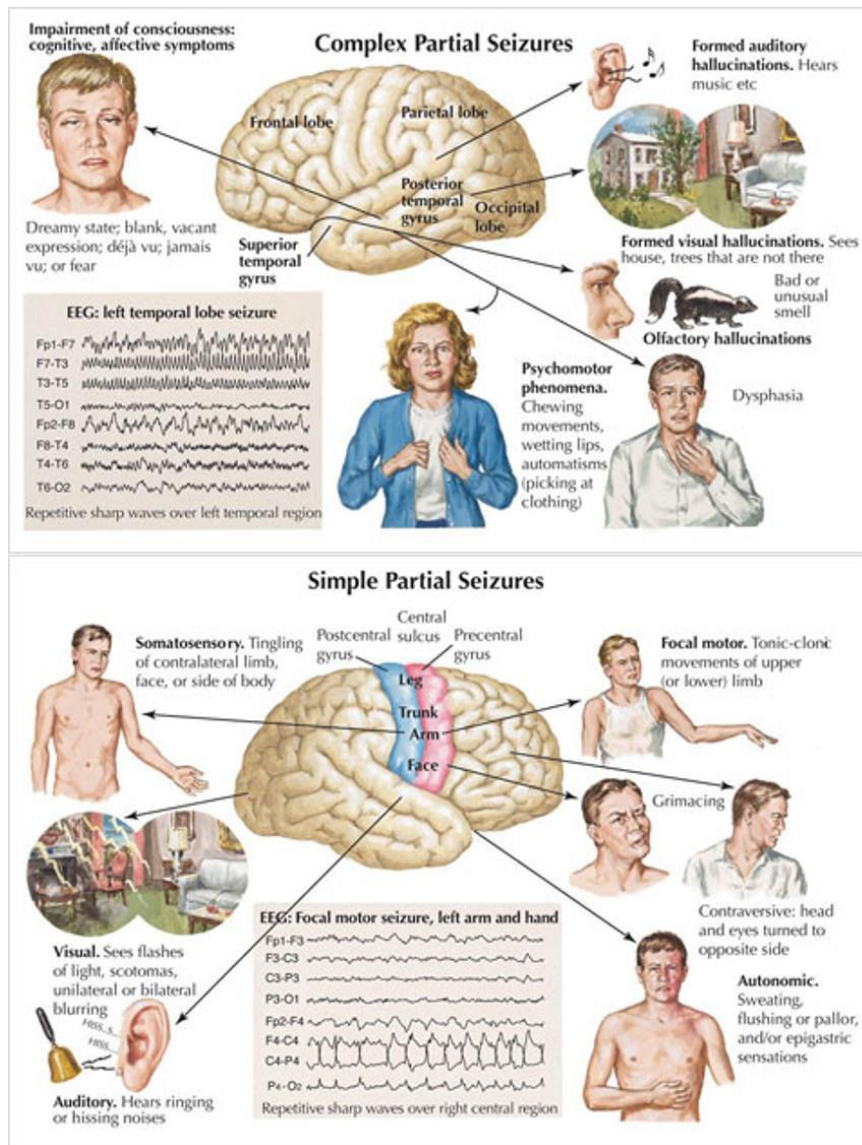
Fig.1.1 – Representation of the different physical manifestations of seizure activity. The manifestation correlates with the area of the brain that is affected. Adapted from (Jones Jr. et al., 2012).

1.2. *Status epilepticus*

Normally seizures are self-limiting and typically after one seizure a complete recovery occurs. Therefore, one seizure is usually not followed by another within a short period of time. A constant seizure activity for the duration of 30 minutes or more is defined as *status epilepticus* (SE), although the classification of *status epilepticus* is currently being revised by the ILAE (Goodkin et al., 2005; Cherian and Thomas, 2009; Reddy and Kuruba, 2013). Observations from experimental models showed that any seizure that persisted for more than 30 minutes results in serious metabolic decompensation and neuronal damage. A spontaneous termination of the seizures becomes progressively less likely the longer the seizure endures, typically after a period of 5 minutes. This suggests that the innate inhibitory mechanisms of the brain are progressively less effective after 5 minutes of SE. Thus, it was proposed

that SE can be defined as a continuous, generalized, convulsive seizure lasting more than 5 minutes, or two or more seizures without recovery of consciousness in between (Lowenstein and Alldredge, 1998). There are several types of SE, which have been generally classified as either generalized or partial seizures by the ILAE; furthermore, they can be convulsive and nonconvulsive (Lowenstein and Alldredge, 1998; Cherian and Thomas, 2009). The pathophysiology of SE is not clearly understood, but it is likely that an ineffective recruitment of inhibitory neurons, together with excessive neuronal excitation, plays a role in the initiation and propagation of the electrical disturbance. It is thought that GABA receptor-mediated inhibition is responsible for the termination of a seizure (Cherian and Thomas, 2009). Several studies have shown that SE becomes progressively more difficult to control as its duration increases (Kapur and Coulter, 1995; Kapur and Macdonald, 1997; Sutula, 2004; Naylor et al., 2005). This may be due to a disruption in the excitatory-inhibitory balance of the brain due to disrupted GABAergic inhibitory receptor-mediated transmission and excessive NMDA excitatory receptor-mediated transmission (Kapur and Lothman, 1989; Kapur et al., 1989; Kapur and Macdonald, 1997; Cherian and Thomas, 2009). In some cases, SE patients are unable of responding to pharmacological treatment and very severe case is classified as refractory SE.

Antiepileptic drugs (AEDs) act on diverse molecular targets to selectively modify the excitability of neurons. Conventional AEDs act by blocking sodium channels or enhancing the function of GABA as a neurotransmitter. Traditionally, the strategies employed to potentiate GABAergic synaptic transmission are based on the upregulation of neurotransmitter release or on the modification of GABA receptor expression and/or activity. Moreover, same AEDs act via inhibition of the glutamatergic synapse (Fig.1.2) (Kobow et al., 2012; Reddy and Kuruba, 2013; Schousboe et al., 2014). Despite the advances made in epilepsy research, nearly 30% of the patients do not respond to pharmacological treatment (Duncan et al., 2006; Banerjee et al., 2009; Reddy and Kuruba, 2013). These observations indicate that further studies are needed in order to unravel the pathophysiological mechanisms of SE and to provide better options for the afflicted people.
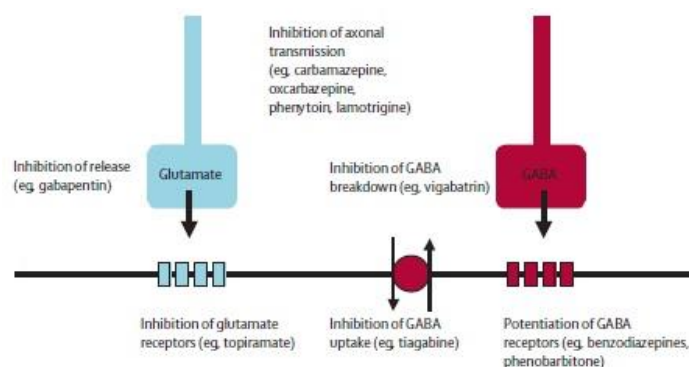
Fig.1.2. – AEDs and their molecular targets for management of seizure activity. Adapted from (Duncan et al., 2006)

1.2.1. Experimental models of epilepsy

Human epilepsies display a wide range of symptoms from clinical, behavioural and electrical point of view. Not surprisingly, a corresponding large number of animal models and *in vitro* models have been used to study this disease.

Over the years, various experimental models have been developed that mimic diverse *status epilepticus* phenotypes, which can be used to study different aspects of the pathology. SE is the most widely used approach for inducing chronic epilepsy, especially TLE. The *in vivo* and *in vitro* epilepsy models available, commonly use chemical or direct electrical stimulation, as described in **Table 1.1**. Typically, these models are characterized by an unbalance in the excitatory/inhibitory equilibrium, by either enhancing neuronal activity or by decreasing neuronal inhibition (Stables et al., 2002; Reddy and Kuruba, 2013). In addition to the models described in Table 1.1, other models are available that recapitulate genetic alterations that define certain forms of epilepsy (Kandratavicius et al., 2014) which lead to recurrent and self-sustained alterations in brain function characterized by excessive discharges of cerebral neurons.

Table 1.1. Classification of the different models of SE. Adapted from (Reddy and Kuruba, 2013)

	Classification	Model
In vivo Models	Electrical Models	Preforant pathway stimulation
		Self-sustaining stimulation
	Chemical Models	Kainic acid
		Pilocarpine
		Lithium-pilocarpine
		Organophosphates
		Flurothyl
		Cobalt-homocysteine thiolactone
	Thermal Models	Hyperthermia or Febrile Seizures
	Refractory Models	Lithium-Pilocarpine
		Kainic Acid
		Diisopropylphosphorofluoridate (DFP)
	***In vitro* Models**	Low Magnesium
		High Potassium
		4-Aminopyridine

Animal models are extremely helpful for the development and validation of anti-epileptic drugs. One of the most common SE animal models is the pharmacological model of pilocarpine. It is one of best established animal models for SE and shares many of the characteristics of human TLE (Curia et al., 2008; Löscher, 2011; Reddy and Kuruba, 2013). Pilocarpine is a muscarinic cholinergic agonist and when administered, it induces robust seizures through cholinergic hyper-activation. There is a sequence of behavioural alterations that after a 1 to 2 hour period progressively develop into limbic SE. EEG activity first appears in the ventral forebrain followed by hippocampus, then the amygdala and neocortex (Reddy and Kuruba, 2013). Within 24 h of pilocarpine injection, the seizures subside and the EEG returns to normal activity (Turski et al., 1983; Curia et al., 2008). Due to the characteristics of this model, it is suited for the study of the generation and spread of seizure activity in the hippocampus and therefore it is extremely useful when studying TLE. Studies suggest that pilocarpine induces SE by cholinergic hyper-activation, but the continuation of seizure activity is likely through a glutamatergic mechanism as neuronal death and spontaneous seizure activity occurs secondary to seizure-induced glutamate release (Curia et al., 2008).

In vitro models of epilepsy are normally performed in cultures of dissociated neurons and organotypic hippocampal slice cultures. These are simple model systems to analyse and more appropriate for studying cellular and molecular mechanisms. Incubation of neurons in a solution lacking Mg^{2+} ($[Mg^{2+}]_0$) is a commonly used *in vitro* model of epileptiform activity, working through the activation of NMDA receptors due to the removal of the Mg^{2+} blockade of NMDA receptor channels (Fueta et al., 2005; Reddy and Kuruba, 2013). In this model the epileptiform activity is progressive and leads to the development of resistance to benzodiazepines after prolonged periods of stimulation. It progresses through two stages: i) the initial response profile is characterized by seizure-like events that are sensitive to benzodiazepines (this profile continues between 10 and 45 minutes of stimulation); ii) the second period, when neuronal activity abruptly changes to late recurrent discharges that are insensitive to benzodiazepines (Kapur and Macdonald, 1997; Naylor et al., 2005). This model is also characterized by synchronized activity, as tested using hippocampal slices (Zhang et al., 1995; Reddy and Kuruba, 2013). Due to the characteristics of this model, it is typically used to determine the mechanisms of epileptiform and antieplileptiform activities. In particular, this model is particularly suited to study the molecular mechanisms mediated by impairment in the inhibitory signalling and the development of pharmacoresistance.

1.3. Molecular mechanisms of epilepsy

Epilepsy is considered a spectrum disorder with a range of etiologies and comorbidities. Epileptiform activity arises from a multitude of different factors that evoke an imbalance between excitation and inhibition in the brain. Due to the complex nature of epilepsy, and the wide variety of etiologies of the disease, the mechanism for development of this condition remains elusive. However, recent efforts in epilepsy research have shown that hyperactivity of excitatory amino acid systems, insufficient $GABA_A$ receptor-mediated neurotransmission, disturbances in neuronal membranes properties and ionic

dysregulation are paramount for the development of the epileptiform activity (Pitkänen and Lukasiuk, 2011; Reddy and Kuruba, 2013; Staley, 2015),. Together, this evidence indicates that epileptiform activity is tightly related to alterations in synaptic transmission. Therefore, in this section we will describe the molecular alterations at the pre- and postsynaptic levels and the dysregulation of ionic homeostasis in epilepsy.

Dysregulation of ionic concentrations in the intra- and extracellular compartments is a prominent mechanism underlying epileptiform activity. Proteins involved in ionic homeostasis are largely distributed in the brain, including transmembrane channels and transporters associated with the plasma membrane and intracellular organelles (Staley, 2015). The disturbed function of the ligand and voltage-dependent sodium, potassium, chloride and calcium channels, possibly caused by changes in expression, polymorphisms, or mutations can contribute to epileptiform activity (Staley, 2015). Considering these alterations in the ion transport systems that have been identified in epilepsy, it is not surprising that ion concentrations in the intra- and extracellular compartments have also been shown to be dysregulated. Furthermore, seizure activity has been shown to disrupt Na^+/K^+ ATPase activity as the excessive K^+ efflux induced by seizure activity overwhelms the capacity of this protein to maintain the cation gradients. This induces a shift in the resting membrane potential of neurons and co-transport of other ions is compromised (Ransom et al., 2000).

Calcium homeostasis has also been shown to be dysregulated in the epileptic brain. Calcium is paramount to life as it is a signalling ion to most of its essential processes. The processing of Ca^{2+} signalling is done by sensor proteins which have the capacity to specifically bind to the cation, resulting in a conformational change of the sensor protein (Ross, 2012). Ca^{2+} signalling is particularly important to neurons as it is a major regulator of synaptic transmission. Furthermore, calcium signalling regulates a multitude of neuronal processes such as the release of neurotransmitters, the process of learning and the formation and consolidation of memory, the regulation of specific gene pools, the long-term potentiation or depression of synaptic transmission, the direct coupling between the depolarization of the plasma membrane and the increase of intracellular Ca^{2+} (Brini et al., 2014). The correct functioning of these processes plays a key role in the maintenance of neuronal life and, therefore, neurons depend on the precise temporal and spatial regulation of Ca^{2+} signals.

Calcium dynamics have been shown to be affected in epilepsy. Studies have shown that large influxes of Ca^{2+} through voltage- and ligand-gated calcium channels disrupt the intracellular calcium homeostasis, thereby altering neurotransmitter release (Staley, 2015). Furthermore, due to its many roles as a second messenger, the excessive intracellular concentration Ca^{2+} evoked by seizure activity can have severe effects on gene expression, thereby inducing long-term effects in neuronal physiology. Calpains, a calcium-dependent protease, can also be activated by the influx of Ca^{2+} rending several molecular targets susceptible to cleavage (Dong et al., 2009). In addition, further increase in the intracellular Ca^{2+} concentration can induce excitotoxicity, where the levels of intracellular calcium exceed the capacity of Ca^{2+} regulatory mechanisms and can lead to metabolic derangements such as the formation of free radicals and cell death (Sattler and Tymianski, 2001). The role of calcium in

epileptogenesis still remains elusive and further study is needed given the plethora of neuronal processes that this ion modulates.

Chloride fluxes have also been shown to be dysregulated in epilepsy. The early extensive activation of GABAergic synaptic activity causes a shift in the $GABA_A$ reversal potential, consequently disrupting inhibition. In normal physiological conditions, the GABA receptor is permeable to both chloride and bicarbonate, being chloride the dominant charge carrier (Staley, 2015). The excessive chloride influx evoked through sustained activity of the GABAergic synapse overloads the neuronal K-Cl co-transporter KCC2 and the neuronal Na-K-2Cl co-transporter isoform 1, NKCC1, which maintain chloride homeostasis (Kaila et al., 2014). Under these conditions bicarbonate becomes the driving force for net ion movement through the $GABA_A R$. The continuous cycle of bicarbonate-carbon dioxide causes bicarbonate to symmetrically distribute on both sides of the membrane causing the bicarbonate driving force to end. This leads to a chloride efflux, shifting the role of the GABAergic synapse from an inhibitory to an excitatory depolarizing profile. This is maintained as long as the co-transporter capacity is overloaded (Staley and Proctor, 1999; Kahle et al., 2008; Lillis et al., 2012). Mutations in the KCC2 and NKCC1 co-transporters have also been shown to be associated with epilepsy, making this mechanism a possible explanation for the excessive neuronal activity and the loss of GABA-mediated inhibition (Kaila et al., 2014).
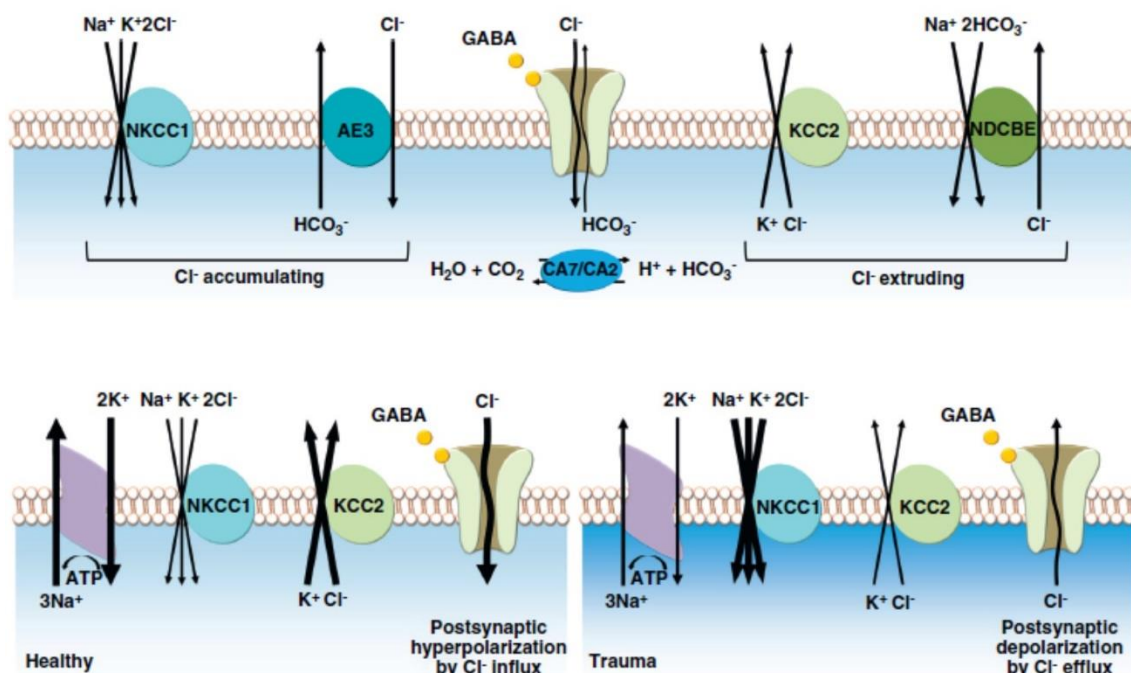

Fig.1.3 – Altered neuronal ion regulation causes a shift in the function of $GABA_A Rs$. Adapted from (Kaila et al., 2014).

Mutations in pre- and postsynaptic proteins were also associated with epilepsy supporting the idea that epileptiform activity is tightly related to abnormal synaptic transmission. Short-term synaptic plasticity in the presynaptic membrane has also been shown to be altered in epilepsy (Staley, 2015). Studies have shown that depression of inhibitory GABAergic synapses onto principal neurons or depression of glutamatergic depression onto inhibitory neurons are possible mechanisms of triggering seizures (Bracci et al., 2001; Le Duigou et al., 2011). Furthermore, neurotransmitter vesicle fusion has been shown to be impaired in epilepsy. The fusion of these vesicles with the presynaptic membrane is dependent on the coordinated activity of several proteins that facilitate docking, priming, fusion of the vesicles and proteins that regulate calcium transport and sensing. Mutation of several of these proteins are associated with epilepsy (Rajakulendran et al., 2012; Lazarevic et al., 2013; Kaeser and Regehr, 2014; Staley, 2015). Despite this evidences suggesting that disrupted short-term synaptic plasticity could trigger seizures it has yet to be demonstrated.

Finally, alterations in long-term synaptic plasticity in the postsynaptic membrane are also likely to trigger seizure events. Mutations in proteins that facilitate neurotransmitter reuptake, receptor desensitization, receptor trafficking and post-translational modifications of receptor subunits affecting transmitter affinity and channel gating have been associated with epilepsy (Staley, 2015). Studies have shown that mutations in the gene encoding for stargazin, a protein associated with regulation of trafficking of AMPA receptors, evoke an epileptic phenotype (Kennard et al., 2011) Furthermore, alteration of the trafficking of NMDA and $GABA_A$ receptors have been shown to be extend epileptiform activity (Naylor et al., 2013). In particular, $GABA_AR$ trafficking has been shown to play an important role in the development of epilepsy and will be further discussed in chapter 1.4.7.

1.4. The GABAergic synapse

In the Central Nervous System (CNS), inhibitory transmission is predominantly mediated by the γ-aminobutyric acid (GABA) (Rudolph and Möhler, 2004). GABA is produced from glutamate by the cytosolic enzyme glutamic acid decarboxylase (GAD) and is stored inside small synaptic vesicles before being exocytosed into synaptic cleft (Roth and Draguhn, 2012). This neurotransmitter exerts its action by activating two classes of receptors with distinct electrophysiological and pharmacological properties: type A GABA receptors ($GABA_AR$) and type B GABA receptors ($GABA_BR$) (Rudolph and Möhler, 2004; Jacob et al., 2008). $GABA_AR$ are ionotropic fast-acting ligand-gated chloride channels (Sieghart 2006) while $GABA_BR$ are metabotropic G protein-coupled receptors (Bettler and Tiao 2006) (Figure 1.4). Activation of $GABA_AR$ leads to the entrance of chloride into the cell according to the concentration gradient, causing membrane hyperpolarization. $GABA_BR$ are responsible for the late and slower component of inhibitory synaptic transmission (Bettler and Tiao 2006).

Previous studies have shown that deficits in the functional expression of $GABA_ARs$ are critical in epilepsy. Furthermore, $GABA_ARs$ are also relevant drug targets for anti-convulsant agents used to manage epilepsy. Therefore, the structure, intracellular traffic and regulation of surface distribution of $GABA_ARs$ will be discussed in the next sections.

1.4.1. Structure of the GABA$_A$Rs

GABA$_A$Rs are part of a Cys loop-type ligand-gated ion channel superfamily which also includes other receptors such as the nicotinic acetylcholine receptors (Corringer et al., 2000), the glycine receptors (Breitinger and Becker, 2002) the 5-hydroxytryptamine 3 receptors (Thompson and Lummis, 2006) and the Zn^{2+}-activated ion channels (Davies et al., 2003). The complexity of GABA$_A$Rs is related with the diversity of subunits that may oligomerize to form these receptors. In humans, there are six types of α subunits, three types of β subunits, three types of γ subunits, three types of ρ subunits, and one type of each of the θ, δ, ϵ, and π subunits, excluding point mutations and splice variants (Sigel and Steinmann, 2012). Each GABA$_A$ receptor is a heteropentameric channel composed by a combination of five subunits. Despite this amazing variability, most GABA$_A$Rs in adult cells are composed of two α subunits, two β subunits and one γ or one δ subunit (Fig 1.4.b) (Rudolph and Möhler, 2004) (Fig.1.4).

One GABA$_A$ receptor subunit is formed by about 450 amino acid residues and shares a common topological organization. The subunits consist of a hydrophilic extracellular N-terminal domain containing the characteristic Cys loop, followed by four transmembrane sequences (TM1−TM4). TM2 lines the ion channel and between TM3 and TM4 there is a large intracellular loop containing phosphorylation sites involved in the modulation of the surface expression of the receptor (Sigel and Steinmann, 2012). The intracellular loop, between TM3 and TM4 of specific GABA$_A$ receptor subunits, also interacts with several proteins and regulates the receptor trafficking and its anchoring at the postsynaptic membrane (Jacob et al., 2008). Both the N- and C-termini of the subunits are placed in the extracellular compartment (Fig.1.4.a).

The subunit composition of GABA$_A$R dictates several aspects of its functionality in the brain. This variation translates in different physiological and pharmacological properties, differential expression throughout the brain and targeting to different subcellular regions (Rudolph and Möhler, 2004; Jacob et al., 2008; Miller and Aricescu, 2014). Previous studies have shown that receptors composed of α1, α2, α3 or α5 subunits, together with β and γ subunits, are sensitive to benzodiazepines and are mostly located at the synapse where they mediate most phasic inhibition in the brain (Rudolph and Möhler, 2004). By contrast, those composed of α4 or α6 subunits, together with β and δ subunits, make up a specialized population of, almost entirely, extrasynaptic receptor subtypes that mediate tonic inhibition. Characteristically, receptors belonging to the latter group are insensitive to benzodiazepine modulation (Fig.1.4.c) (Brünig et al., 2002).
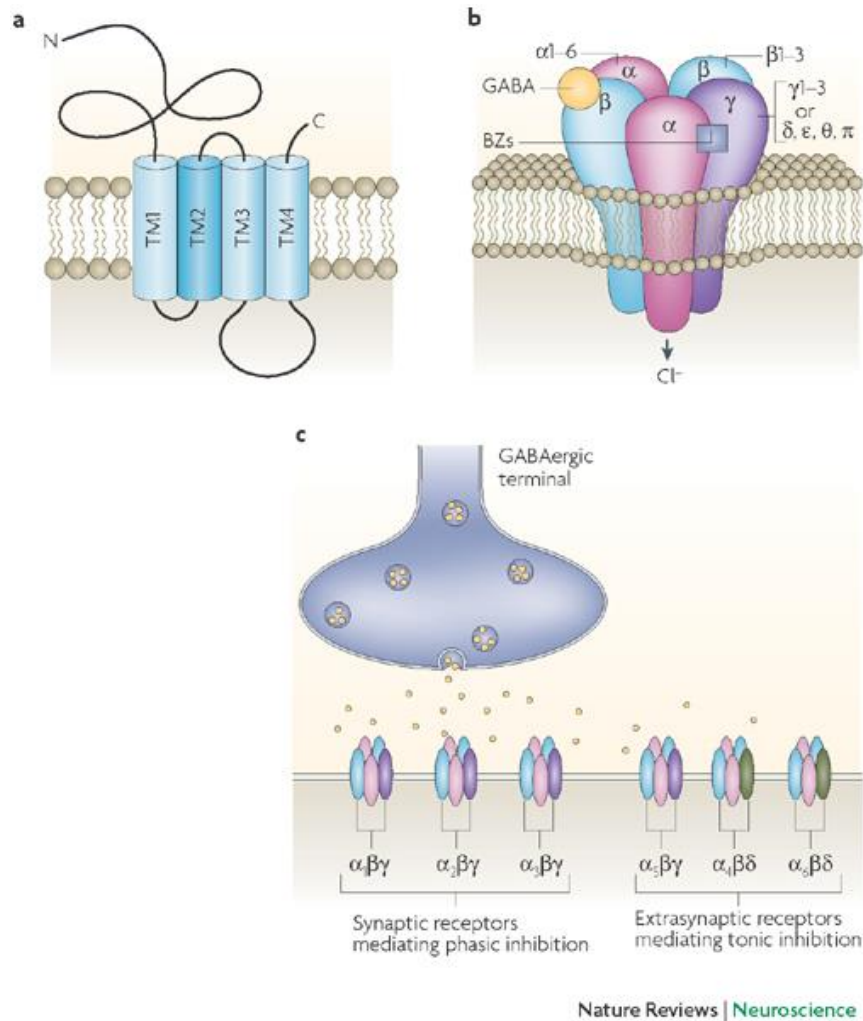
Fig.1.4 – Structure and the subunit composition of the synaptic and extrasynaptic populations of GABA$_A$Rs. Adapted from (Jacob et al., 2008).

1.4.2. GABA$_A$R assembly

Assembly of GABA$_A$Rs from their component subunits occurs in the endoplasmic reticulum (ER). In order to leave the ER, proteins have to reach their appropriate conformation and misfolded proteins are retro-translocated from the ER for degradation in the proteasome (Jacob et al., 2008). The expression and assembly of these subunits is carefully regulated in the ER by mechanisms that involve classical ER-resident chaperones, such as heavy-chain binding protein and calnexin (Connolly et al., 1996). The oligomerization of individual GABA$_A$R subunits into heteromers occurs within 5 minutes of translation. Sequences in the N-terminus of GABA$_A$R subunits control receptor oligomerization and promote the assembly of particular subunit combinations (Kittler et al., 2002). Furthermore, the ER is responsible for the retention and degradation of misfolded or unassembled subunits. Previous studies have shown that homomeric unassembled GABA$_A$R subunits are degraded in this organelle (Bedford et al., 2001). These proteins are degraded by the ER-associated degradation system, which involves protein ubiquitylation and degradation by the ubiquitin–proteasome system (Yi and Ehlers, 2007). This system

is dependent on neuronal activity, since GABA$_A$R subunits were shown to be ubiquitylated in an activity-dependent manner. Thus, blockage of neuronal activity dramatically increases the levels of GABA$_A$R ubiquitylation in the ER and, in contrast, increasing neuronal activity resulted in decreased levels of GABA$_A$R ubiquitylation (Saliba et al., 2007). Therefore, neuronal activity can regulate the ubiquitylation of GABA$_A$Rs in the ER, actively regulating the rate of their degradation by the UPS. It is possible that this is a mechanism that neurons use to homeostatically regulate synaptic inhibition. Ubiquitylated GABA$_A$Rs are also likely to be modulated by their association with the ubiquitin-like proteins PLIC1 and PLIC2. These proteins have been demonstrated to inhibit the degradation of ubiquitylated substrates. PLIC1 binds to the GABA$_A$R subunits through its ubiquitin-associated domain and, as a result, it increases the half-life of GABA$_A$Rs with a consequent upregulation in the availability of receptors for insertion into the membrane (Bedford et al., 2001).

1.4.3. GABA$_A$R trafficking

Once the receptors are correctly assembled in the ER, GABA$_A$Rs are trafficked to the Golgi apparatus and segregated into vesicles for transport to the plasma membrane where they are inserted. These processes are facilitated by a number of GABA$_A$R molecular interactors (Comenencia-Ortiz et al., 2014) (Fig. 1.5). After translocation to the Golgi apparatus, GABA$_A$Rs interact with the GABA$_A$ receptor-associated protein (GABARAP) which binds to the γ2 subunit of the receptor (Wang et al., 1999). N-ethylmaleimide-sensitive factor (NSF) and brefeldin-A-inhibited GDP/GTP exchange factor 2 (BIG2) are also localized to the Golgi network, where they bind to the β subunits of GABA$_A$Rs and modulate GABA$_A$R trafficking (Charych et al., 2004; Goto et al., 2005). NSF is also capable of binding to GABARAP and it was suggested that NSF and GABARAP might act together to promote the forward trafficking of GABA$_A$Rs from the Golgi apparatus (Chen et al., 2007). Another player in the intracellular traffic of GABA$_A$R are the phospholipase-C-related catalytically inactive proteins (PRIPs), which are inositol-1,4,5-trisphosphate binding proteins. It was suggested that PRIPs act as bridging proteins between GABARAP and GABA$_A$Rs, facilitating the transport of γ2-containing receptors (Kanematsu et al., 2002). In addition, PRIPs might also regulate GABA$_A$R function by controlling their phosphorylation. Accordingly, PRIPs inactivate protein phosphatase 1α (PP1α) terminating the phosphorylation-dependent receptor modulation (Terunuma et al., 2004; Mizokami et al., 2007). Furthermore, palmitoylation of γ subunits occurs in the Golgi apparatus via interaction with the Golgi-specific DHHC zinc-finger-domain protein (GODZ). This interaction is involved in the delivery of GABA$_A$Rs to the plasma membrane and in the accumulation of γ2-containing GABA$_A$Rs at synapses for synaptic inhibitory function (Keller et al., 2004; Fang et al., 2006). Finally, GABA$_A$R-interacting factor proteins (GRIFs) interact with the β$_2$ subunit of GABA$_A$Rs and with the microtubule-associated motor protein kinesin, suggesting that these proteins regulate the motor-dependent transport of GABA$_A$Rs (Brickley et al., 2005; Smith et al., 2006). Trafficking of GABA$_A$Rs is extremely complex and we still hold a poor understanding of the whole process.
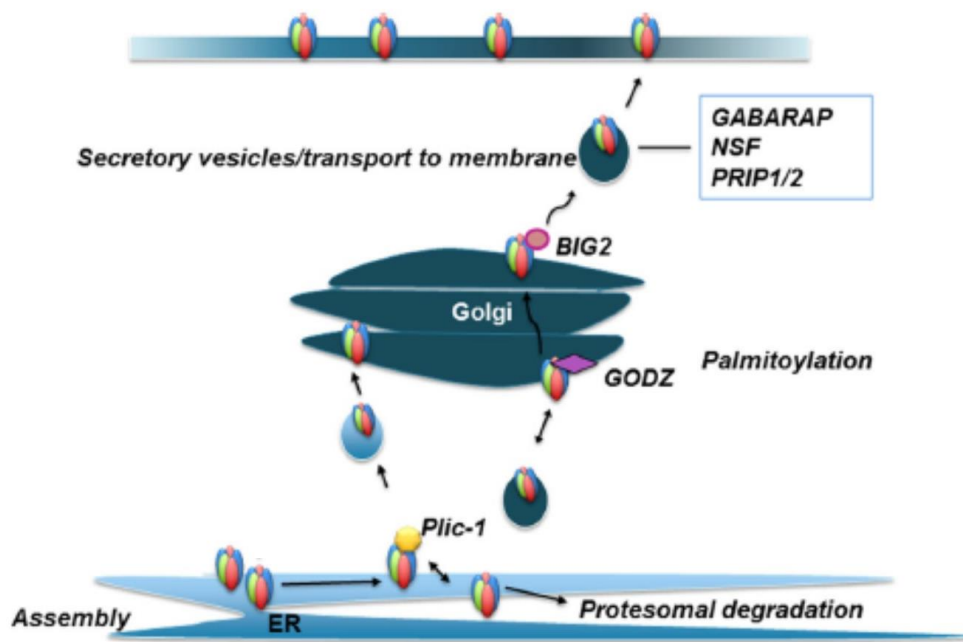
Fig.1.5 - GABA$_A$R trafficking and the molecular interactors of the process. Adapted from (Comenencia-Ortiz et al., 2014).

1.4.4. Synaptic GABA$_A$Rs clustering

1.4.4.1. Gephyrin-depedent clustering of GABA$_A$Rs

After crossing the secretory pathway, GABA$_A$Rs are inserted into the neuronal plasma membrane where they can access either inhibitory postsynapses or extrasynaptic sites, depending on their subunit composition. The fate of GABA$_A$Rs localization in the membrane is facilitated by several mechanisms and is an extremely dynamic process (Fig. 1.6). On the neuronal surface, GABA$_A$Rs exist as either diffuse or clustered populations, being the latter either synaptic or extrasynaptic. The GABA$_A$Rs populations continuously interchange between the different pools through lateral diffusion (Jacob et al., 2005). It was shown that most GABA$_A$Rs are initially inserted at extrasynaptic locations in the membrane. Once there, the receptors migrate to the synaptic sites through lateral diffusion, increasing the population of synaptic receptors over time (Bogdanov et al., 2006). GABA$_A$Rs retain distinct cell surface expression, dependent on their subunit composition. For example, most γ2-containing GABA$_A$Rs have been shown to cluster at the synaptic site, while α5 and δ-containing receptor clusters follow the same pattern and are predominantly extrasynaptic (Jacob et al., 2008).

Gephyrin is a multifunctional protein that has been strongly implicated in the regulation of GABA$_A$Rs clustering at inhibitory synapses. This protein is constituted by three structural domains, G, C and E, and is the principal scaffolding protein in the inhibitory postsynaptic density. The C domain links the G and E domains and is home to numerous sites for post-translational modification and interaction with proteins involved in synapse formation and function (Tyagarajan and Fritschy, 2014). The E domain

possesses a non-conserved surface-exposed loop, which regulates its postsynaptic clustering in an all-or-none fashion. Furthermore, gephyrin undergoes extensive alternative gene splicing and protein post-translational modifications, suggesting that cell and tissue-specific mechanisms regulate its role as the major postsynaptic scaffolding molecule at inhibitory synapses (Saiyed et al., 2007; Tyagarajan and Fritschy, 2014).

Interaction of GABA$_A$Rs with gephyrin modulates their location on the plasma membrane. It was shown that only a subset of GABA$_A$R subtypes containing the α1, α2 or α3-subunit, along with the γ2-subunit, localize postsynaptically with gephyrin (Lardi-Studler et al., 2007). Accordingly, the α1–α3-subunits interact with gephyrin even if with a low binding affinity (Kowalczyk et al., 2013). Inversely, receptors containing the α4, α5 and δ-subunits, which mainly form extrasynaptic GABA$_A$Rs, do not colocalize with gephyrin (Brünig et al., 2002). Gephyrin interacts with other proteins that modulate its role as the major scaffolding protein of the inhibitory synapse. The interaction between gephyrin, neuroligin 2 and collybistin, is of particular importance. Neuroligins (NLGNs) are adhesion molecules that have fundamental roles in the regulation of synapse formation and function (Tyagarajan and Fritschy, 2014). Along with their trans-synaptic partners, the neurexins, they might trigger or facilitate the formation of synapses (Scheiffele et al., 2000; Graf et al., 2004). Of the four NLGNs, NLGN2 is selectively associated with GABAergic synapses (Varoqueaux et al., 2004). Furthermore, among the synaptic adhesion molecules implicated in GABAergic synapse formation, NLGN2 is the only one that is known to interact with gephyrin at GABAergic synapses. It was suggested that NLGN2 drives the formation of gephyrin and GABA$_A$R clusters at nascent postsynaptic GABAergic sites (Poulopoulos et al., 2009).

Collybistin is a neuron-specific guanine nucleotide exchange factor (GEF) belonging to the Dbl family. It is characterized by three functional domains, an amino-terminal type 3 SRC homology (SH3) domain, a catalytic Dbl homology (DH) domain and a pleckstrin homology (PH) domain. The tandem Dbl-homology and pleckstrin-homology domains shared by all members of this family represent the structural module responsible for catalyzing the GDP–GTP exchange reaction of Rho proteins and activate small GTPases of the RHO family (Zheng, 2001). Collybistin directly binds to gephyrin, and its binding site overlaps with those of the GABA$_A$R α2- and α3-subunits. On the other hand, gephyrin binds to collybistin's DH domain and may potentially interfere with its ability to activate CDC42 (Xiang et al., 2006). Fundamental insight into the role of collybistin in gephyrin clustering was provided by studies done in collybistin-null mice. Analyses of their GABAergic system showed cell and synapse-specific alterations. Furthermore, clustering of both gephyrin and GABA$_A$Rs was impaired in hippocampal and cortical pyramidal cells. Interestingly, the same alterations could be induced by conditional inactivation of the collybistin coding gene *Arhgef9* after the period of synaptogenesis, implying that collybistin is also required for GABAergic synapse maintenance (Papadopoulos et al., 2007, 2008).

Gephyrin also depends on both actin microfilaments and microtubules for synaptic targeting and a successful scaffold formation (Kirsch and Betz, 1995; Maas et al., 2006; Papadopoulos et al., 2008). In

addition, the actin-binding proteins profilin and Mena (mammalian enabled)/VASP (vasodilator stimulated phosphoprotein), and the dynein light chains 1 and 2 (Papadopoulos et al., 2008), interact with gephyrin allowing for local lateral movements and removal or addition by microtubule-dependent trafficking. Together, these multiple interactions contribute with additional mechanisms to the regulation of GABAergic synaptic transmission (Tyagarajan and Fritschy, 2014).
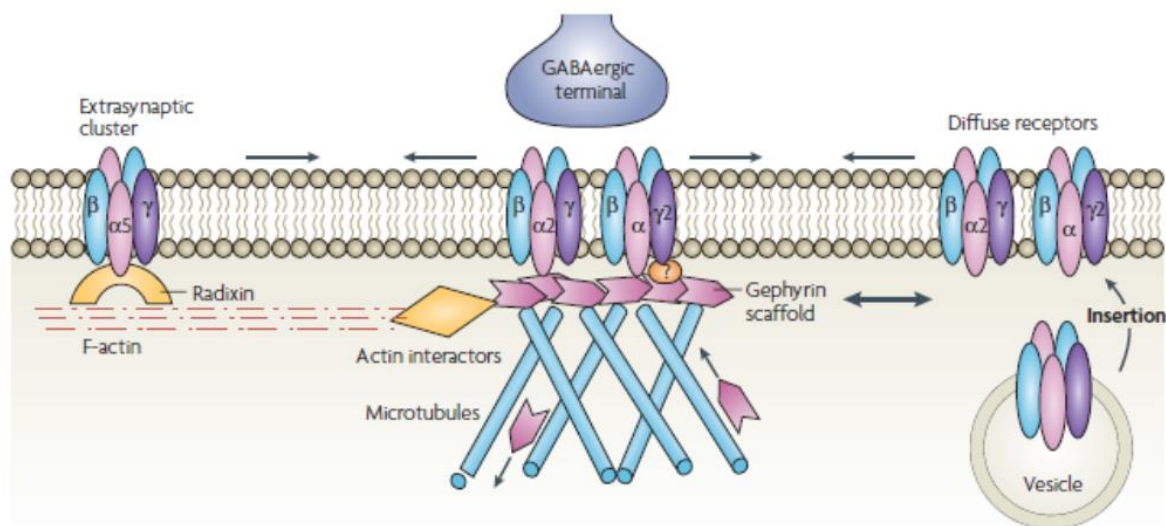
Fig.1.6 - GABA$_A$R synaptic clustering and the dynamic regulation of the receptor at the GABAergic synapse. Adapted from (Jacob et al., 2008).

1.4.4.2. Gephyrin-independent clustering of GABA$_A$Rs

Studies performed in gephyrin-knockout mice showed that despite the lack of gephyrin there were clusteres of GABA$_A$Rs and mIPSCs, suggesting that gephyrin-independent GABA$_A$R clustering mechanisms exist (Kneussel et al., 2001). Radixin, an ERM family protein (ezrin, radixin, moesin), was identified as a specific interactor for the intracellular domain of the α5 subunit of GABA$_A$Rs. Evidence show that depletion of radixin dramatically decreases α5-containing-GABA$_A$R clustering, albeit total cell-surface levels of the α5 subunit remain unchanged (Loebrich et al., 2006). Furthermore, radixin seems to directly establish a link between the α5 subunit and the actin cytoskeleton, as it binds both the α5 subunit and F-actin. The apparent radixin binding domain in the α5 subunit is a highly conserved region that is also found in α1−3 subunits, differing in only the last two amino acids in the α2 subunit. Further work is needed to elucidate the mechanism of radixin-dependent GABA$_A$R anchoring (Jacob et al., 2008).

1.4.5. GABA$_A$R endocytosis

GABA$_A$R surface expression is very dynamic and regulated. When localized in the extrasynaptic compartment the receptors can be removed from the plasma membrane by clathrin- and dynamin-dependent endocytosis (Fig. 1.7) (Kittler et al., 2000). This process is regulated by interactions of the GABA$_A$R β and γ subunits intracellular domains with the clathrin adaptor protein AP2 (Kittler et al. 2000; Kittler et al. 2005; Kittler et al. 2008). AP2 is composed of four distinct subunits, α, β2, μ2 and σ2. It was shown that the μ2 subunit of the AP2 complex directly binds to the β1–3 and γ 2 GABA$_A$R subunits (Kittler et al., 2000). In addition, an AP2 binding motif was identified in the intracellular domains of GABA$_A$R β subunits, which is located in the same region containing the major sites of phosphorylation for PKA and PKC. Phosphorylation of these sites reduces binding to the μ2 subunit of AP2. and a mimetic peptide simulating the β3 subunit motif that binds to AP2 upon dephosphorylation enhanced mIPSC amplitude and whole-cell GABA$_A$R currents (Kittler et al., 2005). Other studies were conducted showing a homologous mechanism with other GABA$_A$Rs subunits. Thus, these evidence indicate that phosphorylation of GABA$_A$R subunits at AP2 binding sites can negatively regulate the cell-surface stability of GABA$_A$Rs and the strength of synaptic inhibition (Kittler et al., 2005, 2008; Terunuma et al., 2008). Moreover, the regulation of protein kinase and phosphatase activity may influence the efficacy of synaptic inhibition by controlling the stoichiometry of GABA$_A$R phosphorylation and, thus, GABA$_A$R endocytosis (Jacob et al., 2008).

1.4.6. GABA$_A$R post-endocytic sorting

After endocytosis, most of the internalized GABA$_A$Rs recycle back to the membrane over short periods of time; however, over longer time periods they are targeted for lysosomal degradation. The fate of internalized GABA$_A$Rs is one more mechanism that control cell-surface receptor levels and thus synaptic inhibition efficacy (Fig.1.7) (Kittler et al., 2004). One protein that plays an important role in this cellular mechanism is the Huntingtin-associated protein 1 (HAP1) (Li et al., 1995). HAP1 is a GABA$_A$R-associated protein that binds to the intracellular loop of β subunits (Kittler et al., 2004). It is constituted of several central coil-coiled domains that are likely to regulate protein–protein interactions. Studies regarding the effects of HAP1 showed that overexpression of HAP1 in neurons inhibits GABA$_A$R degradation and increases receptor recycling. In addition, HAP1 overexpression increases the surface levels of GABA$_A$Rs accompanied by an increase in mIPSC amplitude. This indicates that the increase in surface receptor levels have a dramatic functional effect (Kittler et al., 2004). Despite our current knowledge of this process, the mechanism that underlies post-endocytic GABA$_A$R sorting remains unknown, and the specific role of HAP1 in this process is also an area of active research.
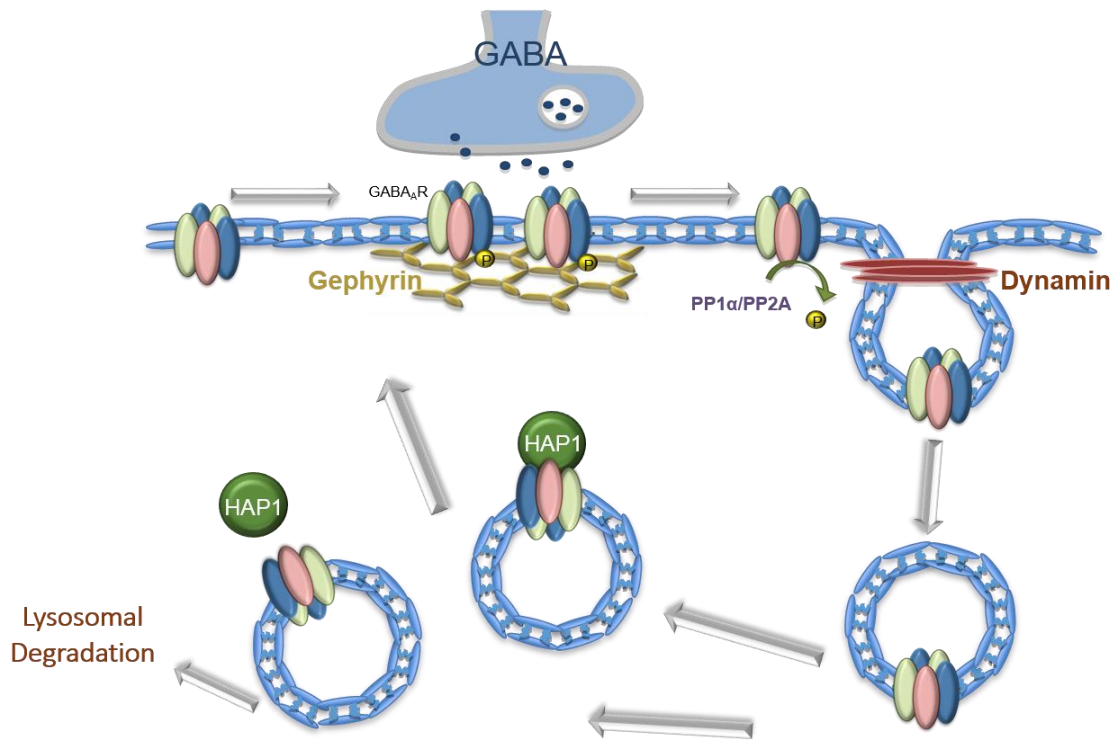
Fig.1.7 – GABA$_A$R endocytosis and post-endocytic sorting. Adapted from (Mele et al., 2014).

1.4.7. GABAergic synapse alterations in epilepsy

Inhibitory neurotransmission in the Central Nervous System (CNS) is largely mediated by γ-aminobutyric acid (GABA) and plays an essential role in maintaining the excitatory/inhibitory balance required for correct brain function. Deficits in the functional expression of GABA$_A$Rs have been implicated in the pathogenesis of several neurological and psychiatric diseases, including brain ischemia, anxiety, depression, schizophrenia, substance abuse and epilepsy (Jacob et al., 2008). Epilepsy is characterized by a dramatic change in excitatory and inhibitory activity balance (Staley, 2015). In Temporal Lobe Epilepsy (TLE) and in different experimental models of epilepsy, the hippocampal CA1 region is hyper-excitable during the chronic stage, being a permissive factor for the genesis and/or propagation of epileptic seizures. Single and recurrent seizures lead to a dysregulation of GABAergic synapses at pre- and post-synaptic levels, but the mechanisms involved are still not fully understood.

Different pre-synaptic changes in GABAergic synapse were suggested to contribute to the development of epileptiform activity. GABA is produced from glutamate by the cytosolic enzyme glutamic acid decarboxylase (GAD) and is stored inside small synaptic vesicles before being exocytosed into synaptic cleft (Roth and Draguhn, 2012). Studies have shown that there is a progressive loss of GAD-positive terminals correlating with the development of seizures (Treiman, 2001). In addition, GAD65 has been shown to be cleaved by calpains under conditions of high neuronal activity (Buddhala et al., 2012). Furthermore, calpain has been shown to cleave high affinity GABA transporter proteins (GATs) (Baliova et al., 2009) and the vesicular GABA transporter (vGATs) (Gomes et al., 2011). However, it

remains to be determined whether these alterations in GABA transporters contribute to the changes in inhibitory activity observed in the epileptic brain.

Mutations in the neuronal P/Q type voltage-gated calcium channel (also known as CaV 2.1) were also associated with epilepsy (Rajakulendran et al., 2012). This channel is paramount for the coupling of calcium influx to neurotransmitter release, but these mutations are likely to affect the release of GABA and glutamate. Furthermore, several alterations in the modulators of synaptic vesicle formation, release, and recycling have been associated with epilepsy (Casillas-Espinosa et al., 2012). The synaptic vesicle protein 2A (SV2A) is a key regulator of synaptic vesicle exocytosis and the vesicular calcium homeostasis and, accordingly, SV2A knockout mice have shown reduced evoked action potential–dependent release of inhibitory neurotransmitters (Chang and Südhof, 2009). Interestingly, SV2A protein levels were shown to be reduced in the hippocampus of epileptic patients and animal models of SE (Van Vliet et al., 2009). Synapsin, a protein responsible for the control synaptic vesicle trafficking between the reserve pool and the readily releasable pool, dynamin, a protein that participate in endocytic vesicle formation, and syndapin, a protein that interacts with dynamin and other vesicular trafficking proteins involved in vesicular endocytosis, have all been shown to be altered in epilepsy and associated with excessive neuronal activity (Casillas-Espinosa et al., 2012).

Alterations in the population of postsynaptic $GABA_AR$ were also suggested to partly contribute to the reduction of GABA-mediated inhibition of principal neurons in *status epilepticus* (SE) (Kapur et al., 1989; Kapur and Coulter, 1995). SE is a life-threatening state of non-terminating seizures. Several studies have shown that single and recurrent seizures result in a reduction in GABA-mediated inhibition during SE (Kapur and Coulter, 1995; Kapur and Macdonald, 1997). This correlates with the observations from animal models of SE which also demonstrate a loss of inhibition during SE, suggesting that SE is a self-reinforcing condition in which there is a progressive reduction of GABA-mediated inhibition (Kapur and Macdonald, 1997; Goodkin et al., 2005). The reduced GABA-mediated inhibition allows the seizure to endure, further decreasing GABA-mediated inhibition. This might explain the perpetuation of the seizure in SE. Studies in SE animal models have also shown decreases in synaptic $GABA_ARs$, resulting from enhanced endocytosis (Naylor et al., 2005). Prolonged SE was shown to reduce GABA-mediated synaptic inhibition, accompanied by an enhanced internalization of $GABA_ARs$ This internalization was shown to be rapid and progressively increased due to the enhanced neuronal activity associated with seizures (Goodkin et al., 2005). Furthermore, a decreased phosphorylation of β3 $GABA_AR$ subunits was observed during SE, with a resulting increased association of the receptors with the clathrin adaptor AP2. These results suggest that SE disrupts the modulation of the synaptic $GABA_ARs$ stability by phosphorylation and induces $GABA_AR$ internalization via AP2 endocytosis (Terunuma et al., 2008). In addition, several studies showed an increased internalization of $GABA_AR$ correlated with a loss of benzodiazepine responsiveness between 10 and 45 minutes of SE (Kapur and Macdonald, 1997; Naylor et al., 2005).

As described in section 1.4.4.2., gephyrin plays an important role in the regulation of synaptic GABA$_A$R clustering and alterations to this protein have been associated with the development of epilepsy. The total expression of gephyrin was shown to be down-regulated in the CA1 region of the hippocampus during the latent period of epileptogenesis, correlating with a down-regulation of GABA$_A$Rs (González, 2013; González et al., 2013). The reduction of gephyrin observed during the latent period of epileptogenesis correlates with the changes in excitability previously observed, and suggests that the loss of gephyrin directly impacts the function of GABA$_A$R (González, 2013). Furthermore, a recent study has shown that a dissociation between GABA$_A$R and gephyrin, together with an increased GABA$_A$R dephosphorylation, are key steps for GABAergic down-modulation under excitotoxic conditions (Mele et al., 2014).

Interestingly, gephyrin clustering was shown to be modulated by phosphorylation on Ser-268 and Ser-270: phosphorylation of these two residues modulates gephyrin cluster size inhibiting further clustering of gephyrin molecules, while their dephosphorylation evokes the clustering of new gephyrin molecules. However, when only one of the residues is dephosphorylated, gephyrin becomes susceptible to calpain cleavage (Tyagarajan et al., 2013). It remains to be determined whether the gephyrin phosphorylation state is altered in the epileptic brain. A recent study demonstrated that several models of excitotoxicity (including NMDA over-activation) induce the cleavage of gephyrin by calpains into stable products. Cleavage of gephyrin decreased the synaptic clustering of the protein and reduced the synaptic pool of GABA$_A$Rs (Costa et al., 2015). Calpains are activated by an increase in the $[Ca^{2+}]_i$, in particular for sustained alterations, rending several molecular targets susceptible to cleavage (Dong et al., 2009). During seizure activity, the excessive calcium influx is likely to activate calpains thereby enhancing the cleavage of gephyrin and the disruption of the synaptic GABA$_A$R clusters. Furthermore, calcium dynamics have been shown to be disrupted in epilepsy (Nagarkatti et al., 2009; Brini et al., 2014; Staley, 2015) and due to the multifunctional nature of this signalling ion there are a multitude of targets that can be affected in this disease.

The disruption of GABAergic synapses due to enhanced internalization of GABA$_A$Rs and disrupted clustering of gephyrin are likely to be major players in the loss of GABAergic mediated inhibition and the development of pharmacoresistance in SE. Together the understanding of these processes can offer novel therapeutic targets for the management of this disease.

Objectives

Evidence point to the contribution of hyper-excitability as a permissive factor for the genesis and/or the propagation of epileptic seizures. Aberrant GABAergic synaptic functionality may be the cause of persistent deficits in functional inhibition in epilepsy.

$GABA_A$ receptors ($GABA_AR$) are the main mediators of inhibitory neurotransmission in the CNS and play an essential role in maintaining the excitatory/inhibitory balance required for the correct function of neuronal networks (Smith and Kittler, 2010). In SE, there are rapid changes in $GABA_A$ receptor ($GABA_AR$) surface expression which have been attributed to an increase in the internalization of the synaptic population of receptors. These alterations in the surface expression of $GABA_AR$ may contribute the generation of pharmacoresistant self-sustaining seizures (Goodkin et al., 2005). However, the specific mechanisms underlying GABAergic dysfunction in epilepsy are not yet established.

The present work was aimed at investigating the molecular mechanisms underlying $GABA_AR$ downregulation in cultured hippocampal neurons subjected to $[Mg^{2+}]_0$, an *in vitro* model of *status epilepticus*. In the first part of the work we implemented and validated this model in the laboratory. More specifically, we investigated the effect of hippocampal neurons exposure of to $[Mg^{2+}]_0$ on:

- Cellular death
- Intracellular calcium alterations evoked by SE at a single cell level through single cell live imaging
- Effect of SE on $GABA_AR$ turn-over. In particular we studied the effect of SE on:
    - The phosphorylation state of $GABA_ARs$ β3 subunit;
    - The levels of truncated gephyrin;
    - The internalization and the recycling $GABA_ARs$, using a antibody-feeding assay.

Materials and Methods

2. Materials and Methods

2.1. Hippocampal neuron cultures

Primary cultures of rat hippocampal neurons were prepared from the hippocampi of E18-19 Wistar rat embryos. After dissection, hippocampi were treated with trypsin (0.06%, for 15 min at 37°C) in Ca^{2+}- and Mg^{2+}- free Hank's balanced salt solution (5.56 mM KCl, 0.44 mM KH_2PO_4. 137 mM NaCl, 4.16 mM $NaHCO_3$, 0.34 mM HEPES and 0.001% phenol red). Trypsin activity was then stopped by washing with HBSS containing 10% fetal bovine serum, and the hippocampi were transferred to Neurobasal medium supplemented with SM1 (1:50 dilution), 25 μM glutamate, 0.5 mM glutamine and 0.12 mg/mL gentamycin. The cells were dissociated in this solution, and the suspension was filtered through a 0.22 μm filter to select the dissociated cells. The cells were counted and plated on 6 well plates, previously coated with poly-D-lysine (0.1 mg/mL), at a density of 90.0 x 10^3 cells/cm^2, or on poly-D-lysine coated glass coverslips, at a density of 80.0 x 10^3 cells/cm^2. The cultures were maintained in a humidified incubator with 5% CO_2 / 95% air, at 37°C, for 15 days. At day 3 *in vitro*, the cell division inhibitor 5-Fluoro-2′-deoxyuridine (FDU, 10 μM) was added to the cultures. After 7 days of incubation, one third of the culture medium was replaced by fresh medium with the same composition but without glutamate.

2.2. Induction of *in vitro status epilepticus*

Cultured hippocampal neurons (15 DIV) were incubated with a $[Mg^{2+}]_0$ medium (148 mM NaCl, 2.5 mM KCl, 2.0 mM $CaCl_2$, 10 mM Glucose, 10 mM HEPES at a final pH of 7.4) in a humidified incubator with 5% CO_2 / 95% air, at 37°C. For experimental conditions with a post-incubation period, the $[Mg^{2+}]_0$ medium was replaced by the conditioned medium and the cells were returned to the incubator for the indicated period of time. Under control conditions the cells remained in Neurobasal medium throughout the experiment. Under Sham control conditions the cells were incubated with a medium with the same composition of the $[Mg^{2+}]_0$ medium supplemented with 2 mM $MgCl_2$, and the NaCl concentration was adjusted to keep the osmolality. These cells were kept in the incubator for the indicated time period. Sham and SE medium have an osmolality of ±300 mOsm/l.

2.3. Nuclear morphology analysis

After stimulation neurons were fixed in 4% sucrose/paraformaldehyde in PBS. After fixation, the cells were washed two times with ice-cold PBS and incubated with the fluorescent dye Hoescht 33342 (1 μg/mL) for 10 min. Finally, the coverslips were washed twice with ice-cold PBS and mounted on glass slides with a fluorescence mounting medium (DAKO). Images were acquired on an Axio Observer 2.1 fluorescence microscope coupled to an Axiocam HRm digital camera, using a 40x objective. For each experimental condition three coverslips were analysed (at least 200 cells per coverslip were counted), and at least three independent experiments were performed, using distinct preparations.

2.4. Calcium fluorometric assay

Cells plated on 24 multiwell plates at a density of 80.0 x 10^3 cells/cm^2 were pre-incubated with 5 µM of Fura-2/AM for 40 min, in Sham solution supplemented with 0.1% BSA and 0.2% Pluronic F-127. When appropriate the cells were pre-incubated with glutamate receptor inhibitor APV (100 µM) for 30 min before the insult, and the drug was also present during and the experiment. After incubation with Fura-2/AM solution, the cells were washed with Sham solution to remove the excess of Fura-2/AM. The fluorescence intensity was measured using a SpectraMax Gemini EX spectrofluorometer at 37°C. Fura-2 fluorescence was recorded at 340 and 380 nm excitation and 548 nm emission for a period of 30 min with an interval of 30 sec between each reading. When appropriate [Mg^{2+}]$_0$ medium was replaced by Sham medium after 15 min reading, and the fluorescence intensity was measured for more 15 min.

2.5 Single cell calcium imaging

2.5.1. Fura-2 imaging

Hippocampal neurons cultured on coverslips at a density of 80.0 x 10^3 cells/cm^2 were pre-incubated with 5 µM Fura-2/AM for 40 min in Sham medium supplemented with 0.1% BSA and 0.2% Pluronic F-127. The coverslips were then washed with Sham medium to removed residual Fura-2/AM and mounted on a RC-20 chamber in a PH3 platform (Warner Instruments), at room temperature, on the stage of an inverted Axiovert 200 (Zeiss) fluorescence microscope. The perfusion chamber was filled with Sham medium and the baseline Fura-2 fluorescence was recorded for 3 min. After the initial 3 min, the Sham medium was replaced by [Mg^{2+}]$_0$ medium until t= 30 min. Finally, the cells were perfused again with Sham medium for the rest of the experiment. The preparations were excited at 340 and 380 nm using a Lambda DG4 lamp (Sutter Instruments Company). Changes in the fluorescence ratio of Fura-2 were acquired with a 40× objective coupled to a CollSNAP HQ digital camera (Roper Scientific) as previously described (Caldeira et al., 2007). Fura-2 fluorescence was in intervals of 10 sec throughout the experiment. Analysis was done via ImageJ analysis software. The results are presented as the ratio of fluorescence intensities after excitation at 340 nm and 380 nm.

The Fura-2-acetoxymethyl ester (Fura-2/AM) is a membrane-permeable fluorescent ratiometric calcium indicator. When added to cells, Fura-2/AM crosses cell membranes and once inside the cell the acetoxymethyl groups are cleaved by esterases. This gives rise to Fura-2 which binds to calcium. Binding of calcium causes the maximum excitation wavelength of Fura-2 to shift from 380 nm to 340 nm. The ratio of fluorescence intensity at these wavelengths can be calculated and used for measuring $[Ca^{2+}]_i$ changes (Fig. 1) (Grynkiewicz et al., 1985; Kikuchi, 2010).
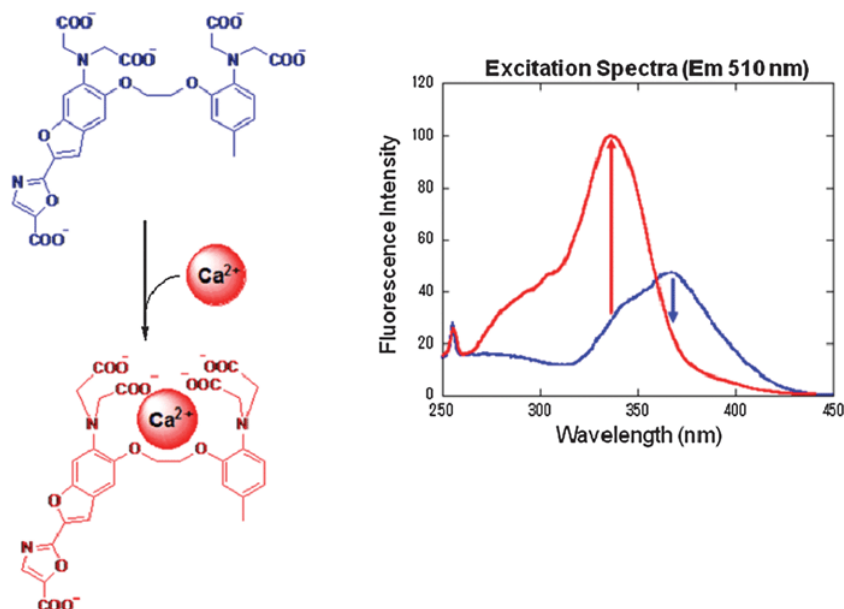
Fig.2.1: Structural and excitation spectral changes of Fura-2 upon Ca2+binding. Adapted from (Kikuchi, 2010).

Ratiometric imaging considerably reduces the effects of uneven loading, leakage and photobleaching of the fluorescent probes, and allows accurate measuring of the $[Ca^{2+}]_i$ in cells of different thicknesses. Measurements of Fura-2 fluorescence can usually be made over a period of an hour without significant loss of fluorescence as a result of either leakage or bleaching. In addition, Fura-2 is bright enough to permit measurements at intracellular concentrations of dye unlikely to cause significant Ca^{2+} buffering or damping of Ca^{2+} transients. However, Fura-2 strongly binds to Ca^{2+}, and as dissociation of Ca^{2+} from the indicator is slow, it is not suited to assess rapid $[Ca^{2+}]_i$ transients (Grynkiewicz et al., 1985; Kikuchi, 2010).

2.5.2. Fluo-4 imaging

Hippocampal neurons cultured on coverslips at a density of 80.0×10^3 cells/cm^2 were pre-incubated for 30 min with Fluo-4/AM (5 μM) prepared in Sham medium supplemented with 0.2% Pluronic F-127. The coverslips were then washed with Sham medium to remove residual Fluo-4/AM and mounted on a chamber filled with the same buffer. The chamber was placed on the microscope for recording and the baseline Fluo-4 fluorescence was recorded for 3 min. After this period, the Sham medium was replaced by $[Mg^{2+}]_0$ medium and the cells were further incubated for 15 or 30 min. Finally, the $[Mg^{2+}]_0$ medium was replaced by Sham medium for the rest of the experiment. When appropriate, Sham medium supplemented with 1 μM TTX was added to the cells after the third spontaneous calcium spike. Fluo-4 fluorescence imaging was performed under an atmosphere of 5% CO_2 / 95% air at 37°C. The preparation was excited at 488 nm using a solid state laser 100mW. Fluo-4 fluorescence was recorded through a Zeiss Cell Observer Spinning Disk microscope with a Plan-Apochromat 20× objective coupled to the highly sensitive electron multiplying camera, EM-CCD Evolve Delta. Fluo-4 fluorescence was recorded in intervals of 10 sec for the first 3 min (baseline). For the rest of the experiment fluorescence was recorded in intervals of 3 sec. Analysis was performed with ImageJ analysis software.

Similarly to Fura-2/AM, the fluo-4-acetoxymethyl ester (Fluo-4/AM) is a membrane-permeable fluorescent calcium indicator. When added to cells, Fluo-4/AM crosses the plasma membrane and once inside the cell the acetoxymethyl groups are cleaved by esterases. This gives rise to Fluo-4 which binds calcium, thereby increasing its fluorescence. Unlike Fura-2, binding of calcium does not cause a spectral shift, maintaining its maximum fluorescence excitation intensity at 488 nm. Instead, binding of calcium produces an >100-fold increase in fluorescence intensity (Fig. 2.2) (Minta et al., 1989).
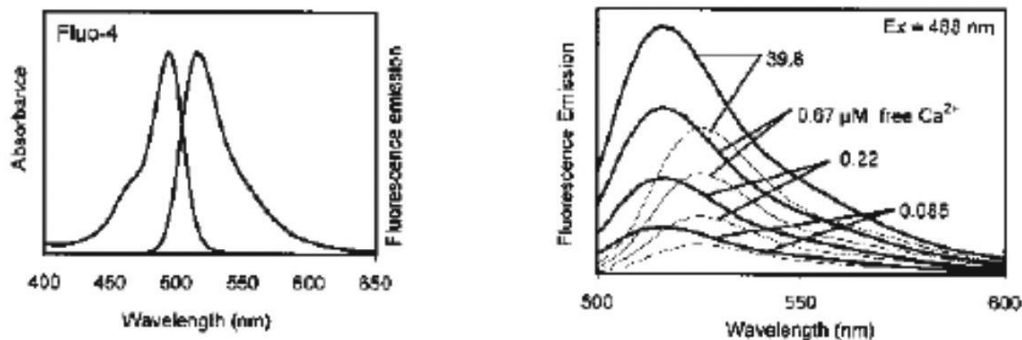
Fig.2.2: Fluo-4 fluorescence increases upon calcium binding without exhibiting a spectral shift. Adapted from (Gee et al., 2000)

The properties of Fluo-4 makes it extremely useful for flow cytometry, as well as in experiments involving photoactivation of 'caged' chelators, second messengers, and neurotransmitters, and for cell-based pharmacological screening. Since Fluo-4 has a low Ca^{2+}-binding affinity, it is suitable for detecting small and rapid changes in the intracellular calcium concentration, thus to assess rapid $[Ca^{2+}]_i$ transients (Gee et al., 2000; Thomas et al., 2000).

2.6. Western blotting

Total cell extracts were prepared after washing the cells twice with ice-cold PBS buffer. The cells were then lysed with RIPA buffer (150 mM NaCl, 50 mM Tris-HCl, 5 mM EGTA, 1% Triton, 0.5% DOC and 0.1% SDS, at a final pH of 7.5) supplemented with a cocktail of protease inhibitors (0.1 mM PMSF, 1 μg/mL chymostatin, 1μg/mL leupeptin, 1μg/mL antipain and 1 μg/mL pepstatin) and phosphatase inhibitors (50 mM NaF, 1.5 mM sodium orthovanadate). After lysis, the lysates were centrifuged for 10 min at 16.000 x g. The supernatants were collected and protein levels contained in the samples were quantified using the bicinchoninic acid (BCA) method. The protein concentration in the samples was equalized to the least concentrated sample and the samples were then diluted either with a 2x or 5x concentrated denaturing buffer (200 mM Tris-HCl, 8% glycerol, 1.6% SDS, 0.001% bromophenol blue and 5% β-mercaptoethanol). The samples were heated at 95°C for 5 min before analysis by SDS-PAGE; samples used in the analysis of GABA$_A$R β3 subunits were not heated. Then, the protein samples were separated by SDS-PAGE using a 10% polyacrylamide gel and the proteins were transferred to Polyvinylidene fluoride (PVDF) membranes overnight at 40 V, followed by a 1 h pulse at 100 V. Membranes were blocked in 5% milk or 3% BSA in TBS-T (20 nM Tris, 13.7 mM NaCl, 0.1% Tween, pH 7.6) for 1 h at room temperature. After blocking, the membranes were incubated with primary antibodies (overnight for anti-phospho-ser[408/409] β3 GABA$_A$ receptor, 2 h at room temperature for anti-gephyrin or 1 h at room temperature for anti-β-actin). The membranes were then washed and incubated with alkaline phosphatase-conjugated secondary antibodies for 1 h at room temperature. Alkaline phosphatase activity was visualized using the ECF system on the Storm 860 gel and blot imaging system. β-actin was used as a loading control.

2.7. Neuron transfection with calcium phosphate

Transfection of cultured hippocampal neurons with a myc-huGABA$_A$R β3 construct was performed by the calcium phosphate co-precipitation method as previously reported (Mele et al., 2014). Briefly, cultured hippocampal neurons were incubated with a cultured-conditioned medium with 2 mM kynurenic acid. 2 μg of plasmid DNA was diluted in Tris-EDTA (TE) at pH 7.3 and mixed with 2.5 M CaCl$_2$. This DNA/TE/calcium mix was added to 10 mM HEPES-buffered saline solution (270 mM NaCl, 10 mM KCl, 1.4 mM Na$_2$HPO$_4$, 11 mM dextrose, 42 mM HEPES at a final pH of 7.2). The precipitates were added drop-wise to each well and incubated for 90 min at 37°C, in an incubator with 5% CO$_2$ / 95% air. The cells were then washed with acidic culture medium containing 2 mM kynurenic acid and returned to the 5% CO$_2$ / 95% air incubator for 20 min at 37°C. Finally, the medium was replaced with the initial culture-conditioned medium, and the cells were further incubated in a 5% CO$_2$ / 95% air incubator for 48 h at 37°C to allow protein expression. Transfected cells were used for assessing receptor internalization and recycling rates in SE through antibody feeding assays.

2.8. Fluorescence assay of receptor internalization

Cultured living hippocampal neurons (15 DIV) were incubated at room temperature for 10 min in the presence of a high concentration (1:300) of an anti-myc antibody (N-terminus). The cells were then washed with PBS at 37°C, to remove the free antibody, and were further incubated in an antibody-free conditioned medium, at the same temperature for 15 min, to allow the internalization of antibody-bound receptors. After this incubation neurons were fixed for 15 min in 4% sucrose/paraformaldehyde (in PBS). Next, neurons were exposed to a super-saturating concentration (1:300) of the first of two secondary antibodies (Alexa Fluor 488) for 1 h at room temperature. After permeabilization (0.3% Triton X-100 in PBS, for 5 min) the cells were blocked with 5% BSA in PBS for 1h at room temperature. After blocking, the cells were incubated with the second secondary antibody (Alexa Fluor 568) for 1 h at RT. This strategy allows distinguishing the surface receptors from those receptors that have been internalized before fixation (Goodkin et al., 2005, 2008; Mele et al., 2014). The coverslips were then mounted on slides with fluorescence mounting medium (DAKO). Images were acquired on Axio Observer 2.1 fluorescence microscope (Zeiss) coupled to an Axiocam HRm digital camera, using a 63× oil objective and the fluorescence intensity was quantified using the ImageJ image analysis software. For each experiment analysed, the cells were imaged using identical settings. The ratio of internalization was calculated using the internalized antibody signal/ total antibody signal ratio.

2.9. Fluorescence assay of receptor recycling

Cultured living hippocampal neurons (15 DIV) were incubated at room for 10 min in the presence of a high concentration (1:300) of an anti-myc antibody (N-terminus). The cells were then washed with PBS at 37°C, to remove the free antibody, and were further incubated in antibody-free conditioned medium, at the same temperature for 15 min, to allow the internalization of antibody-bound receptors. The antibodies that remained on the cell surface were then stripped away by incubation in stripping buffer (0.5 M NaCl and 0.2 M acetic acid) on ice for 4 min. Immediately after the stripping, $GABA_A$ receptors were allowed to recycle for a period of 20 min in culture-conditioned medium. After this incubation the neurons were fixed for 15min in 4% sucrose/paraformaldehyde (in PBS). Next, neurons were exposed to a super-saturating concentration (1:300) of the first of two secondary antibodies (Alexa Fluor 488) for 1 h at room temperature. After permeabilization (0.25% Triton X-100 in PBS, for 5 min) the cells were blocked with 5% BSA in PBS for 1 h at room temperature. After blocking, the cells were incubated with the second secondary antibody (Alexa Fluor 568) for 1h at room temperature. The coverslips were then mounted on slides with the fluorescence mounting medium (DAKO). Images were acquired on Axio Observer 2.1 fluorescence microscope coupled to an Axiocam HRm digital camera, using a 63× oil objective and fluorescence intensity was quantified using the ImageJ image analysis software. For each experiment analysed, the cells were imaged using identical settings. The ratio of recycling was calculated using the recycled antibody signal/ total antibody signal ratio.

2.10. Reagents

Table 2.1. List of Reagents: Compilation of the reagents used for the experiments and respective branding.

Reagent	Brand	Reagent	Brand
APS	Sigma-Aldrich	KH_2PO_4	PanReac
APV	Tocris Bioscience	Kynurenic Acid	Sigma-Aldrich
BCA Method	Thermo Scientific	Lyophylized Milk	Nestle
Bromophenol blue	Merck Millipore	Methanol	Fisher Scientific
BSA	Sigma-Aldrich	$MgCl_2$	Merck Millipore
$CaCl_2$	PanReac	Na_2HPO_4	Merck Millipore
CAPS	Fisher Scientific	NaCl	PanReac
DMSO	Sigma-Aldrich	NAF	Merck Millipore
DOC	Sigma-Aldrich	$NaHCO_3$	Merck Millipore
DTT	NZYTech	Neurobasal Medium	Gibco® Life Technologies
ECF	GE Healthcare	NeuroCult™ SM1	StemCell™
EDTA	PanReac	Paraformaldahyde	Sigma-Aldrich
EGTA	Sigma-Aldrich	Phenol Red	Sigma-Aldrich
FBS	Gibco® Life Technologies	Pluoronic F-127	Molecular Probes™ Life Technologies
Fluo-4/AM	Molecular Probes™ Life Technologies	PMSF	Sigma-Aldrich
Fluorescence Mounting Medium	Dako	Polyacrilamide	Fisher Scientific
Fura-2/AM	Molecular Probes™ Life Technologies	Poly-D-Lysine	Sigma-Aldrich
Gentamycin	Gibco® Life Technologies	Protease Inhibitor Cocktail	Sigma-Aldrich
Glucose	VWR Chemicals	PVDF membranes	Merck Millipore
Glutamate	Sigma-Aldrich	SDS	Fisher Scientific
Glutamine	Sigma-Aldrich	Sodium Orthovanadate	Sigma-Aldrich
Glycerol	Amresco	Sucrose	Fisher Scientific
HCl	Fisher Scientific	Tris	Calbiochem
HEPES	Fisher Scientific	Triton X-100	Sigma-Aldrich
Hoescht 33342	Molecular Probes™ Life Technologies	Trypsin	Sigma-Aldrich
Isopropanol	PanReac	TTX	Tocris Bioscience
KCl	PanReac	Tween 20	Fisher Scientific

	Antibodies	Animal	Dilution	Brand
Primary	β-Actin	Mouse	1:10000	Sigma-Aldrich
	GABA$_A$ β3	Rabbit	1:1000	NeuroMab
	Gephyrin	Mouse	1:2000	Synaptic Systems
	myc (N Terminus)	Rabbit	1:300	Cell-Signaling
	Phospho-Ser$^{408/409}$ β3 GABA$_A$	Rabbit	1:1000	Symansis
Secondary	Alexa Fluor 488-conjugated Rabbit	Goat	1:300	Invitrogen
	Alexa Fluor 568-conjugated Rabbit	Goat	1:500	Invitrogen
	Alkaline Phosphatase-conjugated Mouse	Goat	1:20000	Jackson ImmunoResearch
	Alkaline Phosphatase-conjugated Rabbit	Goat	1:20000	Jackson ImmunoResearch

Table 2.2. List of Antibodies: Representation of the antibodies and their respective dilutions that were used during the experiments. Their respective brand and animal in which they were produced is also presented.

Results

3. Results

3.1. Characterization of $[Mg^{2+}]_0$ in vitro SE model

3.1.1. Evaluation of SE-induced cellular death

Incubation of primary cultures of hippocampal or cortical neurons, or hippocampal slices in a medium lacking Mg^{2+} ($[Mg^{2+}]_0$) is a commonly used *in vitro* model of epileptiform activity (Goodkin et al., 2005; Reddy and Kuruba, 2013). The transient incubation of the cells under these conditions allows the activation of NMDA receptors for glutamate, which was shown to contribute to the epileptiform activity observed after removal of the Mg^{2+}-free solution. Since this model is characterized by an excessive activity of excitatory synapses, which could be toxic to neurons, we measured neuronal viability under the experimental conditions used.

In order to analyse the putative changes in neuronal viability induced by the SE conditions used, we incubated cultured hippocampal neurons (15 DIV) with $[Mg^{2+}]_0$ medium for 30, 60, 90 and 120 minutes. After the stimulus, the $[Mg^{2+}]_0$ medium was replaced by culture-conditioned medium for an additional period of 8h (Post-incubation), and neuronal death was analysed via nuclei staining with Hoechst 33342. Exposure of cultured hippocampal neurons to SE for 60-120 min induced a time-dependent cell death, as determined by analysis of nuclear morphology 8 h after the insult (Fig. 3.1). The shorter period of SE tested (30 min) did not induce significant increase in cell death when compared with the Sham condition, while hippocampal neurons subjected to 60 or 90 min of stimulation showed ~15% increase in cell death, characterized by nuclear shrinking and chromatin condensation. Cell death was increased to ~20% when the cells were exposed to $[Mg^{2+}]_0$ for 120 min.

Considering that the one of the aims of the work was to investigate the alterations in the $[Ca^{2+}]_i$ homeostasis induced by epileptogenic conditions, experimental conditions were chosen where cell death was not observed. Therefore, 60 min was the maximum SE period used in all other experiments performed in this work to avoid artefacts resulting from excitotoxic injury which is coupled to $[Ca^{2+}]_i$ dysregulation.
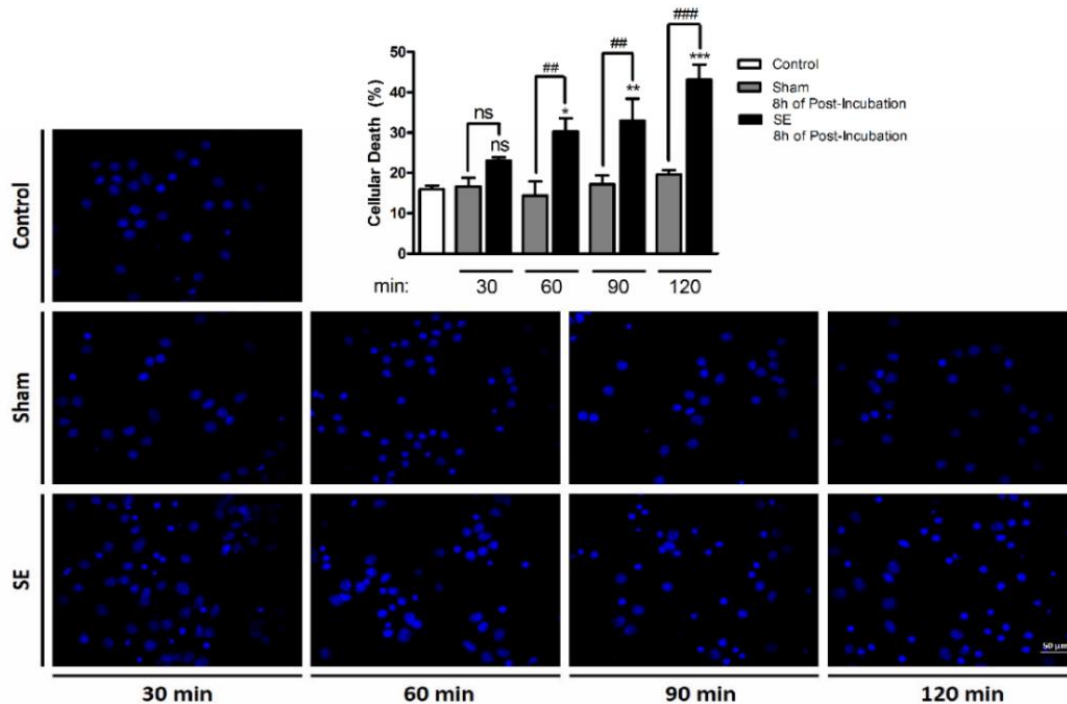
Fig.3.1: SE-induced neuronal cell death - SE was induced in cultured hippocampal neurons (15 DIV) through incubation in $[Mg^{2+}]_0$ medium (SE) for the following time periods: 30 min, 60 min, 90 min and 120 min. Immediately after stimulation the neurons were incubated in culture-conditioned medium for 8 h (post-incubation). Cell death was analysed via nuclei staining with Hoechst 33342. Representative results are shown below. The results are average ± SEM of 3 different experiments performed in duplicate and in independent preparations. Statistical analysis was performed by one-way ANOVA, followed by Dunnett's and Bonferroni's test. *p<0.05, ** p<0.01, *** p<0.001, ##p<0.01, ###p<0.001; significantly different when compared to control conditions. Non-significant differences are indicated as ns.

3.1.2. SE increases the intracellular Ca^{2+} levels by an NMDA receptor-dependent mechanism

The activity of neuronal networks is accompanied by the release of glutamate at excitatory synapses with consequent stimulation of glutamate receptors, including NMDA receptors. The activity of excitatory synapses raises the intracellular Ca^{2+} concentration in post-synaptic cells and, therefore, these $[Ca^{2+}]_i$ transients are tightly related to neuronal function. Calcium-dependent processes have been hypothesized to be involved in the induction of epilepsy. It has been shown that following epileptogenesis there is an alteration of calcium homeostatic mechanisms in hippocampal neuronal cultures (Pal et al., 1999, 2001; Hongo et al., 2015). The characterization of calcium transients in SE is crucial to understand the pathology.

To determine whether the SE stimulus used upregulates neuronal activity we measured the $[Ca^{2+}]_i$ under different experimental conditions. Cultured hippocampal neurons (15 DIV) were incubated with $[Mg^{2+}]_0$ medium for 30 min at 37°C in presence or absence of the NMDA glutamate receptor antagonist APV ((2R)-amino-5-phosphonovaleric acid; 100 μM), and the intracellular calcium concentration was measured with Fura-2, using a plate reader. The results are represented in Fig. 3.2 (panels A and B). SE

significantly increased the $[Ca^{2+}]_i$ for the duration of the stimulus and this effect was abolished in the presence of APV. These results indicate that SE induces an intracellular calcium accumulation through activation of NMDA receptors.

To determine whether the SE-induced $[Ca^{2+}]_i$ increase could be reversed, after incubation in $[Mg^{2+}]_0$ medium (for 15 min, at 37°C) hippocampal neurons were further incubated in a medium with the same composition but supplemented with 2 mM $MgCl_2$ (Sham medium). The $[Ca^{2+}]_i$ was then measured for 15 min and the results are represented in Fig. 3.2 (panels C and D). In control experiments hippocampal neurons were incubated with Sham medium for the same period of time. A complete recovery of the $[Ca^{2+}]_i$ levels was observed when SE was induced for 15 min.

In the experiments described above, Fura-2 fluorescence was analysed in populations of cultured hippocampal neurons. However, since the cultures of hippocampal neurons contain different types of neurons we hypothesized that differential responses could also take place. To address this question we tested the effect of SE at a single cell level by single cell calcium imaging, using the Fura-2 calcium probe. Cultured hippocampal neurons (15 DIV) were maintained in Sham medium (Na^+ salt solution containing Mg^{2+}) for 3 min, to determine the baseline Fura-2 fluorescence, before incubation in SE medium for 27 min. The cells were then incubated in sham medium for 15 min, and the results obtained are shown in Fig. 3.2 (panels E and F). Incubation with SE medium induced a transient increase in Fura-2 fluorescence by ~42%, and an additional incubation with Sham medium did not have a significant effect on the $[Ca^{2+}]_i$ dynamics.

The equipment used for the experiment described in this section did not allow maintaining neurons in a controlled atmosphere and temperature, possibly affecting the $[Ca^{2+}]_i$ profile. Therefore, all other experiments analysing the profile of calcium responses in single cell was performed with a different methodology, as described in the following section.
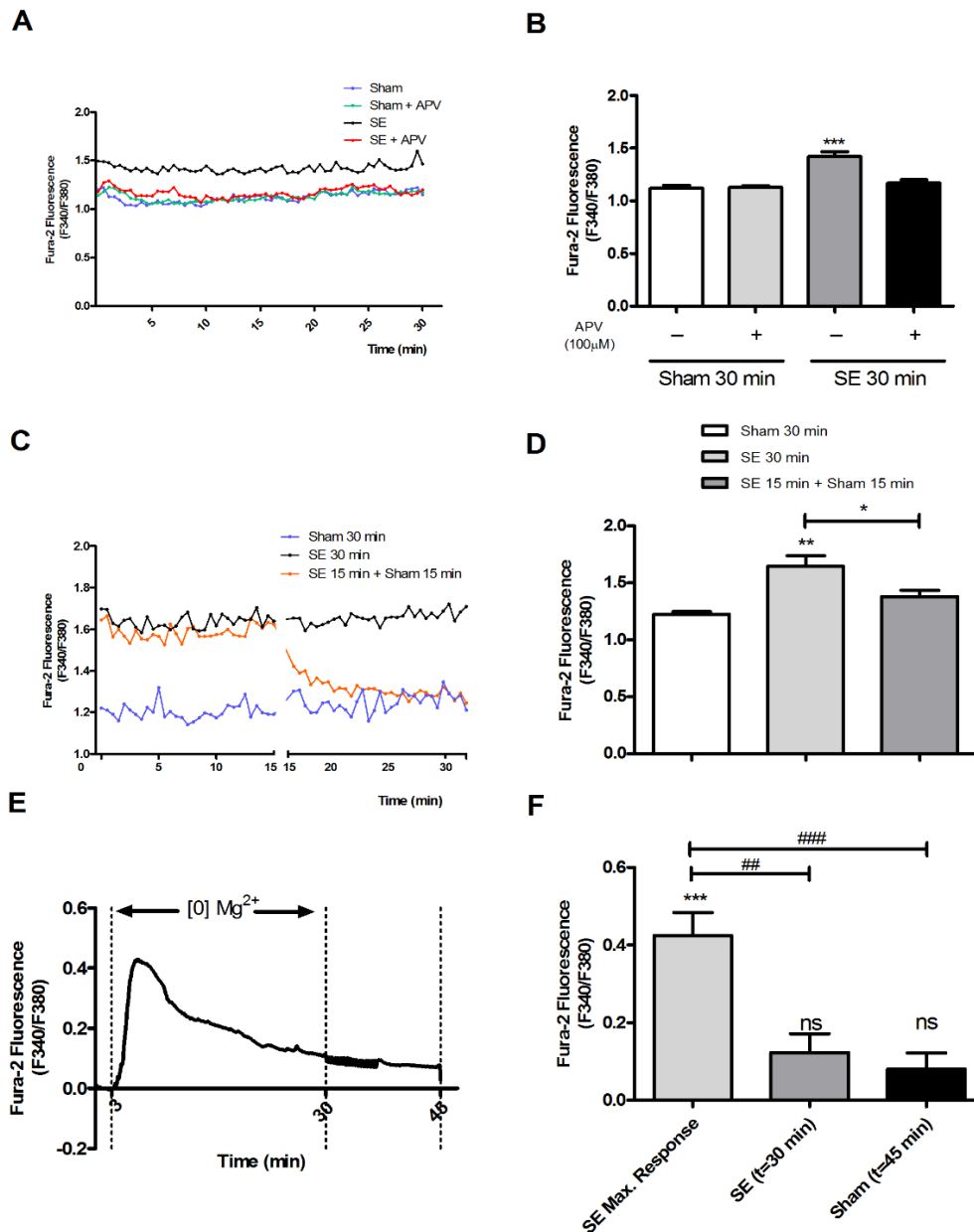
Fig.3.2: SE increases the intracellular Ca^{2+} concentration by a mechanism dependent on the activation of NMDA receptors. [A,B] Cultured hippocampal neurons (15 DIV) were incubated with [Mg^{2+}]$_0$ medium (SE) for 30 min at 37°C in presence or absence of the NMDA glutamate receptor antagonist APV (100 μM), and the [Ca^{2+}]$_i$ was measured with Fura-2, using a plate reader. The Fura-2 fluorescence ratio 340⁄380 nm was used to evaluate cytosolic [Ca^{2+}] levels. **[C,D]** Cultured hippocampal neurons (15 DIV) were incubated with [Mg^{2+}]$_0$ medium at 37°C for 15 min or 30 min. Under the latter condition the SE medium was replaced by Sham medium (Na$^+$ salt solution containing Mg^{2+}) and the cells were further incubated for 15 min. Fura-2 fluorescence was recorded for the duration of the experiment. **[E, F]** Fura-2 fluorescence in cultured hippocampal neurons (15 DIV) was analysed by single cell calcium imaging. The cells were initially incubated with Sham medium (Na$^+$ salt solution containing Mg^{2+}) for 3 min to determine the baseline level. After 3 min, the sham medium was replaced with SE medium for 27 min. The medium was then replaced by sham medium for an additional period of 15 min. Fura-2 fluorescence was recorded for the duration of the experiment. For each time point the results are represented as the ratio 340⁄380 nm subtracted by the ratio values corresponding to the baseline. Values are the means ± SEM of at least three independent experiments performed in triplicate, in the case of single cell calcium imaging results are the average of 17 cells from four independent experiments. One-way ANOVA was performed as statistical analysis, followed by Dunnett's and/or Bonferroni test.*$p< 0.05$, **$p< 0.01$, ***$p< 0.001$, ##$p< 0.01$, ###$p< 0.001$; significantly different when compared to the sham condition or to the indicated experimental condition. Non-significant differences are indicated as ns.

3.2. Characterization of SE-induced calcium transients

3.2.1. SE induces synchronous neuronal activity and the development of spontaneous calcium spiking

To further investigate the effect of SE on the $[Ca^{2+}]_i$ homeostasis we analysed the alteration in neuronal intracellular calcium levels with the Fluo-4 fluorescent calcium indicator, using high speed spinning disk fluorescence microscopy. Changes in Fluo-4 fluorescence were measured under the experimental conditions used in the previous section but at 37°C and with a controlled 5% CO2 / 95% air atmosphere. Representative $[Ca^{2+}]_i$ profiles for three different neurons in the same field are presented in Fig. 3.3. Analysis showed a rapid increase in the $[Ca^{2+}]_i$ immediately after incubation of hippocampal neurons in $[Mg^{2+}]_0$ medium. This $[Ca^{2+}]_i$ response was transient, and the initial peak was followed by a decrease towards a plateau which was maintained until the end of the incubation period in SE medium (t = 30 min). Replacement of the SE medium with a Na^+-salt solution containing 2 mM $MgCl_2$ (Sham medium) induced an additional reduction in the $[Ca^{2+}]_i$, down to levels similar or slightly above those observed under resting conditions. However, the cells developed spontaneous calcium spikes for the rest of the experiment. Interestingly, the $[Ca^{2+}]_i$ profile of the 3 neurons shown in Fig. 3.3 show that SE induces synchronous calcium transients in the cells present in the culture.
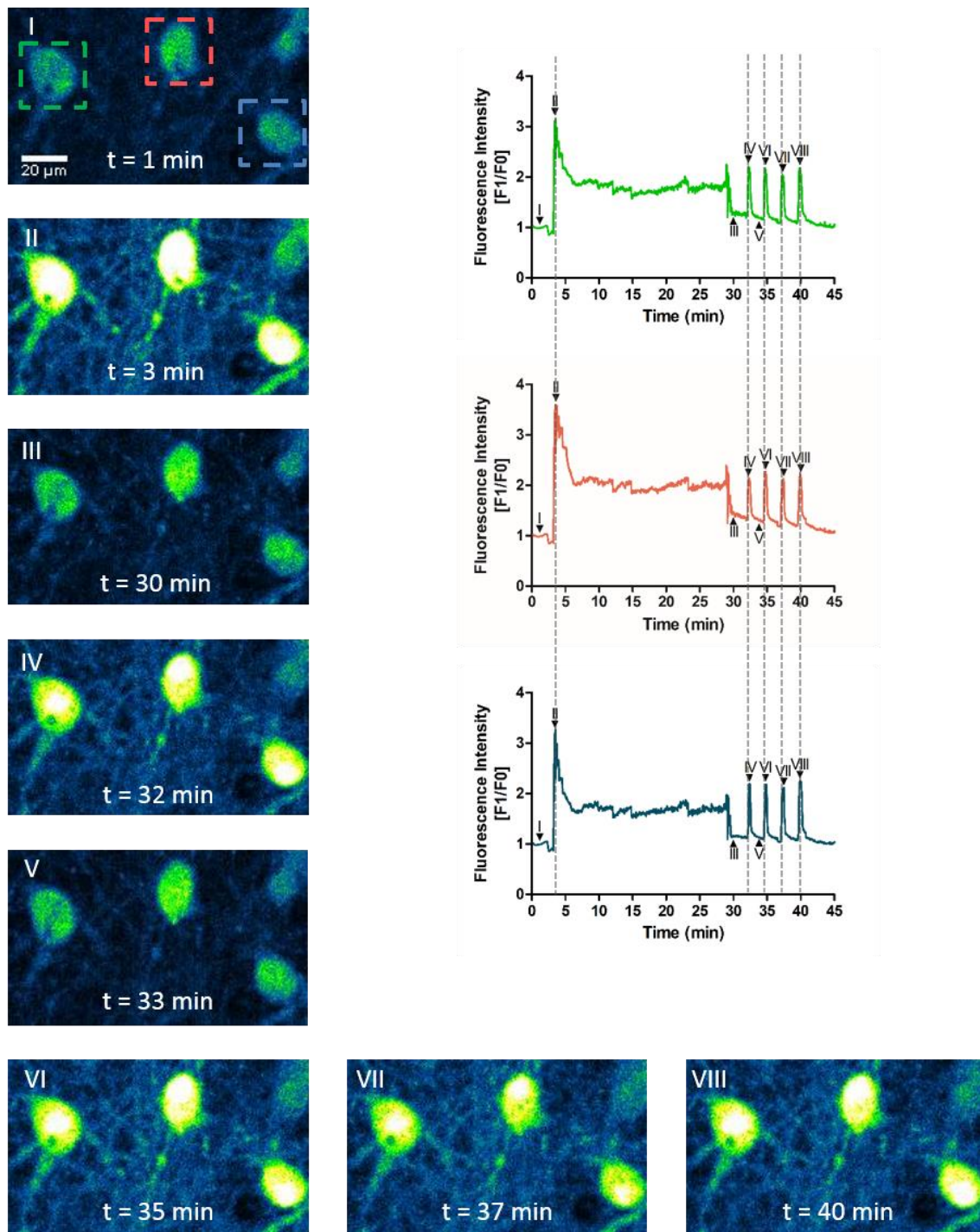
Fig.3.3: **SE induces synchronous neuronal activity and the development of spontaneous calcium spiking** - Cultured hippocampal neurons (15 DIV) were analysed by single cell calcium imaging using the fluorescent Ca^{2+} indicator Fluo-4, with Spinning Disk microscopy. The cells were initially incubated with Sham medium (Na^+-salt solution containing Mg^{2+}) for 3 min to determine the baseline levels of calcium. After 3 min, the Sham medium was replaced with $[Mg^{2+}]_0$ medium (SE) for the indicated stimulation period. At 30 min, the SE medium was replaced by Sham medium for an additional period of 15 min. Fluo-4 fluorescence was recorded for the duration of the incubation. For each time point the results are represented as the normalized intensity of Fluo-4 fluorescence (Fluorescence for a given time point / the baseline fluorescence). Calcium dynamics is represented in a time course visual representation of three different neurons. These neurons are indicated by a coloured square and the corresponding alterations in Fluo-4 are shown in the traces on the right. The images (I to VIII) represent key time points of the Fluo-4 fluorescence recording and their position in the traces is also shown. The dashed lines portray the synchronous neuronal calcium fluctuation pattern.

50

3.2.2. Characterization of 30 min SE-induced calcium transients

A more detailed analysis of the $[Ca^{2+}]_i$ responses to transient exposure of hippocampal neurons to conditions mimicking SE was performed using single cell calcium imaging using Fluo-4. Hippocampal neurons were stimulated with $[Mg^{2+}]_0$ medium for 30 min (SE period) followed by incubation in a Na^+-salt solution containing 2 mM Mg^{2+} (Sham medium), and the results are of Figure 3.4 (panels A-F) showed heterogeneous responses. Among the cells that were analysed (n=282 total cells / n=153 cells submitted to 30 min SE), 91% displayed an increase in the $[Ca^{2+}]_i$ when incubated in $[Mg^{2+}]_0$ medium (Fig. 3.4, G'), 54% of these neurons developed spontaneous calcium spiking upon further incubated in Sham medium; the remaining population of cells did not develop this phenotype. The amplitude of the spontaneous spikes was 80% lower than the initial response to the $[Mg^{2+}]_0$ medium (Fig. 3.4, J), and remained constant throughout the experiment.

In the group of cells that developed spontaneous calcium spiking following incubation in Sham medium, 56% of the neurons recovered the basal $[Ca^{2+}]_i$ during the period between calcium transients (Fig. 3.4, C and D). In contrast, a lower percentage (24%) of the cells that did not develop spontaneous calcium spiking showed a recovery of the calcium levels (Fig. 3.4, G''). We hypothesized that the $[Ca^{2+}]_i$ dysregulation observed in some cells could be attributed to an increased Ca^{2+} entry in response to the initial exposure to the SE buffer. Comparatively, the cells that recovered from the SE stimulus upon incubation in the Sham medium (Fig. 3.4, C and D) showed an initial increase of Fluo-4 fluorescence by ~127% upon incubation with the $[Mg^{2+}]_0$ medium (Fig. 3.4, H). This initial response was followed by a slow decrease towards a plateau at ~47% of the resting Fluo-4 fluorescence (Fig. 3.4, H), and the $[Ca^{2+}]_i$ further decreased upon incubation of the cells in a Na^+-salt solution containing Mg^{2+} (Sham medium) (Fig. 3.4, H). The cells that did not recover from the SE stimulus (Fig. 3.4, E and F) showed a similar (~114%) but sustained increase in Fluo-4 fluorescence when incubated in the $[Mg^{2+}]_0$ medium (Fig. 3.4, I), and the effects were maintained even after incubation with Sham medium (Fig. 3.4, I). Together, these results indicate that under the SE conditions used, the magnitude of the initial $[Ca^{2+}]_i$ does not determine the impairment of the calcium homeostasis mechanisms observed when the cells are exposed again to the Sham medium. On the other hand, it was the delayed $[Ca^{2+}]_i$ response to the incubation in $[Mg^{2+}]_0$ medium (after the initial rapid increase) that correlated with the pattern observed when the SE stimulus was removed.
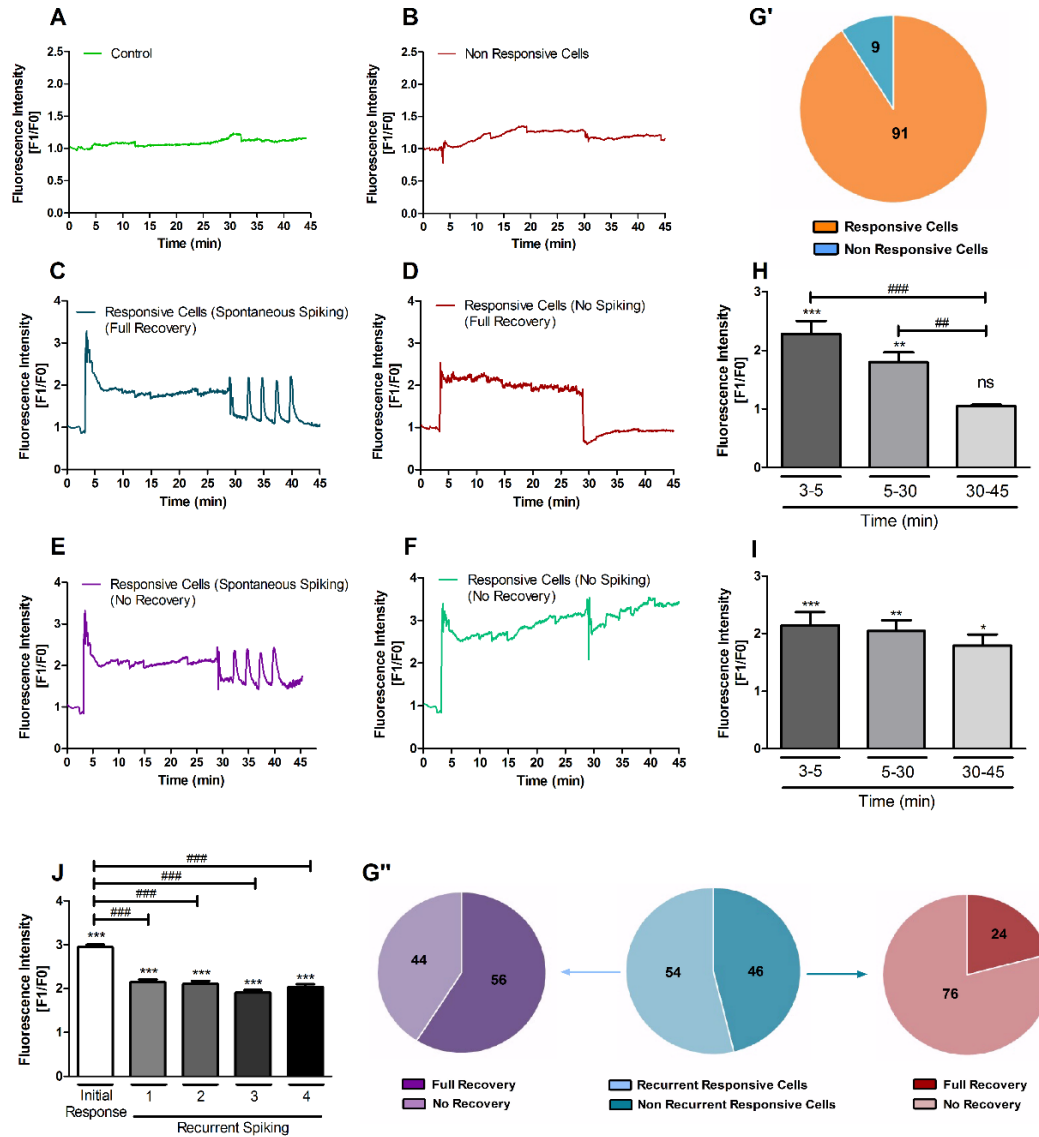
Fig. 3.4: Characterization of SE-induced calcium transients for a 30 minute stimulus - [A-F] Cultured hippocampal neurons (15 DIV) were analysed by single cell calcium imaging using the Fluo-4 fluorescent Ca^{2+} indicator, with Spinning Disk microscopy. The cells were initially incubated with Sham medium (Na^+ salt solution containing Mg^{2+}) for 3 min to determine the baseline level of fluorescence. After 3 min, the Sham medium was replaced with $[Mg^{2+}]_0$ medium for the indicated stimulation time. At t = 30 min, the medium was replaced by Sham medium for an additional period of 15 min. Fluo-4 fluorescence was recorded for the duration of the experiment. For each time point the results are represented as the normalized intensity of Fluo-4 fluorescence (Fluorescence for a given time point divided by the baseline fluorescence). The analyses represent the different types of response to the $[Mg^{2+}]_0$ medium. **[G'-G'']** Pie chart representation of the types of response to $[Mg^{2+}]_0$ medium as a percentage of total cells with the indicated pattern of response. **[H-I]** A comparative analysis of the calcium response profile was done between the cells that showed a recovery to basal calcium levels **[C and D; H]** and the cells that did not, **[E and F; I]**. **[J]** Calcium spikes were comparatively analysed to determine the differences between the initial response to the $[Mg^{2+}]_0$ medium and the spontaneous spikes that developed after the stimulus (in Sham medium). Values are the means ± SEM of at least three independent experiments. One-way ANOVA was performed as statistical analysis, followed by Dunnett's and/or Bonferroni test.*$p < 0.05$, **$p < 0.01$, ***$p < 0.001$, ##$p < 0.01$, ###$p < 0.001$; significantly different when compared to the sham condition or to the indicated column. ns, not significantly different.

3.2.3. Characterization of the calcium transients induced by 15 min SE

The results of section 3.1.1 showed a time-dependent effect of SE in inducing neuronal death (Figure 3.1), indicating that differential responses are evoked depending on the duration of the stimulus. Single cell characterization of calcium transients showed that a 30 min SE stimulus induces the development of spontaneous spiking in a subpopulation of cells when further incubated in Sham conditions (Figure 3.3 and 3.4). Therefore, we hypothesized that different periods of SE could translate into distinct SE phenotypes which could affect the calcium transient profiles. To address this question we compared the calcium transients evoked by 30 min of SE with the profile evoked by incubation of cultured hippocampal neurons with $[Mg^{2+}]_0$ for 15 minutes.

Single cell calcium imaging using Fluo-4 and Spinning Disk microscopy showed an increase in the $[Ca^{2+}]_i$ when the cells were incubated in the solution lacking Mg^{2+}, similarly to the results shown in Figs. 3.3 and 3.4. After 15 min of SE the cells were further incubated for 30 min in a Na^+-salt solution containing Mg^{2+} (Sham medium), and the results showed different calcium response profiles (Figure 3.5, [A-F]). Among the cells analysed (n=282 total cells / n=129 cells submitted to 15 min SE), 91% responded to the initial incubation in $[Mg^{2+}]_0$ medium with an increase in the $[Ca^{2+}]_i$ (Fig.3.5, G'), in agreement with the results of Fig. 3.4. In the latter population of cells, 61% developed spontaneous calcium spiking when the SE medium was replaced with the Sham medium (at t = 15 min); the remaining cells did not show this phenotype. The spontaneous spiking amplitude progressively decreased by ~20% from the first to the third spike, indicating a progressive loss of intensity of the spontaneous calcium transients with time (Fig. 3.5, J).

When spontaneous spiking activity was observed, 82% of the cells showed a recovery of the basal $[Ca^{2+}]_i$ levels during the period between the calcium transients. In contrast, in the population of hippocampal neurons that did not develop spontaneous calcium spiking only 47% of the cells recovered the basal calcium levels (Figure 3.5, G''). To determine whether the $[Ca^{2+}]_i$ dysregulation observed in the latter group of cells could be attributed to an increased Ca^{2+} entry in response to the initial exposure to the SE buffer, we compared the two sets of data. The cells that fully recovered from the 15 min SE stimulus when incubated in Sham medium (Fig.3.5, C and D) showed an initial increase of the Fluo-4 fluorescence by ~64% when exposed to $[Mg^{2+}]_0$ medium (Fig. 3.5, H), followed by a decrease (~10%) towards a plateau (Fig. 3.5, H). The cells in which the $[Ca^{2+}]_i$ did not recover after incubation in Sham medium (Fig. 3.5, E and F) showed a similar (~58%) increase in Fluo-4 fluorescence after stimulation with the $[Mg^{2+}]_0$ medium (Fig. 3.5, I), but in this case the $[Ca^{2+}]_i$ response was maintained during the rest of the stimulus (Fig. 3.5, I). Under the latter conditions, the $[Ca^{2+}]_i$ levels remained unchanged for the rest of the experiment after addition of Sham medium (Fig. 3.5, I). These results show no correlation between the magnitude of the $[Ca^{2+}]_i$ response to the $[Mg^{2+}]_0$ buffer and the delayed dysregulation of the mechanisms that contribute to the maintenance of the resting concentrations of calcium. Similarly to the results obtained for longer SE periods, it was the delayed $[Ca^{2+}]_i$ response to the incubation in

$[Mg^{2+}]_0$ medium (after the initial rapid increase) that correlated with the pattern observed after the epileptogenic period.
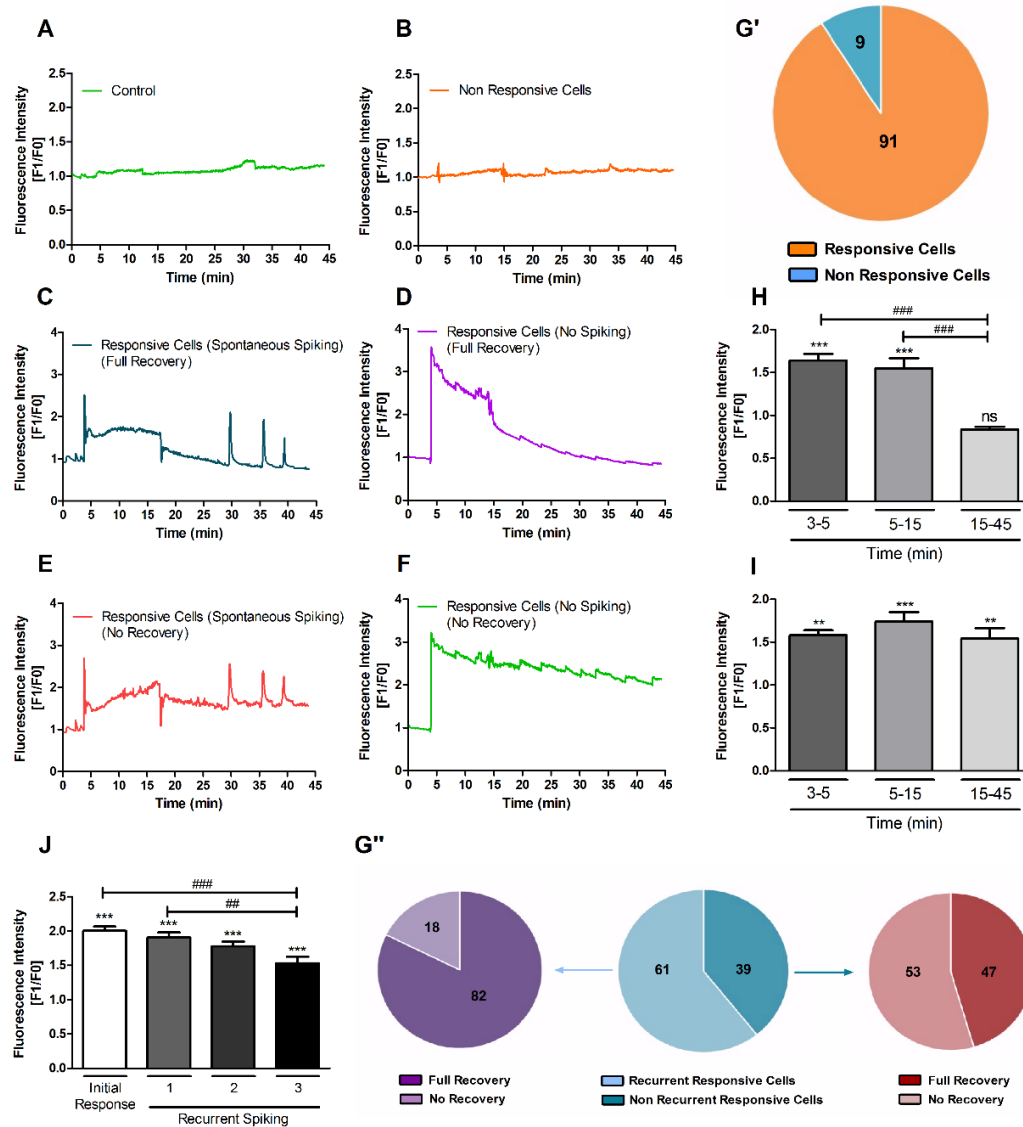

Fig.3.5: Characterization of SE (15 min)-induced calcium transients- [A-F] Cultured hippocampal neurons (15 DIV) were analysed by single cell calcium imaging using the fluorescent Ca^{2+} indicator Fluo-4, with Spinning Disk microscopy. The cells were initially incubated with Sham medium (Na^+-salt solution containing Mg^{2+}) for 3 min to determine the baseline fluorescence level. After 3 min, the Sham medium was replaced with $[Mg^{2+}]_0$ medium for the designated stimulation time. At t = 15 min the medium was replaced by Sham medium for an additional period of 30 min. Fluo-4 fluorescence was recorded for the duration of the experiment. For each time point the results are represented as the normalized intensity of Fluo-4 fluorescence (Fluorescence for a given time point divided by the baseline fluorescence). The analyses represents the different types of response to the $[Mg^{2+}]_0$ medium. **[G'-G'']** Pie chart representation of the types of response to $[Mg^{2+}]_0$ medium in percentage of total cells with the indicated pattern of response. **[H-I]** A comparative analysis of the calcium response profile was done between the cells that were able to recover to basal calcium levels, **[C and D; H]**, and the cells that were not **[E and F; I]**. **[J]** Calcium spikes were comparatively analysed to determine the differences between the initial response to the $[Mg^{2+}]_0$ medium and the spontaneous spikes that developed after the stimulus (in Sham medium). Values are the means ± SEM of at least three independent experiments. One-way ANOVA was performed as statistical analysis, followed by Dunnett's and/or Bonferroni test. **p< 0.01, ***p< 0.001, ##p< 0.01, ###p< 0.001; significantly different when compared to the sham condition or to the indicated column. ns, not significantly different.

54

3.2.4. Longer stimulation times induce faster and more frequent spiking

The results presented above show that the spontaneous calcium spiking profile induced by incubation of hippocampal neurons in a $[Mg^{2+}]_0$ buffer depends on the time of stimulation. In this section a comparative statistical analysis between the two stimulation protocols (30 min and 15 min SE) was performed. Several parameters were analysed: i) the percentage of cells that develop spontaneous spiking (Fig. 3.6, C), ii) the percentage of cells that recover to basal calcium levels after the addiction of Sham medium (Fig. 3.6, D), iii) the spontaneous spiking latency (Fig. 3.6, E), iv) the spontaneous spiking frequency (Fig. 3.6, F) and v) the spontaneous spiking duration (Fig. 3.6, G).

We started by comparing the percentage of cells that developed spontaneous calcium spikes and the capacity of these cells to recover to basal calcium levels between consecutive spikes. There was no significant difference in the number of cells that developed spontaneous calcium spiking between the two protocols tested (Fig. 3.6, C). Interestingly, about 82% of the cells that were subjected to 15 min of SE were capable of recovering to calcium basal levels, while only about 46% of the cells showed the same type of behaviour when 30 min of SE was tested. This suggests that the cells that underwent SE for 30 minutes were less efficient in maintaining the $[Ca^{2+}]_i$ homeostasis (Fig. 3.6, D). However, additional experiments are required to draw conclusions about the differences in the pattern of response.

We also compared the different spiking profile characteristics (latency, frequency and duration) that were induced by either 15 or 30 minutes of SE. The results show that cells that underwent SE for 30 min have a 56% shorter latency of spontaneous calcium spiking development than the cells that underwent SE for 15 minutes (Fig. 3.6, E). In contrast, the frequency of spontaneous calcium spiking is 58% higher in cells that were subjected to 30 min of SE (Fig. 3.6, F). Furthermore, the spiking is 39% faster in the cells that were exposed to 30 min of SE (Fig. 3.6, G). These results indicate that the longer period of SE induces faster and more frequent spontaneous calcium spiking.
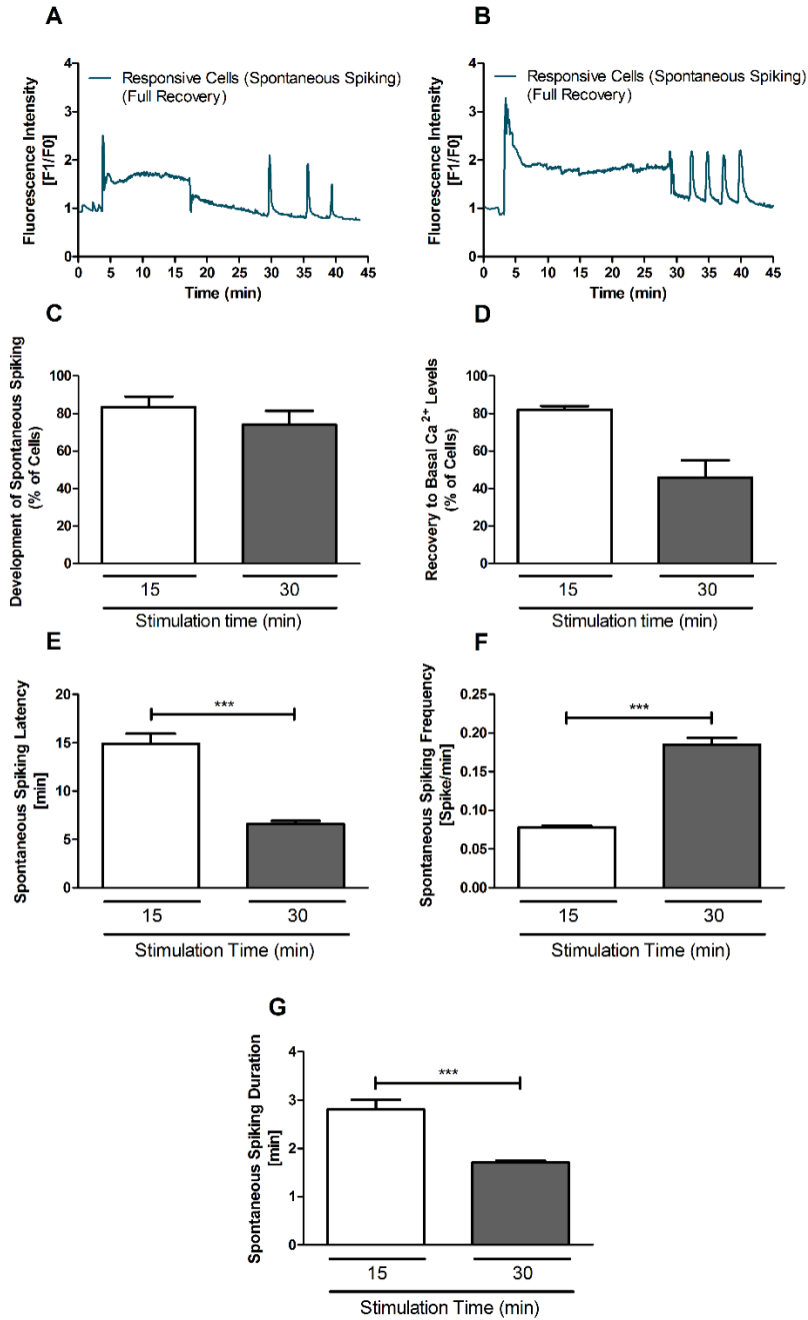
Fig.3.6: Different SE periods induce spontaneous calcium spiking with distinct characteristics - **[A-B]** Cultured hippocampal neurons (15 DIV) were analysed by single cell calcium imaging using the fluorescent Ca^{2+} indicator Fluo-4, with Spinning Disk microscopy. The cells were initially incubated with Sham medium (Na^+-salt solution containing Mg^{2+}) or 3 min to determine the baseline level. After 3 min, the Sham medium was replaced with $[Mg^{2+}]_0$ medium (SE) for the indicated period of time. SE medium was replaced by Sham medium at either the 15 **[A]** or the 30 min, **[B]**, and the cells were further incubated under these conditions for 15 or 30 min, respectively. Fluo-4 fluorescence was recorded for the duration of the experiment. For each time point the results are represented as the normalized intensity of Fluo-4 fluorescence (Fluorescence for a given time point divided by the baseline fluorescence). The analyses represent the different types of response to incubation in $[Mg^{2+}]_0$ medium. **[C-G]** Statistical analysis comparing the response profile of the cells that developed spontaneous calcium spiking after the 15 and the 30 min stimulus with $[Mg^{2+}]_0$ medium. The following parameters were analysed: **[C]** Percentage of cells that develop spontaneous spiking, **[D]** Percentage of cells that recover to basal calcium levels, **[E]** Spontaneous spiking latency, **[F]** Spontaneous spiking frequency, **[G]** Spontaneous spiking duration. Values are the means ± SEM of at least three independent experiments. Non-parametric *t*-test was performed as statistical analysis, followed by Mann Whitney's test. ***p< 0.001, significantly different when compared to the sham condition or to the indicated column.

56

3.2.5. Spontaneous calcium spiking is dependent of neuronal activity

The development of spontaneous calcium spiking occurs during a period when the cells are maintained under non-depolarizing conditions. This suggests that SE induces molecular changes that lead to a chronic state of enhanced neuronal activity. In order to further investigate the mechanisms underlying spontaneous $[Ca^{2+}]_i$ spiking hippocampal neurons were subjected to SE for 30 min, and the cells were further incubated in a Na^+-salt solution containing Mg^{2+}, which allows the development of calcium transients. Once $[Ca^{2+}]_i$ spikes were observed, the cells were perfused in the presence of tetrodotoxin (TTX), a blocker of voltage-gated Na^+ channels. Fig. 3.7 shows that addition of TTX to the medium after the third spontaneous calcium spike completely abolished spiking activity, indicating that this phenomenon is dependent on neuronal activity (Fig.3.7).
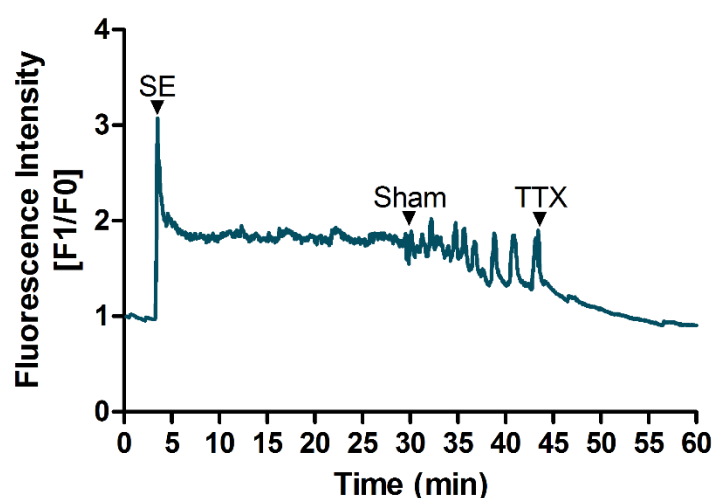

Fig.3.7: Spontaneous calcium spiking is dependent of neuronal activity - Cultured hippocampal neurons (15 DIV) were analysed by single cell calcium imaging using Fluo-4 AM, fluorescent Ca^{+2} indicator coupled with Spinning Disk microscopy. The cells were initially incubated with Sham medium (Na^+ salt solution containing Mg^{2+}) for 3 min to determine the baseline level. After 3 min, the Sham medium was replaced with $[Mg^{2+}]_0$ medium (SE) for the designated stimulation time. At the 30 min mark, the SE medium was replaced by Sham medium for an additional period of 30 min. To assess whether the spontaneous calcium spiking is dependent on neuronal activity, tetrodoxin (TTX; 1 μM), a voltage-gated Na^+ channel inhibitor, was added to the medium after the third spontaneous calcium spike. Fluo-4 fluorescence was recorded for the duration of the experiment. For each time point the results are represented as the normalized intensity of Fluo-4 fluorescence (Fluorescence for a given time point divided by the baseline fluorescence). The results are representative of three experiments performed in distinct preparations (123 cells).

3.3. The effects of SE in GABA$_A$ receptor dynamics

Evidence points to the contribution of hyper-excitability as a permissive factor for the genesis and/or the propagation of epileptic seizures. Aberrant GABAergic synaptic reorganization may be the cause of persistent deficits in functional inhibition in epilepsy. *Status epilepticus* (SE) is also characterized by rapid changes in GABA$_A$R surface expression, and acute increases in AP2-mediated internalization of synaptic GABA$_A$R underlie the generation of pharmacoresistant self-sustaining seizures (Goodkin et al., 2005; Kittler et al., 2005)

The strength of GABAergic synapses is determined by the total number of GABA$_A$R locally available. Synaptic GABA$_A$R are recruited from an extrasynaptic pool, and their insertion in the plasma membrane and internalization occurs extra-synaptically (Bogdanov et al., 2006). The anchoring of GABA$_A$R by gephyrin is an important step involved in GABA$_A$R targeting to the synapse (Tyagarajan and Fritschy, 2014).

In this section we analysed the effect of SE on GABA$_A$R trafficking. In particular we focused the attention on the alterations induced by SE on GABA$_A$R internalization and recycling, on the phosphorylation of β3 GABA$_A$R subunit and on gephyrin protein levels

3.3.1. SE reduces the phosphorylation of β3 GABA$_A$R subunit.

In physiological condition the internalization of GABA$_A$R is negatively regulated by phosphorylation of β3 GABA$_A$R subunit intracellular loop (Kittler et al., 2005, 2008). Therefore, we evaluated GABA$_A$R β3 subunit phosphorylation in hippocampal neurons subjected to $[Mg^{2+}]_0$ medium (SE) for different periods of time (10 - 60 min). In control experiments hippocampal neurons were incubated in Sham medium (Na$^+$-salt solution containing 2 mM Mg^{2+}) for the same period of time. GABA$_A$R β3 subunit phosphorylation was evaluated by western blot analysis using a phospho-specific antibody against the β3 subunit serine residues 408/409 (Fig. 3.8). Short periods of SE (20 min) induced a significant dephosphorylation of the GABA$_A$R β3 subunit (~30%) and similar results were obtained when longer incubations in $[Mg^{2+}]_0$ were tested (24% and ~31% decrease for 30 and 60 min, respectively) (Fig. 3.8, C). Control experiments showed no significant differences in the total amount of GABA$_A$R β3 subunits under the same conditions. Interestingly, when the levels of GABA$_A$R β3 subunit phosphorylation were assessed 8 h after the stimulus, a decrease was also observed but the results were not statistically significant (Fig.3.8, F). These results suggest that the cells may be unable to recover from the SE stimulus.
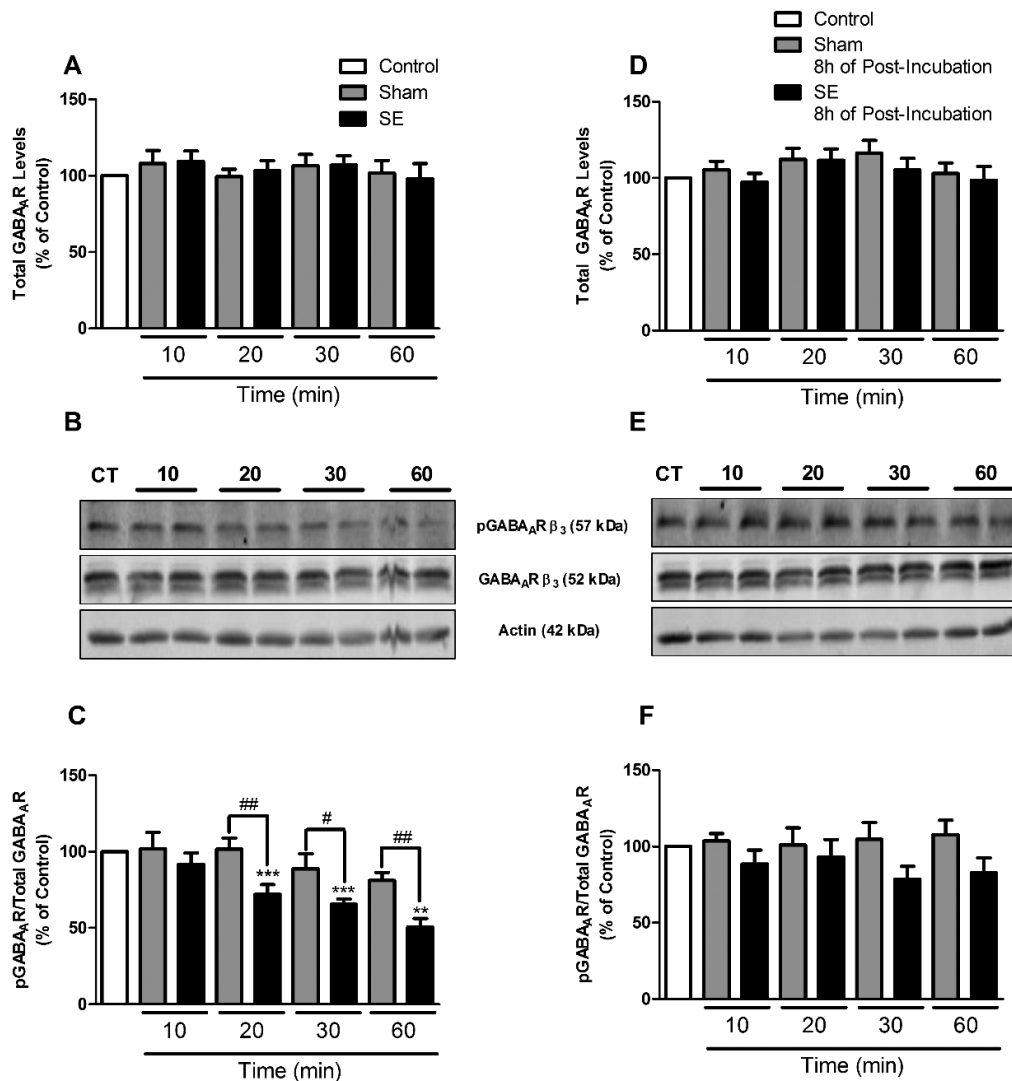
Fig.3.8: SE induces dephosphorylation of the GABA$_A$ Receptor β3 subunits -GABA$_A$R β3 subunit phosphorylation was evaluated immediately after the stimulus (A-C) or 8h later (post incubation) (D-F), by western blot analysis with a phospho-specific antibody against the β3 subunit serine 408/409. (A-F). Hippocampal neurons (15 DIV) were subjected to $[Mg^{2+}]_0$ medium (SE, 10 - 60 min) or maintained under control conditions (Sham medium). Results were normalized to the total protein levels of GABA$_A$R β3 subunit. GABA$_A$R β3 subunit total protein levels was determined under the same conditions by western blot analysis. The results were normalized with the loading control β-actin and were expressed as percentage of the control. The values are average ± SEM of at least 5 independent experiments performed in different preparations. One-way ANOVA was performed as statistical analysis, followed by Dunnett's and Bonferroni test, [**]$p< 0.01$, [***]$p< 0.001$, [#]$p< 0.5$, [##]$p< 0.01$; significantly different when compared to the control condition or to the indicated experimental condition.

3.3.2. SE induces the cleavage of gephyrin

Gephyrin, the principal scaffolding protein at inhibitory postsynapses, is responsible for the clustering and stabilization of synaptic $GABA_A$Rs (Fritschy et al., 2008). $GABA_A$Rs interact with gephyrin at the synapse promoting clustering and dictating their localization(Mukherjee et al., 2011; Kowalczyk et al., 2013; Tyagarajan et al., 2013). Thus, gephyrin is crucial for maintaining the balance of GABAergic inhibition and ultimately the maintenance of the correct functioning of neuronal networks. Recent studies have shown that gephyrin malfunction is implicated in epilepsy (Dejanovic et al., 2014). Furthermore, it has been previously demonstrated that phosphorylation and increased intracellular concentrations of calcium make gephyrin susceptible to proteolysis by calpain (Tyagarajan et al., 2013). SE is characterized by intense neuronal activity through an intracellular calcium accumulation. This can possibly lead to the activation of calpains, disrupting the synaptic cluster of gephyrin and therefore the synaptic stability of $GABA_A$Rs.

Gephyrin cleavage was evaluated by western blot analysis, immediately after the SE stimulus or 8h later (post-incubation), using an antibody against the G domain of gephyrin. Hippocampal neurons (15 DIV) were subjected to SE (incubation with $[Mg^{2+}]_0$ medium) for 10, 20, 30 and 60 min or maintained under control conditions (Sham medium). Samples were analyzed by western blot and gephyrin cleavage was expressed as a percentage of total gephyrin (truncated [TR] gephyrin) (C, D). Total gephyrin protein levels under the same conditions (A, B; full length + truncated [TR] gephyrin) was also calculated (Fig. 3.9 A, C). Immediately after incubation in SE medium there was no significant cleavage of gephyrin. However, when the cleavage of the protein was analysed 8 h after the insult there was a significant increase, even for short SE periods (~29%, ~35 % , ~25% and ~31% increase for 10, 20, 30 and 60 min of SE, respectively) (Fig.3.9 F). No changes in the gephyrin total protein levels were observed in the analysed conditions (Fig.3.9 A and D). Together, the SE-induced gephyrin cleavage and the changes in $GABA_A$R phosphorylation levels suggest that dramatic changes in the GABAergic synapse may occur under these conditions.
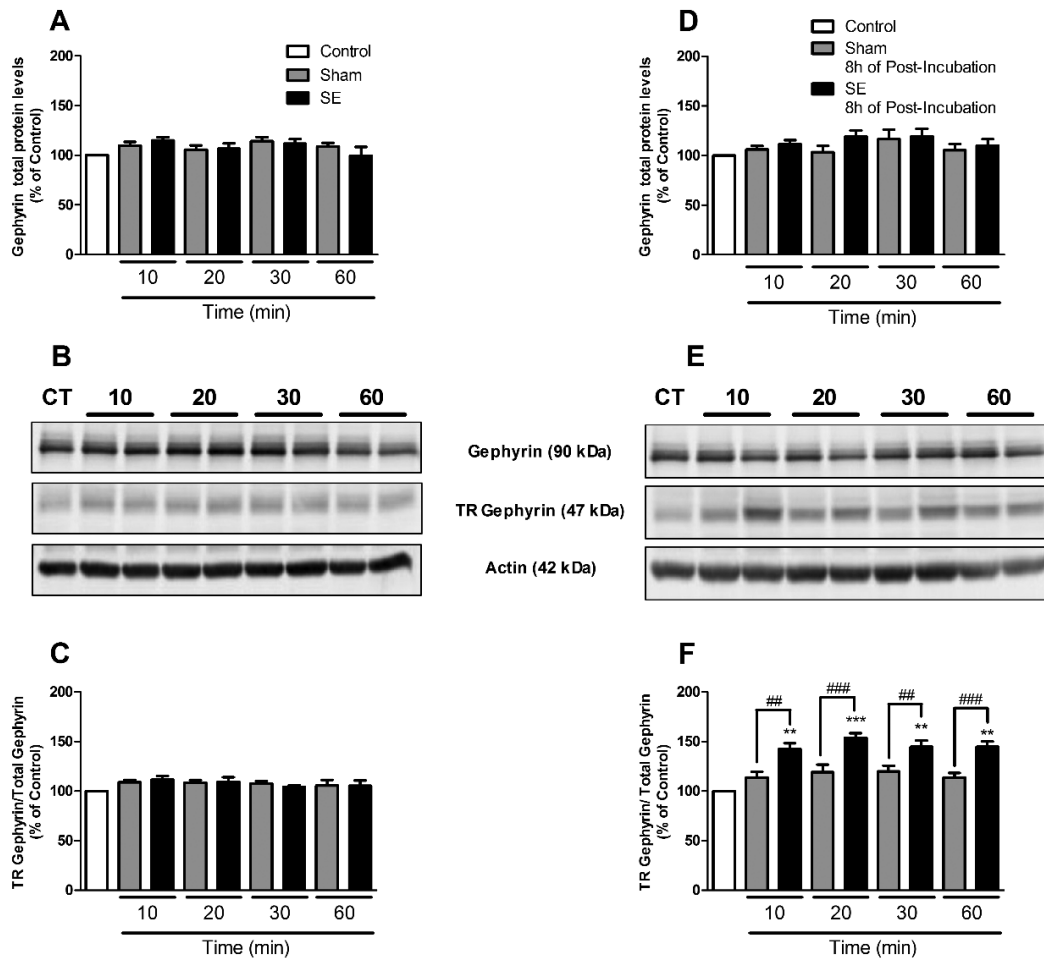
Fig.3.9: SE induces long-term accumulation of truncated gephyrin - Gephyrin cleavage was evaluated immediately after SE or 8h later (post-incubation), by western blot using an antibody against the G domain of gephyrin. Hippocampal neurons (15 DIV) were subjected to SE (incubation with $[Mg^{2+}]_0$ medium; 10 - 60 min) or maintained under control conditions (Sham medium). When a post-incubation was performed, the cells were maintained in culture-conditioned medium for this period of time. The results expressed as a percentage of total gephyrin (truncated [TR] gephyrin) (C, F) or as total gephyrin protein levels (A, D; full length + truncated [TR] gephyrin). Results were normalized with the loading control β-actin and were expressed as percentage of the control (A, C, D, F). The bars represent the means ± SEM of at least 3 independent experiments performed in different preparations. Statistical analysis was performed by one-way ANOVA, followed by Dunnett's or Bonferroni test. **p< 0.01, ***p< 0.001, ##p< 0.01, ###p< 0.001; significantly different when compared to the control condition or to the indicated experimental condition.

3.3.3. SE increases the internalization of GABA$_A$ receptors

Regulation of GABA$_A$R is extremely dynamic, since these receptors are known to undergo cycles of internalization and insertion into the plasma membrane. The results of section 3.3.1. and 3.3.2. showed that SE induces the dephosphorylation of GABA$_A$ receptors and the cleavage of gephyrin, indicating that the GABAergic synapse is damaged by SE.

To assess whether the SE-induced dephosphorylation of GABA$_A$Rs and cleavage of gephyrin are correlated with an increased internalization of the GABA$_A$Rs we transfected cultured hippocampal neurons with myc-tagged GABA$_A$R β3 subunit (tag located at the N-terminus which is extracellular) and receptor internalization was assessed using an antibody-feeding assay with an anti-myc antibody. The cells were incubated with $[Mg^{2+}]_0$ medium for 15 min (internalization period) or, alternatively, the incubation was in Neurobasal medium (Control) or saline medium (Sham) for the same period of time. The results show that SE significantly increased internalization of GABA$_A$Rs by ~22% (Fig. 3.10). This observation correlates with the results showing a GABA$_A$R β3 subunit dephosphorylation, and suggest that the receptor dephosphorylation may contribute to the increased internalization of GABA$_A$Rs after SE.
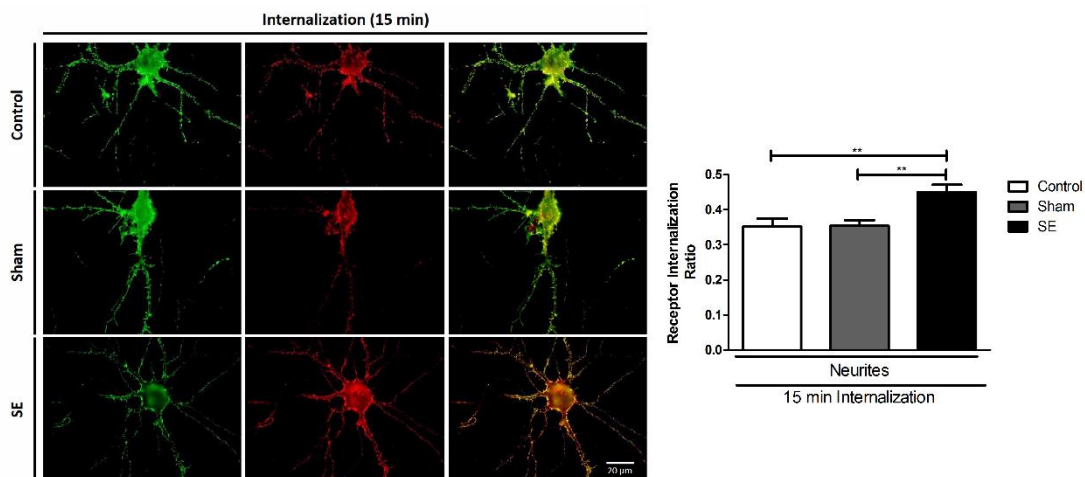

Fig. 3.10: SE increases the internalization of GABA$_A$ receptors - Cultured hippocampal neurons (13 DIV) were transfected with myc-tagged GABA$_A$R β3 subunit and receptor internalization was assessed using an antibody-feeding assay (DIV 15). Changes in the distribution of the receptors were analysed by fluorescence microscopy with an anti-myc antibody which binds to the N-terminal region of the receptor subunit. To assess receptor internalization changes in SE, the cells were incubated with $[Mg^{2+}]_0$ medium for 15 min (internalization period). In control or Sham conditions, the cells were incubated in Neurobasal medium (Control) or saline medium (Sham) for the same period of time. After quantification of the immunoreactivity in the neuritic compartments, the results were expressed as a ratio of internalized receptors/total receptor immunoreactivity. Results are means ±SEM of at least 3 independent experiments, performed in different preparations. At least 10 cells were analysed for each experimental condition. Statistical analysis was performed by one-way ANOVA, followed by Bonferroni's test. **$p < 0.01$, significantly different when compared to control conditions.

3.3.4. SE induces an impairment in GABA$_A$ receptor recycling

After internalization GABA$_A$Rs can be promptly recycled back to the plasma membrane or targeted for lysosomal degradation. This mechanism is crucial for controlling cell-surface receptor levels and thus the inhibitory synaptic strength (Jacob et al., 2008). It is still unknown if SE affects GABA$_A$R recycling. To assess the effect of SE in GABA$_A$R recycling we transfected cultured hippocampal neurons with myc-tagged GABA$_A$R β3 subunits (tag located at the N-terminus) and receptor recycling was assessed with an antibody-feeding assay with an anti-myc antibody. To analyse the changes in receptor recycling upon SE, the cells were initially stimulated with $[Mg^{2+}]_0$ medium for 15 min (internalization period) and after the internalization an acid wash was performed to remove antibodies that were bound to surface receptors. Immediately after the stripping, GABA$_A$ receptors were allowed to recycle for a period of 20 min in culture-conditioned medium. In control or Sham conditions, the stimulus was replaced by either Neurobasal medium (Control) or saline medium (Sham). The results show that SE significantly reduced GABA$_A$Rs recycling in ~30 (Fig. 3.11).
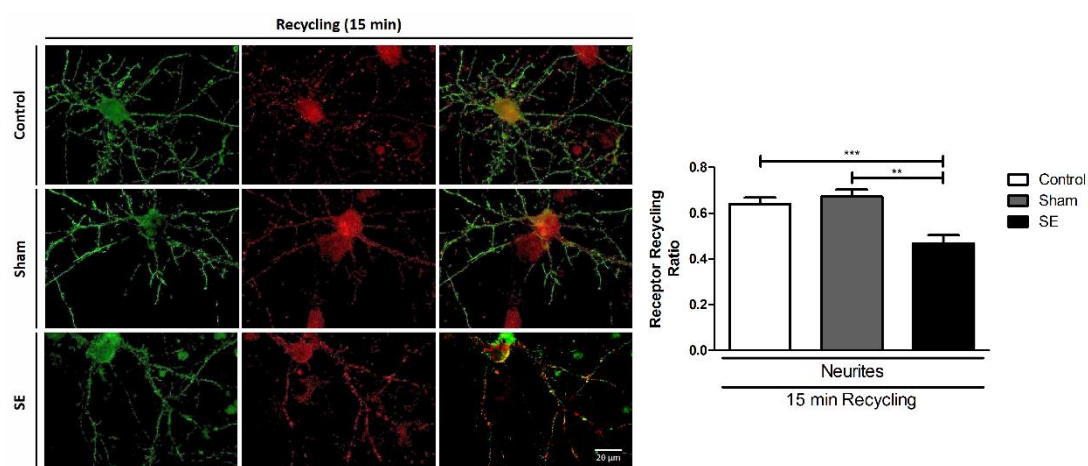

Fig.3.11: SE induces an impairment in GABA$_A$ receptor recycling - Cultured hippocampal neurons (13 DIV) were transfected with myc-tagged GABA$_A$R β3 subunits and receptor recycling was assessed at DIV 15 through an antibody-feeding assay. Changes in the distribution of the receptors were analysed by fluorescence microscopy in cells labelled with an anti-myc (N-terminus) antibody which binds to the N-terminal region of the receptor subunit. To assess changes in receptor recycling upon SE, the cells were initially stimulated with $[Mg^{2+}]_0$ medium for 15 min (internalization period) and after the internalization an acid wash was performed to remove antibodies that were bound to surface receptors. Immediately after the stripping, GABA$_A$ receptors were allowed to recycle for a period of 20 min in culture-conditioned medium. In control or Sham conditions, the stimulus was replaced by either Neurobasal medium (Control) or saline medium (Sham). After quantification of the immunoreactivity in the neuritic compartments, the results were expressed as a ratio of recycled receptors/total receptor immunoreactivity. Results are means ±SEM of at least 3 independent experiments, performed in different preparations. At least 10 cells were analysed for each experimental condition. Statistical analysis was performed by one-way ANOVA, followed by Bonferroni's test. **p< 0.01, ***p< 0.001 significantly different when compared to control conditions.

Discussion

4. Discussion

Epilepsy is an extremely complex disease where a multitude of abnormal physiological alterations induce a dramatic change in the balance between excitatory and inhibitory activities, giving rise to seizures (Pitkänen and Lukasiuk, 2011; Staley, 2015). Evidence points to the contribution of hyper-excitability as a permissive factor for the genesis and/or the propagation of epileptic seizures. Seizures rapidly modify neuronal activity and synaptic function. Aberrant GABAergic synaptic reorganization may be the cause (or one of the causes) of persistent deficits in functional inhibition in epilepsy.

In many patients with epilepsy, seizures are controlled with anti-epileptic drugs (AEDs), including enhancers of GABAergic transmission (Duncan et al., 2006). However, 30% of epileptic patients do not respond to the treatment (Banerjee et al., 2009). The development of pharmacoresistance has been associated to changes in neuronal plasticity. In fact, *status epilepticus* (SE) induces short-term and long-term alterations of $GABA_AR$ transmission (Staley, 2015). One explanation for this occurrence is that recurrent seizures lead to a progressive internalization of postsynaptic $GABA_ARs$ and to a consequent downregulation of inhibition (Goodkin et al., 2005). However, the molecular mechanisms contributing to the alterations in $GABA_AR$ synaptic distribution during epileptogenesis are currently unknown. In this work we report that the enhanced internalization of the $GABA_ARs$ is accompanied by a decrease in the phosphorylation of the β3 subunit and increased levels of cleaved gephyrin. Furthermore, we show that SE also impaired $GABA_ARs$ recycling, indicating that $GABA_AR$ synaptic stability is compromised in this condition.

4.1. $[Mg^{2+}]_0$ *in vitro* model of SE induce a time-dependent increase of cell death and alterations in the $[Ca^{2+}]_i$

The first part of our work was focused on the characterization of the $[Mg^{2+}]_0$ *in vitro* model of SE, to analyse the effects cellular death and the alterations of the $[Ca^{2+}]_i$ in cultured hippocampal neurons. Nuclear morphology analysis showed that SE induced neuronal death in a time-dependent manner for periods of incubation longer than 1 h (Fig.3.1). This is in accordance with previous studies conducted in *in vivo* models of SE and in humans. In humans, it was shown that epilepsy induces a loss of CA1 and CA3 pyramidal cells and of hilar neurons in the hippocampus. Neuronal damage was also found in associated limbic structures, including the amygdala, entorhinal cortex, and dorsomedial thalamus (Kapur, 2003). A similar pattern of neuronal loss was observed in the pilocarpine animal model of temporal lobe epilepsy (Curia et al., 2008).

We also showed that SE induces an increase of intracellular calcium concentration as demonstrated by Ca^{2+} analyses using Fura-2 in the absence of Mg^{2+} (Fig.3.2 A-B). Interestingly, the addition of Sham medium (containing Mg^{2+}) after a SE stimulus of 15 min induced a complete recovery to calcium basal levels (Fig.3.2 C-D), indicating that the cells preserve their capability to restabilising $[Ca^{2+}]_i$ basal levels after a SE insult. In general $[Ca^{2+}]_i$ increases may be due to the release of calcium from intracellular compartments and/or to the intake of extracellular calcium (Brini et al., 2014). Since the NMDA receptor

antagonist APV completely abolished the $[Mg^{2+}]_0$-induced increase in $[Ca^{2+}]_i$. we can conclude that SE increases the $[Ca^{2+}]_i$ through activation of NMDA receptors for glutamate. These results show that the SE-induced increase of $[Ca^{2+}]_i$ is likely due to an influx of extracellular calcium. To exclude the possibility of this mechanism being mediated by mobilization of calcium from intracellular stores, experiments should be performed in a calcium-free medium. In addition, excessive activation of NMDA receptors is known to lead to excitotoxicity through the excessive influx of Ca^{2+} (Sattler and Tymianski, 2001; Wang and Qin, 2010). To some extent the data obtained from single cell calcium imaging using Fura-2 indicated that incubation of hippocampal neurons in $[Mg^{2+}]_0$ medium induces a transient $[Ca^{2+}]_i$ response, may have been influenced by the fact that the experiments were conducted at room temperature. In fact, previous studies have shown that calcium transients are extremely sensitive to temperature (Lee et al., 2005) and the results may have been influenced by a temperature shift effect on NMDA receptor sensitivity (Gray et al., 1997; Lee et al., 2005). Accordingly, a different pattern of [Ca2+]i response was obtained when hippocampal neurons were subjected to SE at 37°C.

The results discussed above showed that SE induces a massive influx of Ca^{2+} through activation of NMDA receptors. As expected, the longer the cells were exposed to SE the higher was cellular death due to excitotoxic mechanisms resulting from an $[Ca^{2+}]_i$ overload. Excitotoxicity is characterized as a deleterious effect resulting from an excessive or prolonged activation of glutamate receptors by excitatory signals. This induces a multitude of deleterious effects, such as impairment of intracellular calcium homeostasis, compromised organelle functions, increase in nitric oxide and free radical production, persistent activation of proteases and kinases, increases in expression of pro-death transcription factors and immediate early genes (Wang and Qin, 2010). In particular, NMDA receptors play a fundamental role in the development of excitoxicity. The massive activation of NMDA receptors results in a more accentuated cell death when compared with the effects resulting from the activation of non-NMDA glutamate receptors or voltage-gated calcium channels (Wang and Qin, 2010). The excessive calcium influx through NMDA receptors has been shown to result in mitochondrial membrane depolarization, increases in free radicals and the activation of caspases, triggering several pathways which culminate in neuronal damage and eventual cellular death (Sattler and Tymianski, 2001; Dong et al., 2009; Wang and Qin, 2010).

4.2. SE evokes synchronous neuronal intracellular calcium transients in a time-dependent manner

Cytosolic calcium ($[Ca^{2+}]_i$) is an important mediator of neuronal signalling and neuronal activity (Burgoyne and Haynes, 2012). Excessive $[Ca^{2+}]_i$ has also been implicated in acute neuronal injury (Wang and Qin, 2010), and calcium-dependent processes have been hypothesized to play a role in the induction of epilepsy (Staley, 2015). Several studies have shown that the epileptogenic period is characterized by an alteration of $[Ca^{2+}]_i$ homeostatic mechanisms, but the intracellular calcium dynamics in SE is still poorly characterized. In this work, single cell Fluo-4 calcium imaging studies showed that SE evokes a synchronous $[Ca^{2+}]_i$ increase in cultured hippocampal neurons (Fig. 3.3). This result was

expected considering that SE induces a massive NMDA receptor activation (Nagarkatti et al., 2009; Reddy and Kuruba, 2013; Hongo et al., 2015). Interestingly, after the SE stimulus, around ~81% of the cells developed spontaneous $[Ca^{2+}]_i$ spiking activity (Fig. 3.6 C). The spontaneous spiking occurred during a period when the cells were no longer incubated in $[Mg^{2+}]_0$ medium, i.e. under conditions that mimic the physiological extracellular $[Mg^{2+}]$. When the cells were maintained in Sham medium throughout the entire experiment, no spontaneous spiking was observed (Fig. 3.4 A and 3.5 A), indicating that this type of behaviour is not due to an artefact of the experimental settings, being instead evoked by SE. In addition, the spontaneous $[Ca^{2+}]_i$ spiking was synchronous between the cells subjected to the SE stimulus. The use of the voltage-gated sodium channels blocker TTX, completely abolished the spontaneous calcium spiking, indicating that this process is dependent of neuronal activity (Fig. 3.7).

We also observed that different times of SE induced distinct $[Ca^{2+}]_i$ profiles in what concerns spontaneous spiking (Fig. 3.6). Thus, cells that were subjected to 30 min of SE developed spontaneous calcium spiking faster than hippocampal neurons exposed to SE for 15 min. The spontaneous calcium spiking was also more frequent, although more transient, in cells subjected to 30 min of SE, indicating that SE evokes different patterns of $[Ca^{2+}]_i$ oscillations in a time-dependent manner. Interestingly, around 82% of the cells that were exposed to SE for 15 min were able to recover the $[Ca^{2+}]_i$ basal levels, after the replacement of $[Mg^{2+}]_0$ with the Sham medium, while only about 46% of the cells that were subjected to 30 min of SE displayed the same pattern of response. This suggests that SE also alters the $[Ca^{2+}]_i$ homeostasis processes in a time-dependent manner.

Epileptic seizures are synchronous and sustained neuronal discharges occur within a group of neurons (Goodkin et al., 2005; Cherian and Thomas, 2009; Reddy and Kuruba, 2013). The resulting alterations in the $[Ca^{2+}]_i$ are likely to have multiple effects in neuronal physiology. For example, the $[Ca^{2+}]_i$ is crucial in controlling the activity of neuronal networks, due to the effects on neurotransmitter release and on plasma membrane ion channels (Nagarkatti et al., 2009; Burgoyne and Haynes, 2012). The pattern of increases in the $[Ca^{2+}]_i$ also plays a key role in gene expression under different conditions, including in neuronal plasticity (Nagarkatti et al., 2009). Our data indicates that SE evokes spontaneous epileptiform activity in cultured hippocampal neurons, possibly through physiological changes that maintain the cells in a state of hyperexcitability. This effect may be more remarkable when longer SE periods are tested, and this may explain the shorter lag-phase for initiation of the $[Ca^{2+}]_i$ transients upon removal of the SE buffer, as well as the increased frequency. It is also possible that the initial epileptogenic SE insult disrupts $[Ca^{2+}]_i$ homeostatic mechanisms, and the resulting transient increase of the $[Ca^{2+}]_i$ may lead to long-term changes in neuronal function and subsequent development of an epileptic phenotype. It will be of interest to further study what is the minimum time of SE required for the cells to develop spontaneous calcium spiking and for being able to fully recover to basal $[Ca^{2+}]_i$, as it would provide insights as to how this condition progresses with time.

In contrast with the data obtained with the Fura-2 probe, a more complex pattern of SE-induced changes in the $[Ca^{2+}]_i$ dynamics was observed when using Fluo-4. It is possible that as these calcium transients

are fast they were not detected by Fura-2, a probe with a much higher calcium binding strength when compared with Fluo-4 (Grynkiewicz et al., 1985; Gee et al., 2000; Thomas et al., 2000; Kikuchi, 2010). Furthermore, the temperature and atmosphere were controlled during the experiments performed with Fluo-4, possibly affecting the $[Ca^{2+}]_i$ dynamics.

The patter of $[Ca^{2+}]_i$ responses observed in cultured hippocampal neurons subjected transiently to SE, which includes spiking activity, validates the $[Mg^{2+}]_0$ model as an experimental strategy to study epileptogenesis *in vitro*. Furthermore, the periods of SE tested are appropriate not only to study the cellular and molecular alterations during SE, but also to investigate the long-term changes induced by SE and the development of chronic epilepsy.

4.3. SE evokes short- and long-term alterations on GABAergic synapses

Seizures are periods of excessive synchronized neuronal activity (Duncan et al., 2006). This induces changes the balance between the excitatory and inhibitory activities, and multiple factors are likely to contribute to alter neuronal behaviour. The massive influx of calcium and other ions as a result of the excessive neuronal activity disrupts ion homeostasis with a consequent severe impairment of neuronal function (Staley, 2015). On the other hand, seizure activity was also shown to alter protein trafficking and proteins mutations. Thus, SE increases $GABA_A$ receptor internalization (Goodkin et al., 2005), although the mechanisms involved have not been elucidated. This was confirmed by our data showing that 15 min SE induces an increase in the $GABA_A$Rs internalization, as demonstrated by antibody feeding assay (Fig.3.10). This observation also correlates with the decrease in GABA-mediated inhibition observed in SE (Kapur and Lothman, 1989; Kapur and Macdonald, 1997). Furthermore, previous evidence also showed that $GABA_A$R internalization is rapid and progressively increases by enhanced neuronal activity associated with seizures (Goodkin et al., 2005).

Under physiological conditions the internalization of $GABA_A$Rs is negatively regulated by the phosphorylation of $GABA_A$R β3 subunit on the serine residues 408 and 409. (Kittler et al. 2000; Kittler et al. 2005; Kittler et al. 2008). Phosphorylation of these residues decreases the binding of $GABA_A$R to the μ2 subunit of AP2, and a mimetic peptide simulating the β3 subunit motif that binds to AP2 upon receptor dephosphorylation enhanced mIPSC amplitude and whole-cell $GABA_A$R currents (Kittler et al., 2005), suggesting a major role in modulation of receptor internalization. Western blot analysis of the levels of phosphorylation of the β3 subunit of $GABA_A$Rs showed that SE induces a rapid decrease in the phosphorylation of Ser408/409 residues of the $GABA_A$Rs β3 subunit (Fig.3.8). Previous experiments have also shown that SE decreases phosphorylation of β3 $GABA_A$R subunits, with a resulting increase association of the receptors with the clathrin adaptor AP2 (Terunuma et al., 2008). Together, these results suggest that $GABA_A$R β3 subunit dephosphorylation may play an important role on the internalization of the receptors after SE. Recent studies also showed that $GABA_A$R dephosphorylation and a decreased interaction with gephyrin are key steps for GABAergic down-modulation in excitotoxic conditions (Mele et al., 2014). It remains to be determined whether a similar

decrease in GABA$_A$R interaction with gephyrin plays a role in the downregulation of GABA$_A$R surface expression in hippocampal neurons subjected to SE.

Several studies showed that an increased internalization of GABA$_A$R is correlated with a loss of benzodiazepine responsiveness between 10 and 45 minutes of SE (Kapur and Macdonald, 1997; Naylor et al., 2005). It is possible that excessive seizure activity evoked by SE alters phosphorylation-mediated modulation of the synaptic GABA$_A$Rs, inducing GABA$_A$R internalization via AP2-mediated endocytosis. Consequently, there is a reduction of the synaptic pool of GABA$_A$Rs, loss of GABA-mediated inhibition and a decrease in the sensivity to benzodiazepine-mediated pharmacological intervention during the SE crisis. This hypothesis may be tested by transfecting hippocampal neurons with a phosphomimetic form of GABA$_A$R which is expected to provide protection against the exacerbated internalization of the receptors.

Western blot analysis of the levels of truncated gephyrin showed that SE induces a long-term increase of truncated gephyrin, suggesting that SE induces the cleavage of the protein (Fig.3.9). This effect was not observed during the period SE stimulation, suggesting that the cleavage of gephyrin is a process that develops at a later point after SE, possible due to the dysregulation in the $[Ca^{2+}]_i$ homeostasis. Gephyrin is the major scaffolding protein of the GABAergic synapse and it is responsible for the anchoring and synaptic stability of GABA$_A$Rs (Tyagarajan and Fritschy, 2014; Costa et al., 2015). Gephyrin was shown to be a target for calpain cleavage under physiological conditions (Tyagarajan et al., 2013). Furthermore, a recent study has shown that several models of excitotoxicity (including NMDA over-activation) induce cleavage of gephyrin by calpains into stable products. Cleavage of gephyrin decreased the synaptic clustering of the protein and reduced the synaptic pool of GABA$_A$Rs (Costa et al., 2015).

Interestingly, our experiments have shown that after SE there is a maintenance of an increased $[Ca^{2+}]_i$, and other studies have also shown that SE evokes an elevated intracellular calcium plateau long after the stimulus (Nagarkatti et al., 2009). This elevated intracellular calcium may activate calpains, which may then target gephyrin thereby disrupting the GABAergic synapse. However it still remains to be determined whether SE triggers this mechanism for cleavage of gephyrin. We could furtherly study this mechanism by evaluating the levels of truncated gephyrin after SE in the presence of calpain inhibitors.

Our data also showed that SE decreases the recycling of GABA$_A$Rs (Fig.3.11), as demonstrated by antibody feeding assay, suggesting that a disruption of the mechanisms for-endocytotic sorting of GABA$_A$Rs may take place. Under physiological conditions, post-endocytotic sorting of GABA$_A$Rs depends on the huntingtin-associated protein 1 (HAP1). Overexpression of HAP1 inhibits GABA$_A$ receptor degradation and consequently increases receptor recycling (Kittler et al., 2004). In addition, the interaction between HAP1 and GABA$_A$Rs is compromised during excitotoxic conditions (unpublished results from our laboratory). Whether this mechanism also takes place during SE still remains to be studied. To elucidate the putative alterations in HAP1 protein levels during SE we could analyse the levels of HAP1 through western blot and characterize its interaction with GABA$_A$Rs via

immunoprecipitation. Overexpression of HAP1 would also allow determining if it has a protective effect on the levels of surface GABA$_A$Rs in hippocampal neurons subjected to SE.

An important emerging mechanism that may also contribute to the downregulation of the inhibitory activity of GABA is a positive shift of the GABA$_A$R reversal potential due to an alteration in chloride homeostasis (Kaila et al., 2014; Staley, 2015). However, whether the SE-induced downmodulation of GABAergic neurotransmission depends on the alteration in Cl$^-$ gradient is not yet established. Interestingly, seizures induce a downregulation of KCC2 activity, a neuronal K-Cl co-transporter responsible for maintaining the homeostasis of Cl$^-$ (Kaila et al., 2014). This downregulation is mediated by dephosphorylation and cleavage by the protease calpain (Medina et al., 2014). Furthermore, calpain cleaves not only KCC2 but also other proteins involved in GABAergic transmission, including GAD65, VGAT and GAT1 (Kaila et al., 2014; Medina et al., 2014). Thus, evidence suggests that the changes in postsynaptic GABA$_A$Rs and KCC2 share similar mechanisms and calpains may play a key role in epileptogenesis with important effects on the GABAergic synapse.

4.4. Final remarks

SE is a known epileptogenic insult and has been shown to induce the development of chronic epilepsy in animal models (Reddy and Kuruba, 2013). Our data suggests that SE induces short and long-term changes in GABAergic synapse. It is possible that during SE the dephosphorylation of GABA$_A$Rs leads to the internalization of the synaptic pool of receptors, which is further exacerbated by the disruption of the recycling process. Together, these alterations lead to a loss of GABA-mediated inhibition which not only makes the condition self-reinforcing but also contributes to the development of pharmacoresistance. After SE the GABAergic synapse suffers further alterations where the GABA$_A$R synaptic clustering by gephryin is disrupted, thereby compromising the synaptic stability of GABA$_A$Rs. The down modulation of GABAergic synapse is reinforced by de fact that upon SE there is also an impairment of GABA$_A$R recycling.

Together, all of our data suggest that SE induces short- and long-term alterations to GABAergic synapses, impairing GABA$_A$R-mediated inhibition. Furthermore, this work shows different processes that cooperate to cause the unbalance between excitatory and inhibitory currents. A better understanding of these mechanisms may provide new targets for the therapy of chronic epilepsy.

Bibliography

5. Bibliography

Baliova M, Knab A, Franekova V, Jursky F (2009) Modification of the cytosolic regions of GABA transporter GAT1 by calpain. Neurochem Int 55:288–294.

Banerjee P, Filippi D, Hauser WA (2009) The descriptive epidemiology of epilepsy—a review. Epilepsy Res 85:31–45.

Bedford FK, Kittler JT, Muller E, Thomas P, Uren JM, Merlo D, Wisden W, Triller a, Smart TG, Moss SJ (2001) GABA(A) receptor cell surface number and subunit stability are regulated by the ubiquitin-like protein Plic-1. Nat Neurosci 4:908–916.

Bogdanov Y, Michels G, Armstrong-Gold C, Haydon PG, Lindstrom J, Pangalos M, Moss SJ (2006) Synaptic GABAA receptors are directly recruited from their extrasynaptic counterparts. EMBO J 25:4381–4389.

Bracci E, Vreugdenhil M, Hack SP, Jefferys JG (2001) Dynamic modulation of excitation and inhibition during stimulation at gamma and beta frequencies in the CA1 hippocampal region. J Neurophysiol 85:2412–2422.

Breitinger HG, Becker CM (2002) The inhibitory glycine receptor - Simple views of a complicated channel. ChemBioChem 3:1042–1052.

Brickley K, Smith MJ, Beck M, Stephenson FA (2005) GRIF-1 and OIP106, members of a novel gene family of coiled-coil domain proteins: Association in vivo and in vitro with kinesin. J Biol Chem 280:14723–14732.

Brini M, Calì T, Ottolini D, Carafoli E (2014) Neuronal calcium signaling: function and dysfunction. Cell Mol Life Sci 71:2787–2814.

Brünig I, Scotti E, Sidler C, Fritschy JM (2002) Intact sorting, targeting, and clustering of γ-aminobutyric acid A receptor subtypes in hippocampal neurons in vitro. J Comp Neurol 443:43–55.

Buddhala C, Suarez M, Modi J, Prentice H, Ma Z, Tao R, Wu JY (2012) Calpain cleavage of brain glutamic acid decarboxylase 65 is pathological and impairs GABA neurotransmission. PLoS ONE 7(3): e33002.

Burgoyne RD, Haynes LP (2012) Understanding the physiological roles of the neuronal calcium sensor proteins. Mol Brain 5:2.

Caldeira M V., Melo C V., Pereira DB, Carvalho RF, Carvalho AL, Duarte CB (2007) BDNF regulates the expression and traffic of NMDA receptors in cultured hippocampal neurons. Mol Cell Neurosci 35:208–219.

Casillas-Espinosa PM, Powell KL, O'Brien TJ (2012) Regulators of synaptic transmission: roles in the pathogenesis and treatment of epilepsy. Epilepsia 53 Suppl 9:41–58.

Chang W-P, Südhof TC (2009) SV2 renders primed synaptic vesicles competent for Ca2+ -induced exocytosis. J Neurosci 29:883–897.

Charych EI, Yu W, Miralles CP, Serwanski DR, Li X, Rubio M, De Blas AL (2004) The brefeldin A-inhibited GDP/GTP exchange factor 2, a protein involved in vesicular trafficking, interacts with the β subunits of the GABA A receptors. J Neurochem 90:173–189.

Chen Z-W, Chang C-SS, Leil T a, Olsen RW (2007) C-terminal modification is required for GABARAP-mediated GABA(A) receptor trafficking. J Neurosci 27:6655–6663.

Cherian A, Thomas S (2009) Status Epilepticus. Ann Indian Acad Neurol 12:140–153.

Comenencia-Ortiz E, Moss SJ, Davies P a. (2014) Phosphorylation of GABAA receptors influences receptor trafficking and neurosteroid actions. Psychopharmacology (2014) 231:3453‑3465.

Connolly CN, Krishek BJ, McDonald BJ, Smart TG, Moss SJ (1996) Assembly and cell surface expression of heteromeric and homomeric gamma-aminobutyric acid type A receptors. J Biol Chem 271:89–96.

Corringer P-J, Le Novère N, Changeux J-P (2000) Nicotinic Receptors at the Amino Acid Level. Annu Rev Pharmacol Toxicol 40:431–458.

Costa JT, Mele M, Baptista MS, Gomes JR, Ruscher K, Nobre RJ, de Almeida LP, Wieloch T, Duarte CB (2015) Gephyrin Cleavage in In Vitro Brain Ischemia Decreases GABAA Receptor Clustering and Contributes to Neuronal Death. Mol Neurobiol (in press).

Curia G, Longo D, Biagini G, Jones RSG, Avoli M (2008) The pilocarpine model of temporal lobe epilepsy. J Neurosci Methods 172:143–157.

Curia G, Lucchi C, Vinet J, Gualtieri F, Marinelli C, Torsello a, Costantino L, Biagini G (2014) Pathophysiogenesis of mesial temporal lobe epilepsy: is prevention of damage antiepileptogenic? Curr Med Chem 21:663–688.

Davies P a., Wang W, Hales TG, Kirkness EF (2003) A novel class of ligand-gated ion channel is activated by Zn^{2+}. J Biol Chem 278:712–717.

Dejanovic B, Lal D, Catarino CB, Arjune S, Belaidi A a., Trucks H, Vollmar C, Surges R, Kunz WS, Motameny S, Altmüller J, Köhler A, Neubauer B a., EPICURE Consortium, Nürnberg P, Noachtar S, Schwarz G, Sander T (2014) Exonic microdeletions of the gephyrin gene impair GABAergic synaptic inhibition in patients with idiopathic generalized epilepsy. Neurobiol Dis 67:88–96.

Dong X, Wang Y, Qin Z (2009) Molecular mechanisms of excitotoxicity and their relevance to pathogenesis of neurodegenerative diseases. Acta Pharmacol Sin 30:379–387.

Dudek FE, Staley KJ (2011) The time course of acquired epilepsy: Implications for therapeutic intervention to suppress epileptogenesis. Neurosci Lett 497:240–246.

Duncan JS, Sander JW, Sisodiya SM, Walker MC (2006) Adult epilepsy. Lancet 367:1087–1100.

Engel J (2001) ILAE Commission Report A Proposed Diagnostic Scheme for People with Epileptic Seizures and with Epilepsy : Report of the ILAE Task Force on Classification and Terminology. Epilepsia 42:796–803.

Fang C, Deng L, Keller CA, Fukata M, Fukata Y, Chen G, Lüscher B (2006) GODZ-Mediated Palmitoylation of GABAA Receptors is Required for Normal Assembly and Function of GABAergic Inhibitory Synapses. J Neurosci 26:12758–12768.

Fisher RS, Acevedo C, Arzimanoglou A, Bogacz A, Cross JH, Elger CE, Engel J, Forsgren L, French J a., Glynn M, Hesdorffer DC, Lee BI, Mathern GW, Moshé SL, Perucca E, Scheffer IE, Tomson T, Watanabe M, Wiebe S (2014) ILAE Official Report: A practical clinical definition of epilepsy. Epilepsia 55:475–482.

Fritschy JM, Harvey RJ, Schwarz G (2008) Gephyrin: where do we stand, where do we go? Trends Neurosci 31:257–264.

Fueta Y, Kunugita N, Schwarz W (2005) Antiepileptic action induced by a combination of vigabatrin and tiagabine. Neuroscience 132:335–345.

Gee KR, Brown K a, Chen WN, Bishop-Stewart J, Gray D, Johnson I (2000) Chemical and physiological characterization of fluo-4 Ca(2+)-indicator dyes. Cell Calcium 27:97–106.

Gomes JR, Lobo AC, Melo C V, Inácio AR, Takano J, Iwata N, Saido TC, de Almeida LP, Wieloch T, Duarte CB (2011) Cleavage of the vesicular GABA transporter under excitotoxic conditions is followed by accumulation of the truncated transporter in nonsynaptic sites. J Neurosci 31:4622–4635.

González MI (2013) The possible role of GABAA receptors and gephyrin in epileptogenesis. Front Cell Neurosci 7:113.

González MI, Cruz Del Angel Y, Brooks-Kayal A (2013) Down-regulation of gephyrin and GABAA receptor subunits during epileptogenesis in the CA1 region of hippocampus. Epilepsia 54:616–624.

Goodkin H, Yeh J, Kapur J (2005) Status epilepticus increases the intracellular accumulation of GABAA receptors. J Neurosci 25:5511–5520.

Goodkin HP, Joshi S, Mtchedlishvili Z, Brar J, Kapur J (2008) Subunit-specific trafficking of GABA(A) receptors during status epilepticus. J Neurosci 28:2527–2538.

Goto H, Terunuma M, Kanematsu T, Misumi Y, Moss SJ, Hirata M (2005) Direct interaction of N-ethylmaleimide-sensitive factor with GABA(A) receptor beta subunits. Mol Cell Neurosci 30:197–206.

Graf ER, Zhang X, Jin SX, Linhoff MW, Craig AM (2004) Neurexins induce differentiation of GABA and glutamate postsynaptic specializations via neuroligins. Cell 119:1013–1026.

Gray AT, Buck LT, Feiner JR, Bickler PE (1997) Interactive Effects of pH and Temperature on N-Methyl-D-Aspartate Receptor Activity in Rat Cortical Brain Slices. J Neurosurg Anesthesiol 9:180–187.

Grynkiewicz G, Poenie M, Tsien RY (1985) A new generation of Ca2+ indicators with greatly improved fluorescence properties. J Biol Chem 260:3440–3450.

Hongo Y, Takasu K, Ikegaya Y, Hasegawa M, Sakaguchi G, Ogawa K (2015) Heterogeneous effects of antiepileptic drugs in an in vitro epilepsy model: a functional multineuron calcium imaging study. European Journal of Neuroscience. doi: 10.1111/ejn.12945

Jacob TC, Bogdanov YD, Magnus C, Saliba RS, Kittler JT, Haydon PG, Moss SJ (2005) Gephyrin regulates the cell surface dynamics of synaptic GABAA receptors. J Neurosci 25:10469–10478.

Jacob TC, Moss SJ, Jurd R (2008) GABA(A) receptor trafficking and its role in the dynamic modulation of neuronal inhibition. Nat Rev Neurosci 9:331–343.

Jacobs MP, Leblanc GG, Brooks-Kayal A, Jensen FE, Lowenstein DH, Noebels JL, Spencer DD, Swann JW (2009) Curing epilepsy: Progress and future directions. Epilepsy Behav 14:438–445.

Jones Jr. HR, Srinivasan J, Allam GJ, Baker RA (2012) Netter's Neurology (Clinic L, ed)., 2nd ed. Elsevier Health.

Josephson CB, Pohlmann-Eden B (2012) The "Natural" History of Medically Treated Temporal Lobe Epilepsy: What Can an Evidence-Based Approach Tell Us? Epilepsy Research and Treatment, vol. 2012, Article ID 216510, 8 pages, 2012. doi:10.1155/2012/216510.

Kaeser PS, Regehr WG (2014) Molecular mechanisms for synchronous, asynchronous, and spontaneous neurotransmitter release. Annu Rev Physiol 76:333–363.

Kahle KT, Staley KJ, Nahed B V, Gamba G, Hebert SC, Lifton RP, Mount DB (2008) Roles of the cation-chloride cotransporters in neurological disease. Nat Clin Pract Neurol 4:490–503.

Kaila K, Ruusuvuori E, Seja P, Voipio J, Puskarjov M (2014) GABA actions and ionic plasticity in epilepsy. Curr Opin Neurobiol 26:34–41.

Kandratavicius L, Balista PA, Lopes-Aguiar C, Ruggiero RN, Umeoka EH, Garcia-Cairasco N, Bueno-Junior LS, Leite JP (2014) Animal models of epilepsy: use and limitations. Neuropsychiatr Dis Treat 10:1693–1705.

Kanematsu T, Jang IS, Yamaguchi T, Nagahama H, Yoshimura K, Hidaka K, Matsuda M, Takeuchi H, Misumi Y, Nakayama K, Yamamoto T, Akaike N, Hirata M, Nakayama KI (2002) Role of the PLC-related, catalytically inactive protein p130 in GABAA receptor function. EMBO J 21:1004–1011.

Kapur J (2003) Role of Neuronal Loss in the Pathogenesis of Recurrent Spontaneous Seizures. Epilepsy Curr 3:166–167.

Kapur J, Coulter D a. (1995) Experimental status epilepticus alters γ-aminobutyric acid type A receptor function in CA1 pyramidal neurons. Ann Neurol 38:893–900.

Kapur J, Lothman EW (1989) Loss of inhibition precedes delayed spontaneous seizures in the hippocampus after tetanic electrical stimulation. J Neurophysiol 61:427–434.

Kapur J, Macdonald RL (1997) Rapid seizure-induced reduction of benzodiazepine and Zn2+ sensitivity of hippocampal dentate granule cell GABAA receptors. J Neurosci 17:7532–7540.

Kapur J, Stringer JL, Lothman EW (1989) Evidence that repetitive seizures in the hippocampus cause a lasting reduction of GABAergic inhibition. J Neurophysiol 61:417–426.

Keller CA, Yuan X, Panzanelli P, Martin ML, Alldred M, Sassoè-Pognetto M, Lüscher B (2004) The Gamma2 Subunit of GABA A Receptors Is a Substrate for Palmitoylation by GODZ. J Neurosci 24:5881–5891.

Kennard JTT, Barmanray R, Sampurno S, Ozturk E, Reid C a., Paradiso L, D'Abaco GM, Kaye a. H, Foote SJ, O'Brien TJ, Powell KL (2011) Stargazin and AMPA receptor membrane expression is increased in the somatosensory cortex of Genetic Absence Epilepsy Rats from Strasbourg. Neurobiol Dis 42:48–54.

Kikuchi K (2010) Design, synthesis and biological application of chemical probes for bio-imaging. Chem Soc Rev 39:2048–2053.

Kirsch J, Betz H (1995) The postsynaptic localization of the glycine receptor-associated protein gephyrin is regulated by the cytoskeleton. J Neurosci 15:4148–4156.

Kittler JT, Chen G, Honing S, Bogdanov Y, McAinsh K, Arancibia-Carcamo IL, Jovanovic JN, Pangalos MN, Haucke V, Yan Z, Moss SJ (2005) Phospho-dependent binding of the clathrin AP2 adaptor complex to GABAA receptors regulates the efficacy of inhibitory synaptic transmission. Proc Natl Acad Sci U S A 102:14871–14876.

Kittler JT, Chen G, Kukhtina V, Vahedi-Faridi A, Gu Z, Tretter V, Smith KR, McAinsh K, Arancibia-Carcamo IL, Saenger W, Haucke V, Yan Z, Moss SJ (2008) Regulation of synaptic inhibition by phospho-dependent binding of the AP2 complex to a YECL motif in the GABAA receptor gamma2 subunit. Proc Natl Acad Sci U S A 105:3616–3621.

Kittler JT, Delmas P, Jovanovic JN, Brown D a, Smart TG, Moss SJ (2000) Constitutive endocytosis of GABAA receptors by an association with the adaptin AP2 complex modulates inhibitory synaptic currents in hippocampal neurons. J Neurosci 20:7972–7977.

Kittler JT, McAinsh K, Moss SJ (2002) Mechanisms of GABAA receptor assembly and trafficking: implications for the modulation of inhibitory neurotransmission. Mol Neurobiol 26:251–268.

Kittler JT, Thomas P, Tretter V, Bogdanov YD, Haucke V, Smart TG, Moss SJ (2004) Huntingtin-associated protein 1 regulates inhibitory synaptic transmission by modulating gamma-aminobutyric acid type A receptor membrane trafficking. Proc Natl Acad Sci U S A 101:12736–12741.

Kneussel M, Brandstätter JH, Gasnier B, Feng G, Sanes JR, Betz H (2001) Gephyrin-independent clustering of postsynaptic GABA(A) receptor subtypes. Mol Cell Neurosci 17:973–982.

Kobow K, Auvin S, Jensen F, Löscher W, Mody I, Potschka H, Prince D, Sierra A, Simonato M, Pitkänen A, Nehlig A, Rho JM (2012) Finding a better drug for epilepsy: antiepileptogenesis targets. Epilepsia 53:1868–1876.

Kowalczyk S, Winkelmann A, Smolinsky B, Förstera B, Neundorf I, Schwarz G, Meier JC (2013) Direct binding of GABAA receptor β2 and β3 subunits to gephyrin. Eur J Neurosci 37:544–554.

Lardi-Studler B, Smolinsky B, Petitjean CM, Koenig F, Sidler C, Meier JC, Fritschy J-M, Schwarz G (2007) Vertebrate-specific sequences in the gephyrin E-domain regulate cytosolic aggregation and postsynaptic clustering. J Cell Sci 120:1371–1382.

Lazarevic V, Pothula S, Andres-Alonso M, Fejtova A (2013) Molecular mechanisms driving homeostatic plasticity of neurotransmitter release. Front Cell Neurosci 7:244.

Le Duigou C, Holden T, Kullmann DM (2011) Short- and long-term depression at glutamatergic synapses on hippocampal interneurons by group i mGluR activation. Neuropharmacology 60:748–756.

Lee JCF, Callaway JC, Foehring RC (2005) Effects of Temperature on Calcium Transients and Ca 2+ - Dependent Afterhyperpolarizaions in Neocortical Pyramidal Neurons. J Neurophysiol 93:2012–2020.

Li X-J, Li S-H, Sharp AH, Nucifora Jr FC, Schilling G, Lanahan A, Worley P, Snyder SH, Ross CA (1995) A huntingtin-associated protein enriched in brain with implications for pathology. Nature 378:398–402.

Lillis KP, Kramer MA, Mertz J, Staley KJ, White JA (2012) Pyramidal cells accumulate chloride at seizure onset. Neurobiol Dis 47:358–366.

Loebrich S, Bähring R, Katsuno T, Tsukita S, Kneussel M (2006) Activated radixin is essential for GABAA receptor alpha5 subunit anchoring at the actin cytoskeleton. EMBO J 25:987–999.

Löscher W (2011) Critical review of current animal models of seizures and epilepsy used in the discovery and development of new antiepileptic drugs. Seizure 20:359–368.

Lowenstein DH, Alldredge B (1998) Clinical features of generalized status epilepticus. N Engl J Med 338:970–976.

Maas C, Tagnaouti N, Loebrich S, Behrend B, Lappe-Siefke C, Kneussel M (2006) Neuronal cotransport of glycine receptor and the scaffold protein gephyrin. J Cell Biol 172:441–451.

Magiorkinis E, Diamantis A, Sidiropoulou K, Panteliadis C (2014) Highlights in the History of Epilepsy : The Last 200 Years. Epilepsy Research and Treatment, vol. 2014, Article ID 582039, 13 pages, 2014. doi:10.1155/2014/582039.

Medina I, Friedel P, Rivera C, Kahle KT, Kourdougli N, Uvarov P, Pellegrino C (2014) Current view on the functional regulation of the neuronal K(+)-Cl(-) cotransporter KCC2. Front Cell Neurosci 8:27.

Mele M, Ribeiro L, Inácio AR, Wieloch T, Duarte CB (2014) GABA(A) receptor dephosphorylation followed by internalization is coupled to neuronal death in in vitro ischemia. Neurobiol Dis 65:220–232.

Miller PS, Aricescu a R (2014) Crystal structure of a human GABAA receptor. Nature 512:270–275.

Minta a., Kao JPY, Tsien RY (1989) Fluorescent indicators for cytosolic calcium based on rhodamine and fluorescein chromophores. J Biol Chem 264:8171–8178.

Mizokami A, Kanematsu T, Ishibashi H, Yamaguchi T, Tanida I, Takenaka K, Nakayama KI, Fukami K, Takenawa T, Kominami E, Moss SJ, Yamamoto T, Nabekura J, Hirata M (2007) Phospholipase C-related inactive protein is involved in trafficking of gamma2 subunit-containing GABA(A) receptors to the cell surface. J Neurosci 27:1692–1701.

Mukherjee J, Kretschmannova K, Gouzer G, Maric H-M, Ramsden S, Tretter V, Harvey K, Davies P a., Triller a., Schindelin H, Moss SJ (2011) The Residence Time of GABAARs at Inhibitory Synapses Is Determined by Direct Binding of the Receptor 1 Subunit to Gephyrin. J Neurosci 31:14677–14687.

Nagarkatti N, Deshpande LS, DeLorenzo RJ (2009) Development of the calcium plateau following status epilepticus: role of calcium in epileptogenesis. Expert Rev Neurother 9:813–824.

Naylor DE, Liu H, Niquet J, Wasterlain CG (2013) Rapid surface accumulation of NMDA receptors increases glutamatergic excitation during status epilepticus. Neurobiol Dis 54:225–238.

Naylor DE, Liu H, Wasterlain CG (2005) Trafficking of GABA(A) receptors, loss of inhibition, and a mechanism for pharmacoresistance in status epilepticus. J Neurosci 25:7724–7733.

Pal S, Sombati S, Limbrick DD, DeLorenzo RJ (1999) In vitro status epilepticus causes sustained elevation of intracellular calcium levels in hippocampal neurons. Brain Res 851:20–31.

Pal S, Sun D, Limbrick D, Rafiq a, DeLorenzo RJ (2001) Epileptogenesis induces long-term alterations in intracellular calcium release and sequestration mechanisms in the hippocampal neuronal culture model of epilepsy. Cell Calcium 30:285–296.

Papadopoulos T, Eulenburg V, Reddy-Alla S, Mansuy IM, Li Y, Betz H (2008) Collybistin is required for both the formation and maintenance of GABAergic postsynapses in the hippocampus. Mol Cell Neurosci 39:161–169.

Papadopoulos T, Korte M, Eulenburg V, Kubota H, Retiounskaia M, Harvey RJ, Harvey K, O'Sullivan G a, Laube B, Hülsmann S, Geiger JRP, Betz H (2007) Impaired GABAergic transmission and altered hippocampal synaptic plasticity in collybistin-deficient mice. EMBO J 26:3888–3899.

Pitkänen A, Lukasiuk K (2011) Mechanisms of epileptogenesis and potential treatment targets. Lancet Neurol 10:173–186.

Poulopoulos A, Aramuni G, Meyer G, Soykan T, Hoon M, Papadopoulos T, Zhang M, Paarmann I, Fuchs C, Harvey K, Jedlicka P, Schwarzacher SW, Betz H, Harvey RJ, Brose N, Zhang W, Varoqueaux F (2009) Neuroligin 2 Drives Postsynaptic Assembly at Perisomatic Inhibitory Synapses through Gephyrin and Collybistin. Neuron 63:628–642.

Rajakulendran S, Kaski D, Hanna M (2012) Neuronal P/Q-type calcium channel dysfunction in inherited disorders of the CNS. Nat Publ Gr 8:86–96.

Ransom CB, Ransom BR, Sontheimer H (2000) Activity-dependent extracellular K+ accumulation in rat optic nerve: the role of glial and axonal Na+ pumps. J Physiol 522 Pt 3:427–442.

Reddy DS, Kuruba R (2013) Experimental models of status epilepticus and neuronal injury for evaluation of therapeutic interventions. Int J Mol Sci 14:18284–18318.

Ross WN (2012) Understanding calcium waves and sparks in central neurons. Nat Rev Neurosci 13:157–168.

Roth FC, Draguhn A (2012) GABA metabolism and transport: Effects on synaptic efficacy. Neural Plasticity, vol. 2012, Article ID 805830, 12 pages, 2012. doi:10.1155/2012/805830

Rudolph U, Möhler H (2004) Analysis of GABAA receptor function and dissection of the pharmacology of benzodiazepines and general anesthetics through mouse genetics. Annu Rev Pharmacol Toxicol 44:475–498.

Saiyed T, Paarmann I, Schmitt B, Haeger S, Sola M, Schmalzing G, Weissenhorn W, Betz H (2007) Molecular basis of gephyrin clustering at inhibitory synapses: Role of G- and E-domain interactions. J Biol Chem 282:5625–5632.

Saliba RS, Michels G, Jacob TC, Pangalos MN, Moss SJ (2007) Activity-dependent ubiquitination of GABA(A) receptors regulates their accumulation at synaptic sites. J Neurosci 27:13341–13351.

Sattler R, Tymianski M (2001) Molecular mechanisms of glutamate receptor-mediated excitotoxic neuronal cell death. Mol Neurobiol 24:107–129.

Scheiffele P, Fan J, Choih J, Fetter R, Serafini T (2000) Neuroligin expressed in nonneuronal cells triggers presynaptic development in contacting axons. Cell 101:657–669.

Schousboe A, Madsen KK, Barker-Haliski ML, White HS (2014) The GABA Synapse as a Target for Antiepileptic Drugs: A Historical Overview Focused on GABA Transporters. Neurochem Res 39:1980–1987.

Sigel E, Steinmann ME (2012) Structure, function, and modulation of GABAA receptors. J Biol Chem 287:40224–40231.

Smith MJ, Pozo K, Brickley K, Stephenson FA (2006) Mapping the GRIF-1 binding domain of the kinesin, KIF5C, substantiates a role for GRIF-1 as an adaptor protein in the anterograde trafficking of cargoes. J Biol Chem 281:27216–27228.

Stables JP, Bertram EH, White HS, Coulter D a, Dichter M a, Jacobs MP, Loscher W, Lowenstein DH, Moshe SL, Noebels JL, Davis M (2002) Models for epilepsy and epileptogenesis: report from the NIH workshop, Bethesda, Maryland. Epilepsia 43:1410–1420.

Staley K (2015) Molecular mechanisms of epilepsy. Nat Neurosci 18:367–372.

Staley KJ, Proctor WR (1999) Modulation of mammalian dendritic GABA A receptor function by the kinetics of Cl - and HCO 3 - transport. J Physiol 519:693–712.

Sutula TP (2004) Mechanisms of epilepsy progression: Current theories and perspectives from neuroplasticity in adulthood and development. Epilepsy Res 60:161–171.

Terunuma M, Jang I-S, Ha SH, Kittler JT, Kanematsu T, Jovanovic JN, Nakayama KI, Akaike N, Ryu SH, Moss SJ, Hirata M (2004) GABAA receptor phospho-dependent modulation is regulated by phospholipase C-related inactive protein type 1, a novel protein phosphatase 1 anchoring protein. J Neurosci 24:7074–7084.

Terunuma M, Xu J, Vithlani M, Sieghart W, Kittler J, Pangalos M, Haydon PG, Coulter D a, Moss SJ (2008) Deficits in phosphorylation of GABA(A) receptors by intimately associated protein kinase C activity underlie compromised synaptic inhibition during status epilepticus. J Neurosci 28:376–384.

Thomas D, Tovey SC, Collins TJ, Bootman MD, Berridge MJ, Lipp P (2000) A comparison of fluorescent Ca2+ indicator properties and their use in measuring elementary and global Ca2+ signals. Cell Calcium 28:213–223.

Thompson a J, Lummis SCR (2006) 5-HT3 receptors. Curr Pharm Des 12:3615–3630.

Treiman DM (2001) GABAergic mechanisms in epilepsy. Epilepsia 42:8–12.

Turski W, Cavalheiro E, Schwarz M, Czuczwar S, Kleinrok Z, Turski L (1983) Limbic seizures produced by pilocarpine in rats: behavioural, electroencephalographic and neuropathological study. Behav Brain Res 9:315–335.

Tyagarajan SK, Fritschy J-M (2014) Gephyrin: a master regulator of neuronal function? Nat Rev Neurosci 15:141–156.

Tyagarajan SK, Ghosh H, Yévenes GE, Imanishi SY, Zeilhofer HU, Gerrits B, Fritschy J-M (2013) Regulated kinase and glycogen synthase kinase 3β regulate gephyrin postsynaptic aggregation and GABAergic synaptic function in a calpain-dependent mechanism. J Biol Chem 288:9634–9647.

Van Vliet E a., Aronica E, Redeker S, Boer K, Gorter J a. (2009) Decreased expression of synaptic vesicle protein 2A, the binding site for levetiracetam, during epileptogenesis and chronic epilepsy. Epilepsia 50:422–433.

Varoqueaux F, Jamain S, Brose N (2004) Neuroligin 2 is exclusively localized to inhibitory synapses. Eur J Cell Biol 83:449–456.

Wang H, Bedford FK, Brandon NJ, Moss SJ, Olsen RW (1999) GABA(A)-receptor-associated protein links GABA(A) receptors and the cytoskeleton. Nature 397:69–72.

Wang Y, Qin Z-H (2010) Molecular and cellular mechanisms of excitotoxic neuronal death. Apoptosis 15:1382–1402.

Xiang S, Kim EY, Connelly JJ, Nassar N, Kirsch J, Winking J, Schwarz G, Schindelin H (2006) The Crystal Structure of Cdc42 in Complex with Collybistin II, a Gephyrin-interacting Guanine Nucleotide Exchange Factor. J Mol Biol 359:35–46.

Yi JJ, Ehlers MD (2007) Emerging roles for ubiquitin and protein degradation in neuronal function. Pharmacol Rev 59:14–39.

Zhang CL, Dreier JP, Heinemann U (1995) Paroxysmal epileptiform discharges in temporal lobe slices after prolonged exposure to low magnesium are resistant to clinically used anticonvulsants. Epilepsy Res 20:105–111.

Zheng Y (2001) Dbl family guanine nucleotide exchange factors. Trends Biochem Sci 26:724–732.